Distribution Agreement

In presenting this thesis or dissertation as a partial fulfillment of the requirements for an advanced degree from Emory University, I hereby grant to Emory University and its agents the non-exclusive license to archive, make accessible, and display my thesis or dissertation in whole or in part in all forms of media, now or hereafter known, including display on the world wide web. I understand that I may select some access restrictions as part of the online submission of this thesis or dissertation. I retain all ownership rights to the copyright of the thesis or dissertation. I also retain the right to use in future works (such as articles or books) all or part of this thesis or dissertation.

Signature:

_____ _____

April D Ratliff Date

Mechanisms of plasticity in sympathetic preganglionic and postganglionic neurons of the chick embryo

By

April D Ratliff
Doctor of Philosophy

Graduate Division of Biological and Biomedical Sciences: Neuroscience

---

Peter Wenner, Ph.D.
Advisor

Nicholas Au Yong, M.D., Ph.D.
Committee Member

Shawn Hochman, Ph.D.
Committee Member

Marie-Claude Perreault, Ph.D.
Committee Member

Astrid Prinz, Ph.D.
Committee Member

Accepted:

Kimberly Jacob Arriola
Dean of the James T. Laney School of Graduate Studies

Date

Mechanisms of plasticity in sympathetic preganglionic and postganglionic neurons of the chick embryo

By

April D Ratliff
B.S., Duke University, NC, 2015

Advisor: Peter Wenner, Ph.D.

An abstract of
A dissertation submitted to the Faculty of the
James T. Laney School of Graduate Studies of Emory University
in partial fulfillment of the requirements for the degree of
Doctor of Philosophy
in Graduate Division of Biological and Biomedical Sciences: Neuroscience
2023

Abstract

Mechanisms of plasticity in sympathetic preganglionic and postganglionic neurons of the chick embryo
By April D Ratliff

Throughout development, the nervous system is faced with countless challenges to which the cells in the system must have the ability to respond. The autonomic nervous system (ANS), in particular, is designed to respond to internal and environmental changes, to alter the function of different organs and tissues, ultimately regulating body temperature, heart rate, muscle tone, and numerous other important functions. In order to accomplish this, the ANS must be able to transiently sense a change, for example in external temperature, and respond by influencing the tissue appropriately, in this example blood vessel dilation or constriction. However, it is important that once the ideal temperature is reached, and target tissue activation is no longer needed, the system must be able to return to some setpoint of firing rate for the output from the autonomic nervous system, also known as baseline autonomic tone. It is not well known, however, what kinds of cellular mechanisms establish this setpoint, which likely occurs early in development. As we know, there are instances where baseline autonomic tone is chronically imbalanced, such as in hypertension. Therefore, understanding the cellular mechanisms for setting a healthy set point for autonomic tone has important implications for human health. Here, we test whether mechanisms of plasticity, which may play a role in setting up the trajectory for autonomic tone, are expressed during embryonic development of the sympathetic nervous system (SNS).

Mechanisms of plasticity in sympathetic preganglionic and postganglionic neurons of the chick embryo

By

April D Ratliff
B.S., Duke University, NC, 2015

Advisor: Peter Wenner, Ph.D.

A dissertation submitted to the Faculty of the
James T. Laney School of Graduate Studies of Emory University
in partial fulfillment of the requirements for the degree of
Doctor of Philosophy
in Graduate Division of Biological and Biomedical Sciences: Neuroscience
2023

Acknowledgments

The pursuit of my Ph.D. has been an incredibly rewarding yet, at times, a challenging journey. This achievement would not have been possible without the unwavering support of numerous mentors and friends who guided me along this path. Completing this dissertation project in the Wenner Lab has been an honor, and I feel immensely fortunate to have collaborated with an exceptional team of scientists. My heartfelt gratitude goes out to each one of them.

Foremost, I extend my deepest appreciation to my Ph.D. advisor, Dr. Pete Wenner. Your mentorship has been exemplary in numerous ways, and I want to emphasize a few key aspects that have profoundly impacted my journey. Your continuous support, from taking a chance on a trainee from a vastly different scientific background to providing hands-on training and navigating countless obstacles, exemplifies your exceptional kindness, patience, and endless support. You not only imparted a new set of skills but also significantly enhanced my scientific writing, and fostered belief in my capacity to innovate. Moreover, your unyielding enthusiasm and passion for scientific pursuits, and even non-scientific interests (Ultimate Frisbee forever!), made our lab environment not just productive but also very enjoyable. Your optimism and humor were a guiding light through challenging experiments. Moreover, the sense of camaraderie fostered in the lab, during our lab outings and shared experiences like supporting Atlanta United, made me feel an integral part of the team, and gave us labmembers lots to talk, laugh, and debate about. Under your guidance, I've evolved immensely as a scientist, writer, and thinker. I would also like to thank all of the members of the Wenner lab, especially Dr. Carlos Gonzalez-Islas, Dr. Dobromila Pekala, and Alishah Lakhani for being incredible mentors and friends. You made the lab an enjoyable place to be and you have each shared so much wisdom with me. You have set the bar very high for my future coworkers!

In addition to my primary mentor and labmates, I am profoundly grateful to the

distinguished members of my thesis committee: Dr. Nicholas Au Yong, Dr. Shawn Hochman, Dr. Marie-Claude Perreault, and Dr. Astrid Prinz. Each of you provided invaluable advice, feedback, and encouragement. Nick, your brilliant insights and assistance with signal processing tools were instrumental. Collaborating with you was an enriching experience. Shawn, your thoughtful feedback and wealth of knowledge in spinal cord physiology were immensely appreciated in refining my manuscript. Marie-Claude, your continued support and timely encouragement have been invaluable, especially during challenging transitions. Your thoughtful review of my thesis manuscript was incredibly helpful as well. Astrid, thank you so much for spending time helping me prepare for my grant proposal. I believe my successful award was in large part due to your guidance! Your friendly conversations were always a delight and I will never forget being your Teaching Assistant for the Neurobiology course. Additionally, I want to express my profound gratitude to two former Directors of Graduate Studies for the Emory Neuroscience Program, Dr. Sam Sober and Dr. Malú Tansey, for their unwavering support through a series of unique challenges. To all of you: thank you for believing in me and dedicating your invaluable time and energy to helping me become a better scientist.

On a personal note, I would like to express my appreciation and love for my mother, Leslie Ramirez, my brother Daniel, and my sister Violet. And, to the rest of my family, thank you so much. Without your continuous love and support, none of my achievements would have been possible. Thank you for always having a warm place for me to come home to for the holidays and for keeping me laughing. I would also like to say thank you to my Aunt and Godmother, Donna. Thank you for supporting me when I was sending out my graduate school applications and for celebrating my defense with me. You were there from beginning to end and I appreciate you so much!

I would also like to express my deep gratitude for the friends I have made during my time here at Emory. Thank you for making Atlanta feel like home. My classmates

and my Ultimate Frisbee teammates helped me stay sane throughout this journey. Thank you for supporting me through the difficult times, and for being there to celebrate the wins as well! I would especially like to thank Makalele Provost, who has been an incredible advocate and source of joy in my life. I would also like to give a very special thank you to my amazing partner Dr. James McGregor. Thank you for always making me smile, giving me great advice and going on adventures with me. I can't wait to see what comes next, now that we are both doctors!

This dissertation is dedicated to my father, Stephen Ratliff. I know he would be very proud of me and very excited to read my dissertation from cover to cover!

Contents

List of Figures

List of Tables

Chapter 1

Introduction

1.1 Background

The autonomic nervous system (ANS), is a system that we rely on constantly to regulate a wide array of bodily functions in an involuntary manner. In vertebrate species, the ANS coordinates involuntary actions across tissues, glands, and organs to orchestrate functioning in response to environmental stimuli, and to achieve a state of global homeostasis in the body. The ANS consists of two branches, the sympathetic nervous system (SNS) and the parasympathetic nervous system (PNS). In simple terms, the PNS is well-understood to coordinate the "rest and digest" functions that must be conducted under conditions of safety such as mating and food-seeking behaviors. Meanwhile the SNS is considered "fight or flight" system, mobilizing the body for action during times of stress, and then returning to an appropriate baseline afterwards. For instance, in order to stabilize blood oxygen levels during exertion, sympathetic output increases and afterwards returns to baseline level of output and thus return blood pressure to a baseline vascular tone. Importantly, the baseline firing rate of the SNS, known as baseline sympathetic tone, plays a role in maintaining metabolic activity during normal conditions. For example, sympathetic tone is influential in

the generation of respiratory and cardiac rhythms. A stable and biologically relevant baseline for autonomic output, known as autonomic tone, is crucial for proper functioning of the circuit. Anatomical and functional studies of the ANS have been studied over the past several centuries [34, 129, 130, 187, 253], yet several questions about this system remain. For instance, how does the ANS, a system that ensures global homeostasis, regulate its own output? The cellular or synaptic mechanisms which are engaged to define the baseline for autonomic tone are not well understood. Furthermore, it is not fully understood how, or when, this baseline is first established. As the ANS includes both SNS and PNS branches, ANS dysregulation could theoretically lead to either hyper- or hypo-excitability, respectively. For this dissertation, my research focuses on hyperexcitability of the SNS, as this has been described previously. For example, several findings suggest that early stages of development are particularly vulnerable to autonomic disturbances and can lead to long-term negative consequences for health of the SNS [35, 96, 112, 144, 161]. This suggests that a critical period may exist in the SNS during which perturbations in the developing circuit are translated into a hyperexcitability of autonomic tone later in life. The mechanisms which underly this process are not well understood. One form of neuroplasticity, known as homeostatic plasticity, works to monitor cellular or network activity and respond in a compensatory manner to any challenges. This may be a mechanism which is expressed during an early sensitive window of autonomic development, and it could play a role in the establishment of a healthy autonomic tone. Furthermore, it is known that mechanisms of homeostatic plasticity are robustly expressed during early development and even during critical periods in developing circuits and therefore homeostatic plasticity is a likely set of candidate mechanisms for this process of baseline establishment. In this thesis project, I sought to determine whether mechanisms of homeostatic plasticity are expressed in the spinal and peripheral neurons of the SNS during embryonic development. As previously stated, the SNS will be the target

of this study as dysfunction in this system is highly associated with life-threatening disease, and the SNS has been reasonably well characterized in the adult system. In addition, homeostatic plasticity has been demonstrated in the mature SNS [241].

Elements of SNS anatomy, connectivity, development, and vulnerability to disease have been explored for centuries in detail [130, 253], however the system is rarely studied through the more modern lens of neural homeostatic plasticity [227] or in the context of critical periods [33**?** , 174]. Critical periods are defined as distinct windows in development during which there is a heightened expression of some kind of neural plasticity, such that perturbations during this period can change the trajectory of development of the fully mature system [75]. On the other hand, perturbations that occur outside this window of a critical period typically don't have the same effect.

During critical periods, different forms of plasticity can be expressed which may determine the circuit excitability during early development. Forms of homeostatic plasticity are thought to maintain some function of neural operation (e.g. spiking or neurotransmission) by regulating cell excitability and/or synaptic strength [227, 234, 247]. These mechanisms could play an important role in establishing baseline sympathetic tone, such that the SNS can return to this setpoint and maintain homeostasis with regard to the entire nervous system. The set point for sympathetic tone should ideally be maintained at an optimal level for the health of the organism. With a sympathetic tone that is tuned to proper level, the SNS can avoid a state of chronically hyper- or hypoexcitability. However, this proper setpoint is not always achieved. For example, in hypertension, a disease of autonomic dysregulation, patients experience chronically elevated levels of sympathetic output, resulting in chronically high blood pressure. Could it be that diseases of autonomic dysregulation such as hypertension represent a malfunctioning of homeostatic plasticity in the SNS during a critical period? Or perhaps could the induction of homeostatic plasticity mechanisms function during this period and actively alter baseline excitability,

leaving the SNS circuit vulnerable to aberrant excitability [74]? In fact, certain autonomic disturbances during prenatal and early neonatal life such as in preterm birth [9, 92, 178] or prenatal alcohol exposure [112, 144], cause a disruption in normal SNS signaling and can impact overall autonomic health later in life [35, 92, 96, 165]. Therefore, this early developmental time likely represents a critical period for the establishment of a stable setpoint for sympathetic tone [29]. In summary, understanding the mechanisms which govern the SNS circuit during early development in the context of homeostatic plasticity and critical periods has widespread clinical relevance.

For my thesis project, I examined two components of the sympathetic nervous system, the sympathetic preganglionic neurons (SPNs) as well as the postganglionic neurons (PGNs). I tested the possibility that these cells express homeostatic plasticity during embryonic development, a time when the SNS circuit is constructed and when homeostatic plasticity is known to be robustly expressed. To explore whether these cells express homeostatic plasticity during embryonic development, my studies were focused on the embryonic chick model system. In this introductory chapter, I will discuss the background literature that motivated this study. In the following two chapters, I will present the experimental methodology that was used to test my hypotheses, I will report my results, and I will interpret my findings for each of the experiments. In Chapter 2, I tested the hypothesis that homeostatic plasticity is expressed in the spinal and peripheral neurons of the SNS in the developing chick embryo. To this end, I conducted a pharmacological blockade of synaptic transmission *in ovo* in the chick embryo in an attempt to induce a homeostatic cellular response. To examine whether synaptic blockade induced changes that are indicative of homeostatic plasticity, I examined neurons in the SNS using both ex vivo fluorescence imaging and electrophysiological recordings. Ultimately, my findings demonstrated that a chloride-mediated mechanism of synaptic scaling is expressed in the SPNs in

response to synaptic blockade. However, in the PGNs, a paradoxical decrease in intrinsic excitability of the membrane was observed. These results are interpreted and discussed at the end of Chapter 2. In Chapter 3, I studied an increase in muscarinic activation in the PGNs, which could represent a homeostatic response. Finally, in Chapter 4, I explain the conclusions that can be inferred from the data presented and place these findings in the context of the surrounding health and basic science literature. Finally, at the end of Chapter 4, I propose future directions which should be conducted to further identify the role of homeostatic plasticity in the developing SNS.

1.2 Characterization of the sympathetic preganglionic neurons

In the spinal cord, SPNs receive descending synaptic input from autonomic nuclei in the brainstem and hypothalamus [54]. The circuitry which provides the input to the SPNs is part of a larger circuit which coordinates the function of the SNS and extends from the cortex all the way to the peripheral tissues (Figure 1.1). In the cortex, brain regions such as the prefrontal cortex (PFC), the insular cortex, and the anterior cingulate cortex (ACC) are responsible for integrating information and sending their output to the amygdala in the temporal lobe, often referred to as the "emotional center of the brain" due to its prominent role in fear learning and aggression. From the amygdala [222] as well as from the subfornical organ [10, 114], projections extend to the hypothalamus to innervate both the dorsomedial hypothalamus (DMH) and the paraventricular nucleus (PVN), two hypothalamic subregions which act as centers for sympathetic signaling (Figure 1.1). Next, the PVN sends output to the brainstem nuclei which include the rostral ventrolateral medulla (RVLM), the caudal ventrolateral medulla (CVLM) and the nucleus tractus solitarius (NTS). Finally, the RVLM

descending projections form synapses onto the SPNs in the IML of the spinal cord (mammals) or the Column of Terni (avian species) [192]. The PVN can also form direct innervation onto SPNs as well, bypassing the brainstem nuclei [200]. Finally, SPNs, also called 'autonomic motoneurons', extend their axonal projections out of the ventral root of the spinal cord, where they gather into collection of myelinated axons which are known as the 'white rami', and subsequently form cholinergic synapses onto their target neurons in the autonomic ganglia, a unique population of neurons which will be discussed in the next section.

In avian species, there are a few notable differences in the spinal cord SNS organization when compared to the spinal cord of mammals. For example, the chicken has seven segments which make up the thoracic region, while mammals typically have twelve (primates) or thirteen (rodents). In the chick, the lumbar and sacral segments are referred to as a single group known as the lumbo-sacral (LS) segments, which will be the focus of our studies. In addition to the differences in segment delineation, the spinal column in which the SPNs are organized differs between murine and avian species (see Figure 1.2). In rodents, the majority of SPNs coalesce in the intermediolateral (IML) nucleus, in the lateral most part of the grey matter of the spinal cord at vertebrae levels T1 through L3 [214], though some SPNs are in more medial positions [54]. On the other hand, the SPNs in the chick spinal cord has a more central location, close to the central canal [133, 139, 186, 261] (Figure 1.2). This cell column has been deemed the Column of Terni [225], and it spans from the C16 segment to the LS 2 segment. *For this thesis, discussion of the SNS will be in the context of the avian system, as the embryonic chick will serve as the model system.*

Interestingly, although the SPNs are often referred to as a single, homogeneous group of neurons, there are numerous accounts of a transcriptionally heterogenous population of many subtypes of neurons within preganglionic clusters [6, 19]. The diversity of SPN subtypes is thought to represent different functionalities, as certain

Figure 1.1: The major components of the SNS circuit

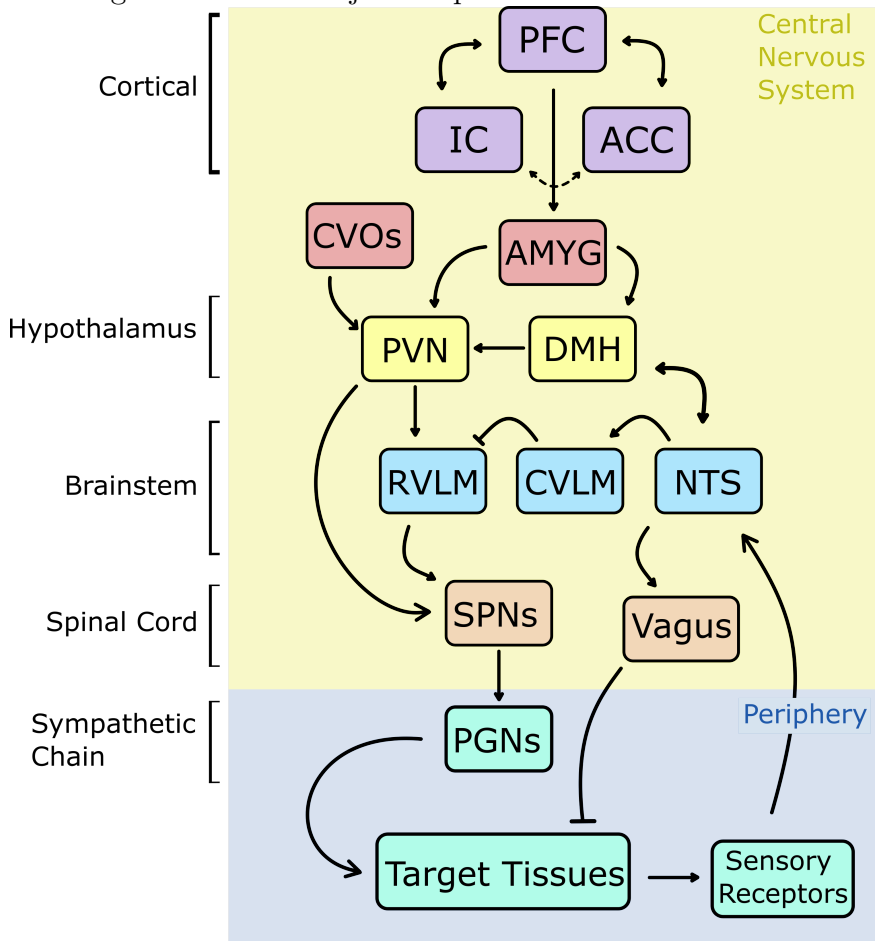

Non-exhaustive circuit which controls, influences, or provides input to the sympathetic nervous system. In particular, the prefrontal cortex (PFC) interacts with the anterior cingulate cortex (ACC) and insular cortex (IC) to send output to the amygdala (AMYG). From here, the dorsomedial hypothalamus (DMH) as well as the paraventricular nucleus (PVN) of the hypothalamus receive excitatory input. The PVN also receives peptidergic input from other circumventricular organs (CVOs), which famously include the subfornical organ and the pineal gland (not pictured here). The PVN integrates this incoming information and sends descending projections to the rostral ventrolateral medulla (RVLM) in the brainstem, as well as direct projections to the sympathetic preganglionic neurons (SPNs) in the spinal cord. The SPNs send projections out of the spinal cord and into the periphery, forming synapses onto postganglionic neurons (PGNs) in the sympathetic chain. From here, the PGNs send their output to their target tissues, blood vessels, or glands. Notably, the activity from these output organs or target tissues, can be sensed by sensory receptors and this ascending information to the nucleus tractus solitarius (NTS) of the brainstem, forming a negative feedback loop. The NTS is the primary visceral sensory organ of the medulla, and its output has been shown to influence both the caudal ventrolateral medullary (CVLM) reticular formation which sends inhibitory input back to the RVLM. The NTS also can directly influence the Vagus nerve of the parasympathetic nervous system, which in turn acts to reduce the tone of certain target tissues.

Figure 1.2: The SPNs of avian species are more medial than that of rodents

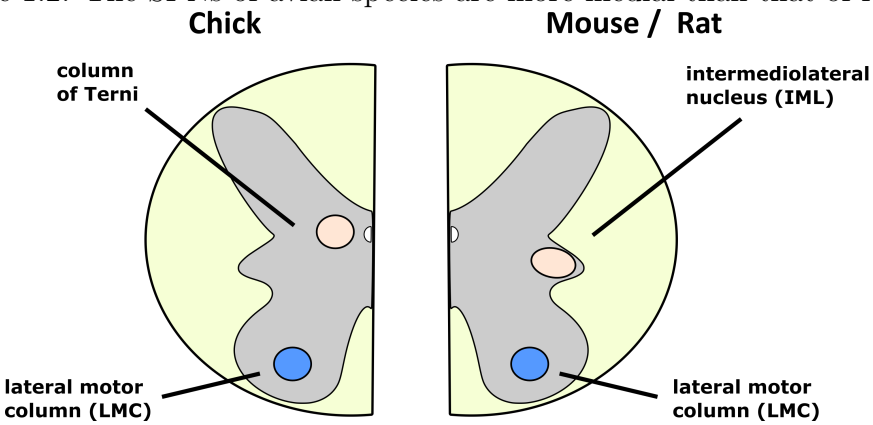

An illustrative comparison of anatomical location of sympathetic preganglionic neuron (SPN) between animal classes. Schematic of axial slice of spinal cord demonstrates that the SPNs of avian species have a more medial location than the majority of SPNs in rodents.

subtypes may express protein profiles that are specific to the type of function which they encode. For example, the population of SPNs which are immune-positive for the label CART, are the same SPNs whose targets ultimately innervate the cardiac circuit [81]. Further, subtypes of SPNs have been delineated based on their membrane properties [270], their activity patterns [76] and their responses to various pharmacological agents [77]. While the exact mapping of subtype to function is not completely understood, it is abundantly clear that SPNs can encode vastly different inputs and signals and are therefore differentiable from other SPN cellular clusters based on these biomarkers and patterns of activation. The heterogeneity of SPNs in the spinal cord suggests that there could be numerous subtypes in this cellular population, or possibly even a vast continuum of various cell properties. Either of which would allow the SPNs to be precisely tuned to their unique inputs. In the present study, we acknowledge our limitation in ability to separate analysis of SPNs based on subtype and are instead examining the SPNs as one single group. That said, in the present study, the values recorded from the SPNs have resulted in normal distributions rather than multimodal distributions, suggesting that we may not have captured several clearly distinct subpopulations (see Chapter 2). Thus, treating the SPNs as a single group

is a reasonable first approach for these data. Over the past several decades, SPNs have been examined using numerous techniques to elucidate their connectivity and neurochemistry. To start, information regarding the various neurotransmitter inputs to the SPNs have been explored, and are known to contain the main excitatory (Glutamate) [76] and inhibitory (GABA) receptors [266], and are also sensitive to several other modulators including 5-HT [150, 184], noradrenaline [70, 264], dopamine [77], and peptides [19]. It is crucial to note that in the embryonic system, GABA transmission is depolarizing due to the nature of chloride gradients which express higher intracellular chloride levels in immature circuits [13, 14, 180], and this phenomenon will be discussed in detail later in this chapter. In addition to the chemical messengers which can provide input to the SPNs, gap junctions are also thought to play a prominent role in the signaling that occurs between SPNs. Gap junctions are intercellular channels that form bridges between adjacent cell membranes, permitting transfer of ions and other small molecules [87]. The presence of gap junctions in the SPNs is evidenced by the analysis of immunoreactivity to connexin36, a gap junction channel protein important for the formation of these gap junctions [151]. This form of ion transmission is thought to be important for orchestrating cation conductances which drive the tonic, rhythmic activity seen in the SPNs [150, 184].

Next, the pattern of projection and anatomical connectivity have been extensively studied. While it is obvious that the SPNs project out of the spinal cord and into the periphery via the ventral root, the exact organization of projection and neural specification is still not fully understood [66]. During the mid 20th century, the projection pattern and the number of synaptic targets that are made by SPNs were heavily studied to illuminate some part of this question. In the mid 1980's researchers were invested in determining the projection pattern of the SPNs. Bennett et al [15] used retrograde labeling with horseradish peroxidase to determine that in dogs and cats, each white ramus is innervated only by the segments immediately surrounding

the labeled ramus. This shows that SPNs project out of the spinal cord either from the same segment as their somas, or a segment that is immediately adjacent to their somas. Around the same time, Yip [259] also ventured to determine the segmental specificity of ganglionic innervation in the embryonic chick. In this case, the observations were made using both electrical recordings as well as retrograde labeling directly from the ganglion itself, rather than from the white rami. In this case, it was shown that the cells in each ganglia are innervated by a characteristic set of SPNs which are located in a contiguous span of segments that are typically 0-4 segments away from that cell's ganglia [259]. To further clarify the stereotyped projection patterns of the SPNs in the chick embryo, a considerable number of studies determined that a single SPN could extend its projections rostrally, caudally, or both, after reaching the paravertebral chain . To this end, researchers examined individual segments of ventral root, to determine the segments at which preganglionic projections travel in a rostral direction, and those which travel in caudal fashion [55, 259]. At segment T1 and above, SPN axons primarily project upwards to the more rostral ganglia [259, 262]. In segments T5 to LS1, however, the SPN projections travel primarily in a caudal direction [68, 259, 262]. Alternatively, between said segments, it appears that the SPNs project either rostrally or caudally to form cholinergic synapses onto PGNs [68, 260, 263]. Further studies from the Yip group were directed at determining the mechanism that governs the projection pattern of SPNs to their targets. To answer this, experimenters surgically removed the neural crest tissue which contains the precursors for the target cells (PGNs) and observed how the preganglionic projections developed [260]. In this case, the SPNs showed similar axon pathfinding trajectories to reach their target ganglia, even though the target cells in the ganglia had never developed. In other words, whatever neurochemical signal that dictated the pre- to post-ganglionic projection pattern was clearly not dependent on the target PGNs. The Yip group then shifted their studies to the SPNs themselves. Could it be that

the fate of the SPNs was determined locally, in the spinal cord? If so, when, and how did this occur? To answer these questions, Yip [261] transplanted spinal cord tissue which contained SPNs from one of two donor sources 1) SPNs from different spinal segments, or 2) SPNs from spinal cords of embryos at older ages. Through this method, Yip determined that both the timing and projection pattern of the SPNs are, in fact, driven by the local environment of the spinal cord [261]. Altogether, these studies confirmed that cues within the spinal cord are necessary for the organization of the SPN projections, regardless of cues from the periphery.

1.3 Characterization of the sympathetic postganglionic neurons

The PGNs are a heterogenous [65, 66] densely packed population of small cells located in the sympathetic paravertebral ganglia, which extends bilaterally alongside the spinal cord (Figure 1.3). These cells receive input from one primary source: cholinergic projections from the SPNs which travel through the ventral root, along white rami, and into the ganglia. While the vast majority of input is cholinergic, some early studies have suggested non-cholinergic activation in some peripheral neurons in the SNS [60, 59, 108]. The PGNs express two modalities of acetylcholine receptors which are activated by the release and subsequent binding of acetylcholine: the fast-responding, ionotropic nicotinic acetylcholine receptors and the g-protein coupled metabotropic muscarinic acetylcholine receptors, which have much longer latency for activation and subsequent dissociation (for a review, see [123]). When the endogenous ligand, acetylcholine, is released from the presynaptic terminal, it enters the synaptic cleft and binds to the orthosteric binding sites on the acetylcholine receptors on the postsynaptic cell membrane.

Another fascinating mechanism of these receptors is that, in some cases, they are

Figure 1.3: The SPNs send information from central nervous system to the PGNs in periphery

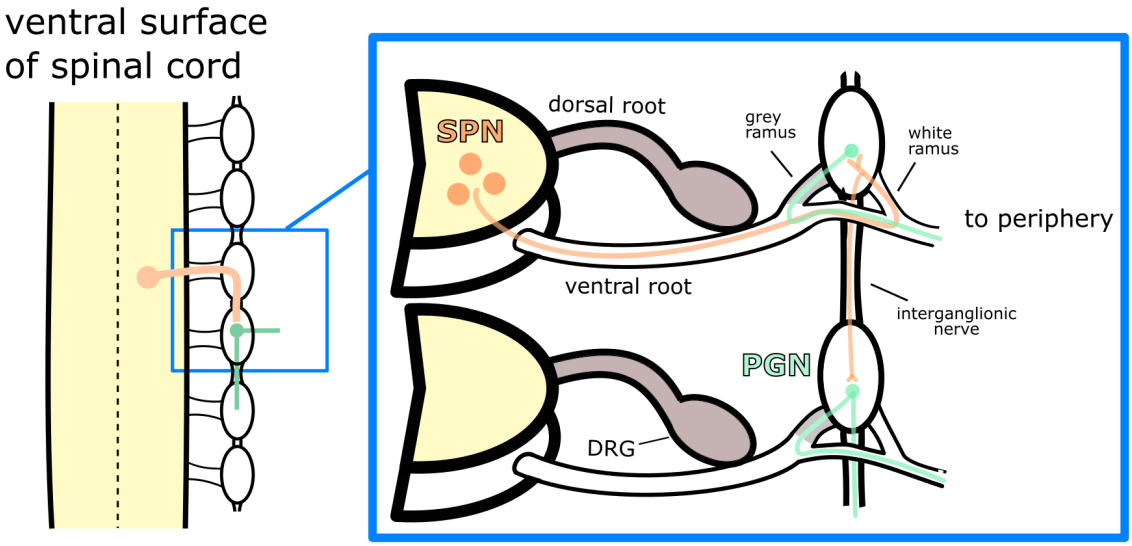

Schematic of the ventral surface of the spinal cord demonstrates that sympathetic preganglionic neurons (SPNS, orange) are located in the spinal cord. These neurons project out of the ventral root, can either project upward or downward (downward pictured here) to a neighboring ganglia, or form a bundle of fibers known as the white rami, which form synapses with the sympathetic postganglionic neurons (PGNs, green) which are located in the sympathetic ganglia of the paravertebral chain, also referred to as the sympathetic chain. The PGNs send their output via the grey rami and extend these projections to their target tissue, although they can also form projections through the interganglionic nerve (IGN) to a neighboring ganglia, as seen here. DRG: dorsal root ganglion.

expressed on presynaptic terminals, and their activation has an effect on presynaptic vesicle release [39, 156]. Although this is thought to be less common in synapses of the peripheral nervous system [105, 271], the expression of presynaptic acetylcholine receptors has even been observed in target tissue, at the terminals of the postganglionic projections [251]. While the expression of presynaptic nicotinic receptors has not been fully explored in the SPN-PGN synapse in the embryonic chick, it does not alter the overall effect of the application of ganglionic blockade, which is to reduce nicotinic neurotransmission. I will discuss each of these two forms of acetylcholine neurotransmitter receptor in the following sections.

1.4 Nicotinic acetylcholine receptor neurotransmission

The binding of acetylcholine to the nicotinic receptor causes a confirmational change which results in the opening of the ion channel. This channel opening causes depolarization of the cell membrane via conductance of cations including potassium (K^+) and sodium (Na^+). In some cases, calcium (Ca^{2+}) enters through direct permeation or indirectly through voltage-dependent influx. For a review, see [189, 207]. The nicotinic acetylcholine receptors contain the typical, orthosteric binding sites that acetylcholine binds to [271], as well as allosteric binding sites in the spaces between certain subunits at which various modulators can bind [31].

The synaptic neurotransmission of acetylcholine in the ganglion takes effect within a few milliseconds due to the fast ionotropic action of nicotinic receptors, however the effect of the acetylcholine on the postsynaptic cell membrane is fleeting due to the rapid dissociation from the receptor and subsequent enzymatic degradation of the neurotransmitter which occurs in the synapse shortly after the release [105]. The enzyme which catalyzes this process is called acetylcholinesterase, and it acts in the cleft to hydrolyze acetylcholine into acetate and choline [155]. The event of ligand dissociation from the receptor and subsequent degradation occurs rapidly [105], though the rate has been shown to vary between subtypes of the receptor. The rate of this process is highly important, especially in muscle type nicotinic receptors, as it allows for abrupt cessation of ionic signaling, and the receptors are therefore able to prepare to respond again should additional acetylcholine enter the cleft. This process of ligand dissociation and receptor reactivation, however, is made slightly more complicated by the fact that receptors can be in numerous configurations. For example, in addition to receptors being unbound, closed and therefore non-conducting, there is the equally obvious configuration of being ligand-bound and therefore open. There are also states

where the agonist is bound to the receptor, but the receptor is in a non-conducting state, known as the "desensitized", or otherwise inactivated state [105]. The speed of receptor desensitization is known to occur at different latencies across the various subtype compositions [31]. In fact, the different subtype cominations and specific stoichiometry of nicotinic receptors vary greatly in their pattern of expression in the nervous system, affinity for ligand binding [153], kinetics and probability of channel opening, patterns of up- or down-regulation [153, 204, 269, 271] as well as their specific ion permeability [189]. I will briefly discuss some of the notable subtypes and their properties.

The nicotinic receptors are a pentameric composition of subunits including α subunits numbered 2-9 and β subunits numbered 2-4 [271]. These subunits can be expressed in a homomeric or heteromeric fashion. Homomeric subunit expression refers to those receptors which express 5 of the same subunit, such as the $\alpha 7$ subtype [39]. Heteromeric subunit expression, on the other hand, describes a receptor that expresses two or more different subunit species, such as the $\alpha 3\beta 4$ subtype. The $\alpha 3\beta 4$ subtype is expressed at the highest rates in the peripheral autonomic ganglia and is therefore often deemed that "ganglionic subtype". It is important to note, however, that there is plenty of overlap. In fact, there is significant evidence to suggest that the $\alpha 7$ subtype is also expressed in the autonomic ganglia, as autoradiography examination of mRNA in rat ganglia suggests [197]. Another study that demonstrated that $\alpha 7$ subunits were expressed in the sympathetic ganglia was shown through the binding of α-bungarotoxin [88], as $\alpha 7$ are among the subtypes that are sensitive to α-bungarotoxin, but $\alpha 3\beta 4$ are not [271]. Moreover, the precise stoichiometry of the $\alpha 3\beta 4$ receptor subtype can vary, such that the fifth accessory subunit can be either of the two subunits. For example $(\alpha 3)3(\beta 2)2$ and $(\alpha 3)2(\beta 2)3$ subtype stoichiometries are differentially expressed in separate contexts [121], and with varying affinities for various ligands [89, 105]. Nonetheless, the $\alpha 3\beta 4$ subtype (considering both sto-

ichiometries) will hereafter be referred to in this thesis as the 'ganglionic nicotinic receptors' for simplicity, though it should be noted that there is non-negligible overlap in subtype expression between muscle, brain, and autonomic systems.

The ganglionic nicotinic receptors can be targeted pharmacologically using endogenous ligands, pharmacologically synthesized agonists and antagonists, or any number of allosteric ("non-competitive") modulators. The approach of using drugs known as "ganglionic blockers" is supposed to limit the impact of other receptor subtypes, such as those at the neuromuscular junction (NMJ). However, as with most pharmacology, there is considerable overlap which cannot be ignored [58]. Among the long list of drugs which act at the PGNs is a non-competitive antagonist, or "negative allosteric modulator" [31] of the ganglionic-type receptor known as Hexamethonium (Hex). This ganglionic drug was at one time prescribed to treat hypertension [26] but has been discontinued due to its lack of specificity and adverse side effects. Despite its clinical discontinuation, Hex has proven to be incredibly useful for research purposes [118, 122, 131, 220], and was used in this thesis project to induce reduction of synaptic transmission in the PGNs. This blockade occurs when Hex binds to the nicotinic acetylcholine receptor at an allosteric site [3, 131]. The mechanism by which this binding causes a dramatic reduction in the permeability to sodium (Na^+) and potassium (K^+) ions) is not entirely understood [131]. Some propose that it binds in a non-competitive site and therefore reduces the affinity for acetylcholine itself, thus preventing the channel from opening [131]. In some cases, the binding of Hex actually blocks the ion pore itself [8], and this has been shown for other allosteric modulators [31] and other methonium groups [90]. Hex has also been found to have an ion channel blocking effect at the endplate [3]. In addition to using Hex for ganglionic blockade, studies have shown that d-tubocurare (dTC) has an even more widespread antagonistic function on the ganglionic nicotinic receptors [59, 179], which we have found to further reduce ganglionic synaptic transmission in some cases where Hex

was introduced beforehand. The cholinergic synaptic neurotransmission experienced at the ganglionic nicotinic synapse can also be increased using agonists such as nicotine or carbachol, or even acetylcholinesterase inhibitors such as neostigmine, which allows acetylcholine to remain in the synaptic cleft for a longer period.

Interestingly, nicotine receptors show robust neuroplasticity, yet prior studies are conflicting on the types of plasticity that are expressed. In the literature, evidence of exhibiting both upregulation and downregulation in response to increased activation of the nicotinic receptor can be found. Exposure to nicotine and other nicotinic agonists can upregulate the expression of certain subtypes of nicotinic receptors [271]. Another study showed that while acute nicotine exposure was associated with increases in nicotine receptor accumulation, at higher doses, however, researchers saw down regulation, particularly in subtypes expressing the $\alpha 5$ subunit [269]. In fact, nicotine exposure in cell cultures can cause both up- and down-regulation, and this process differs basesd on the dose of nicotine, the duration of treatment, and the subtype of receptor [115].

Again, these studies show that the nicotinic acetylcholine receptors are highly plastic, yet the expression of distinct cellular regulatory mechanisms is decidedly dependent on receptor subtype and subunit stoichiometry [204]. These studies provide evidence for the robust expression of nicotinic receptor activity-dependent plasticity in numerous model systems, suggesting that in the present study we may observe similar responses after synaptic blockade of nicotinic receptors in the PGNs of the embryonic chick.

Table 1.1: Common pharmacological tools for studying preganglionic and postganglionic neurons of the SNS (* indicates that this drug was utilized in the present studies)

Drug name	**Target and specificity**	**Mechanism of action**
αbungarotoxin	α7 Nicotinic ACh receptor	Competetive antagonist
Atropine*	Muscarinic ACh (non-specific)	Competetive antagonist
dTC*	Nicotinic ACh (non-specific)	Competetive antagonist
Gabazine*	$GABA_A$ receptor	Allosteric inhibitor (non-comepetive antagonist)
Hexamethonium*	$\alpha 3\beta 4$ Nicotinic ACh	Allosteric negative modulator (non-competitive antagonist)
Lidocaine	voltage-gated Na+ channels	Ion channel blocker
Neostigmine	acetylcholine-esterase	acetylcholine-esterase competetive inhibitor

1.5 Muscarinic acetylcholine receptor neurotransmission

In addition to the ionotropic nicotinic acetylcholine receptors, the ganglionic neurons also have muscarinic acetylcholine receptors, which are metabotropic g-protein coupled receptors that are activated by acetylcholine on a slower time scale than the nicotinic receptors [23]. There are 5 known subtypes of muscarinic receptors, and the M1, M2, and M4 subtypes are associated with autonomic ganglionic function [23]. Neurotransmission in these muscarinic receptors can be blocked or facilitated with countless pharmacological agents. The list of antagonists which block this receptor is very long. Notably, this list includes toxins from venomous snakes [88, 267] as well as atropine [60], which was used in this project to examine muscarinic transmission. This neurotransmission can also be increased using agonists of the muscarinic receptor, including a chemical called muscarine, the namesake of the receptor. Muscarine is a molecule that can either be derived from Amanita muscaria mushrooms [27] or synthesized chemically, and mimics the effect of acetylcholine. However, muscarine has been described as more potent than acetylcholine because muscarine lacks the type of enzymatic hydrolysis that occurs in transmission of acetylcholine [155]. With either antagonists or agonists, the effects caused by these drugs which act on the muscarinic receptor are not perfectly specific to the ganglion. Several key pharmacological agents are described in Table 1.1.

1.6 The lumbosacral segments of the sympathetic nervous system

The postganglionic axons exit the paravertebral chain using several pathways. The first is the most typical, which is by exiting the ganglia through the grey rami, and traveling along the spinal nerves. The second is through the sympathetic nerves such as the cephalic periarterial nerves or splanchnic nerves, in the case of some visceral organs such as the heart. The third is to project toward a neighboring ganglion via the interganglionic nerve (IGN, see Figure 2.1-2.2) [102, 213]. The different synaptic targets of the PGNs depend on the region of the spinal cord from which the cells project. As such, the sympathetic chain is roughly organized by function in a rostral-caudal fashion. While this is a simplification of a more complicated system, the upper thoracic and cervical ganglia innervate organs in the upper body such as the heart and the lungs, while the lower lumbar and sacral regions innervate the organs in the pelvic region such as the bladder [229]. Importantly, you can find PGNs all along the length of the paravertebral chain which innervate the vasculature that is associated with the tissues of that region. In the periphery, PGNs project out of the paravertebral chain to form synapses onto their target tissues, organs, or glands, and these synapses are typically adrenergic, though some cholinergic transmission is present as well [230]. In many studies, PGNs from cervical and upper thoracic segments of the spinal cord have been examined, such as the superior cervical ganglia [49] or stellate ganglia [47] as they are easily accessible and have effects on heart hemodynamics [141].

The lumbosacral segments, however, are the focus of this study for several reasons. First, there is a wealth of knowledge about the somatic motoneurons in the lumbosacral regions such that circuit development and mechanisms of homeostatic plasticity are well-understood in the lumbosacral spinal cord of the embryonic chick [246, 247]. The lumbosacral region also provides an ideal readout of spinal activity

in the intact system, as both somatic motoneurons and SPNs (see Chapter 2) in the lumbosacral region are active during spontaneous movements of the lower limbs in the chick embryo [128, 172, 171, 249, 250]. Therefore, we can take advantage of the fact that the patterns of spontaneous activity in this lumbosacral region can be readily observed. Another benefit of studying the lower thoracic and rostral lumbar region of autonomic motoneurons is that the outflow is distinctly sympathetic [66], thus eliminating the accidental stimulation of parasympathetic axons during recordings, which would make the results more difficult to interpret. Finally, the ganglionic chain in this region is dominated by caudally-projecting preganglionic axons which allow for straightforward, orthodromic stimulation without the additional confounds from regions which include both rostral and caudal projecting fibers [259].

The caudal thoracic and upper lumbosacral PGNs project to the tissues and the majority of the visceral organs in the lower abdomen and pelvis. Among these tissues innervated by this region are the large intestine, kidney, pancreas, gonads, and bladder. Additionally, blood vessels (with the exception of capillaries), sudomotor tissues (sweat glands) of the lower body are innervated by the lower thoracic and upper lumbar sympathetic neruons. A unique exception is the adrenal gland, in which the chromaffin cells are innervated directly by preganglionic fibers [66, 229].

1.7 Synaptic transmission at the SPN - PGN synapse

The monosynaptic connection between SPNs and PGNs is a seemingly crucial junction for establishing a proper input and output relationship between the central and peripheral arms of the SNS as this is the last step for sympathetic instructions coming from the CNS and entering the periphery. In the SPNs, descending information from upstream centers of the ANS including brainstem and hypothalamus are integrated with input from interneurons and sensory afferents [53], before sending instructions

out of the ventral root and to the PGNs in the paravertebral ganglia. Therefore, this synapse is the final step for the modulation of signal from the CNS, before it determines the final sympathetic output onto the target tissues. The transmission from SPN to PGN was not always considered to be highly malleable, however. Many researchers have demonstrated that orthodromic stimulation of the preganglionic projections will produce action potentials, followed by a fast, nicotinic EPSP in the postganglionic neurons [60, 61, 107], as well as a slower, muscarinic potential [107, 108]. This activity forms the basis of neurotransmission from the central arm to the peripheral arm of the SNS. Still, the mechanisms which govern the monitoring and regulation of this neurotransmission are not well understood. In the past, the PGNs have been considered to be a passive relay from the CNS [158], without integration or computation. However, recent studies using more precise electrophysiological recordings and neuron modeling have demonstrated that PGNs are capable of synaptic summation, repetitive firing, and have much higher estimations of cellular excitability [103, 124, 157, 212, 248], compared to studies that used sharp, impaling microelectrodes. Therefore, the PGNs can considerably amplify the signal they receive from the CNS and enhance the sympathetic outflow before it reaches the target tissue. Already, there is considerable signal amplification from the CNS simply due to the anatomical structure of the circuit. For instance, while the ratio of pre-to-post ganglionic transmission was once thought to be approximately 1:4 preganglionic axons to postganglionic cells [22], this number has more recently been assessed to be dramatically different, with estimates of the ratio of preganglionic to postganglionic being around 1:200 [53, 111]. This demonstrates how sympathetic signals from the CNS can be highly amplified and widely dispersed on their path to the periphery simply based on the circuit innervation. Further, there is strong evidence which suggests that cellular mechanisms including synaptic plasticity also contribute to the signal gain [103, 124, 248]. These mechanisms demonstrate that the signal from the

CNS can be amplified in PGNs at a single-cell level, in addition to being widely distributed due to the ratio of pre-to-post innervation. Taken together, the clear evidence of signal amplification provides important background for understanding the signal transduction of the SPN-PGN synapse and suggests the need for a tightly controlled regulation of output at the PGN, such that hyperactivity does not occur in the periphery. It is unclear, however, whether there are cellular mechanisms of synaptic regulation, adjustments of input/output relationship, which are capable of homeostatically regulating this transmission at this synapse.

Taken together, the prior literature on the anatomical circuitry and, more recently, the electrical signaling reveals that there is obvious magnification of neural signal as it travels through the central-to-peripheral synapses of the SNS. Thus, this synapse could be a crucial component of the SNS at which homeostatic mechanisms are expressed to tune and regulate the input/output relationship. As such, the baseline ought to be properly established at a biologically relevant point. It may be that mechanisms of homeostatic plasticity play a crucial role in the early establishment of this baseline input/output at this autonomic synapse during early stages of circuit development. The SPNs and PGNs, however, have been largely ignored in the field of homeostatic plasticity, as the explosion of anatomical studies of the SNS in the mid to late 20^{th} century occurred decades prior to our current understanding of homeostatic plasticity. That said, there exists a prominent gap in knowledge in the literature surrounding the SNS and the field of homeostatic plasticity. Moreover, there is a clear translational importance to this question, as there are obvious instances which demonstrate the negative outcomes that can occur when biological regulation of SNS output is not performing optimally. A prevalent example of autonomic dysregulation is seen in the case of hypertension.

1.8 Disease and disorder in the autonomic nervous system

Hypertension is a disease of the autonomic nervous system in which sympathetic tone is aberrantly and chronically elevated. This disease is among the top 20 leading causes of death (CDC, 2021) and affects a huge portion of the human population. Studies funded by the World Health Organization (WHO) report over 1.2 billion cases estimated in 2019 [268]. Estimates from this same study suggest that this number has nearly doubled since 1999. In the United States, roughly 29% of adult population were estimated to have hypertension in 2016. Of these, only 48% have it under control with medical treatment [71], while 8.9% of adults with hypertension meet the criteria for treatment resistant hypertension [182]. Further, hypertension prevalence varies across socioeconomic status and race [210] (CDC, 2021). Stage 1 hypertensive disease is characterized by a blood pressure level that is above 130/80 mmHG, CDC website) and stage 2 hypertension is defined as 140/90 mmHg [71]. This elevation in blood pressure level over long periods of time can prevent the SNS from being responsive to incoming signals. Moreover, a chronically high vascular tone can cause damage to blood vessels and tissues and is associated with heart disease and even premature death. Such complications include end organ tissue damage and blood vessel deterioration, particularly in the kidneys. Even among children, rates of hypertension were as high as 4% globally [211]. The prevalence of hypertension underlines the importance of understanding the mechanisms which can regulate autonomic output. Furthermore, while some of these autonomic diseases develop progressively over years due to lifestyle or living conditions, it is also well known that some predispositions are present at birth and risk factors associated with hypertension include early life disturbances in ANS signaling, as discussed below. In fact, issues with autonomic health can be present in adults, who experienced certain early life events known to

disrupt ANS signaling. As such, early life vulnerability to autonomic disorder (discussed below) states the need to understand how autonomic setpoints are defined during early development.

There is evidence to suggest that perturbations which occur during early neonatal and even prenatal periods can result in disrupted autonomic functioning. For example, there are many complications that can occur with preterm births and low-weight births. This is a form of autonomic interruption and is well known to complicate ANS development in neonates [48, 164]. Measures of cardiac control are significantly altered in these infants for the duration of the study, from newborn stage and all the way up to term-equivalent age [178], demonstrating that preterm birth results in robust autonomic disturbance. Prenatal exposure to alcohol [112] is also associated with alterations in basal sympathetic tone or signaling. Among these alterations is a change in heart rate variability (HRV), which is a measure of the changes in RR intervals, which is the time elapsed between two successive "R" waves of the QRS signal on an electrocardiogram. This is an excellent measure of autonomic tone [37, 48, 112], and therefore demonstrates the impact of a prenatal disruption to postnatal autonomic functioning. In addition, elevations in basal heart rate have been measured in neonates who experienced prenatal alcohol exposure [154]. Clearly, each of these different early life perturbations can induce immediate challenges to the neonatal nervous system. These challenges can range from mild tachycardia (elevated heart rate) to more intense complications and in severe cases, these complications can be fatal. In infants who survive these acute complications, an important question in the field is: what are the effects later in life? Evidence of long-lasting changes in autonomic health associated with these early life challenges would support the theory that the window surrounding prenatal and early neonatal development is a critical period for the establishment of healthy, tonic output from the SNS.

Above, I have discussed the impact of early life complications on measures of au-

tonomic functioning shortly thereafter. Further, going beyond the first few months of development, individuals who experienced autonomic disruptions early in life may have negative health consequences years later, and even in adulthood. For example, individuals who had very low birth weight had significantly higher blood pressure measures at 20 years of age, compared to those born at a typical weight, and for females, this was true even when controlled for the effects of later body size [92]. This lab group also discovered that young adults who were born weighing less than 1500g had higher rates of neurosensory impairments and lower rates of educational success even when adjusted for socioeconomic status and sex [91]. Low birth weight has also been associated with organ health consequences up to 20 years later [166]. In a fascinating two-cohort study, another group demonstrated that in infants with higher numbers of complications associated with premature births (such as needing ventilation, neonatal sepsis, etc), these numbers were more strongly predictive of later autonomic health, compared to the predictive value of the gestational age at birth [202]. This suggests that, in fact, the actual stressors to the ANS prior to and immediately following birth are associated with long term health outcomes. In another study, researchers determined that prenatal alcohol exposure (PAE) could result in higher rates of symptoms of attention-deficit hyperactivity disorder at the 5-year mark [63]. This outcome could be the result of the impact of PAE on the ANS during this early period. In fact, children with ADHD show specific alterations in HRV which suggest "sympathetic dominance" of cardiac rhythm [196], and perturbed resting HRV has been linked with cognitive measures during tasks which test attention and accuracy [252] in adults with and without ADHD diagnoses. The common link between these studies suggests that ADHD is associated with changes in autonomic tone which could be prompted by early life disturbances in autonomic signaling, but any causal relationship or early life risk factors have yet to be confirmed. Finally, ANS disruptions during this early period are associated with higher rates of neuropsychiatric disorders

throughout adulthood [165], perhaps because these perturbations affect one's ability to regulate their SNS once it is engaged. In fact, this poor SNS regulation is shown at the physiological level in young adults during exercise, as the subjects who were born pre-term had a lower VO_2 max and slower heart rate [96]. Could it be that prenatal and neonatal disruptions to the ANS lead to chronic elevations in sympathetic tone? If the early establishment of autonomic setpoint coincided with this kind of disruption during a critical period, it would stand to reason that the SNS could therefore be programmed to maintain its output at a heightened level. Perhaps, long term autonomic dysregulation occurs when the baseline is set at a higher level, and after the window of plasticity has closed, the system now maintains this level. An estimated 8-20% of patients treated for hypertension have what is known as "resistant hypertension" [182], which means blood pressure is not controlled even after taking multiple medications, and about 5% of that population has an even more severe version of this, called "refractory hypertension" [208]. This suggests that in extreme cases, the adult SNS is chronically maintaining a dangerously high baseline, even with several medications, as though it were programmed to maintain a high output. Together, these data support the notion that the SNS is governed by a critical period that is expressed very early in development [29] during which the "thermostat" for sympathetic output is set. If this is the case, an important next step would be to examine the mechanisms which underly this critical period. Typically, critical periods are characterized by the expression of a window of plasticity which tunes excitability of the circuit. Still, it is unclear whether plasticity mechanisms are expressed by the SNS circuit during embryonic development, and whether they may contribute to this sensitive period.

There are mechanisms of neuroplasticity that are expressed to tune excitability in many developing circuits during critical periods. Among these are a set of mechanisms known as homeostatic plasticity. Embryonic development is a period in which

there is robust plasticity in spinal networks and is also the stage when SNS circuitry is first becoming connected. Because homeostatic plasticity is known to regulate excitability in other systems during early development, we are interested in determining whether these same mechanisms could contribute to a critical period in the SNS. It is unknown, however, whether mechanisms of homeostatic plasticity are even expressed in these neurons. Therefore, an important first step would be to test these mechanisms in the SNS of the embryonic system. In this project, I examined both spinal (SPNs) and peripheral (PGNs) cell populations which comprise an important connection from central nervous system to the periphery, to examine whether mechanisms of homeostatic plasticity are expressed in one, both, or none of the cell populations. This will help us to understand the mechanisms that play a role in the maturation of network excitability in the SNS. First, I will describe the background of homeostatic plasticity, which lays the groundwork for our current understanding of these mechanisms.

1.9 Homeostatic plasticity

Homeostatic plasticity provides neural circuits and cells with mechanisms to maintain a stable feature of neural signaling by adjusting intrinsic membrane excitability or neurotransmitter receptor activation, after such a feature is perturbed. This set of mechanisms describes a process by which a neuron can "sense" a disturbance in baseline input and make the necessary regulations to its functioning, to return to a baseline level of output. This is typically engaged in order to maintain some feature of neural activity. The mechanism surrounding this phenomenon was described in the early 1990s, when it was found that a single neuron that was isolated from the lobster stomatogastric ganglion (STG) and plated on a culture dish would eventually regain its distinct rhythmic pattern of activity following a period of quiescence despite

having no synaptic inputs [232]. This observation made it clear that there must be a mechanism by which cells can regulate their own constellations of ionic conductance in response to changes in sensed activity, a long-held theory that was proposed using model neurons a year prior [138]. Such a mechanism of plasticity was considered "homeostatic", as it was expressed as a response to a perturbation and intervened by adjusting the circuit excitability in some fashion, to return some feature of neural activity back to its baseline. Further, additional forms of this homeostatic form of neuroplasticity were described in which synapses could strengthen or weaken as a compensatory response to activity changes [235].

Homeostatic plasticity is sometimes represented as a negative feedback system that is engaged when some feature of neural activity falls outside a certain range, as a way of placing limits on runaway synaptic strengthening which could be driven by the effects of Hebbian forms of plasticity [97]. The understanding of the expression of mechanisms of homeostatic plasticity has evolved throughout the years to include more nuance as we discover new phenomena surrounding this important facet of neural plasticity. Throughout its study, however, its relevance to the overall health of a nervous system has remained in the forefront, as it is well established that dysfunction in homeostatic plasticity has been observed in several disorders of the nervous system including Fragile X syndrome [21, 20, 24, 25], Rett syndrome and altered MecP2 expression [119, 143, 188, 237], autism spectrum disorders that arise from altered expression of Shank3 [40] (a molecule thought to be important for synaptic plasticity mechanisms [223]), and even schizophrenia [56].

Cellular mechanisms which result in homeostatic adjustments may occur through the enactment of several distinct models. For example, a homeostatic response to a perturbation could be engaged by adjusting the excitability of the postsynaptic cell membrane, or by adjusting the strength of synapses within a circuit [50]. Importantly, homeostatic responses can be bidirectional. For example, if the level of input in a

neural circuit is reduced below a setpoint, neurons may increase their responsiveness to incoming signals. Conversely, if the level of activity is increased from baseline, neurons may reduce their responsiveness by weakening their synapses or reducing their excitability [227]. The regulatory mechanisms described under the umbrella of homeostatic plasticity have been explored in many forms, model systems, and contexts since the field of homeostatic plasticity was first established in earnest in the late 20^{th} century. Each of these well-documented mechanisms, as well as other seminal discoveries within the field of homeostatic plasticity are discussed in the following sections.

1.9.1 Synaptic scaling

The first form of homeostatic plasticity which I will discuss is synaptic scaling. Synaptic scaling is defined as the process by which the strengths of synaptic currents between neurons are adjusted either upward (known as upscaling) or downwards (referred to as downscaling) to maintain stability in the overall level of spiking activity or to maintain the magnitude of synaptic neurotransmission in a neural network [193, 231, 235]. Homeostatic compensations in synaptic strength can occur by insertion or removal of neurotransmitter receptors on the postsynaptic cell membrane [117, 175, 235], or even by adjusting the subtype expression of postsynaptic receptors [72, 217]. In either case, the net effect involves maintaining some feature of neural activity by increasing or decreasing the impact of vesicular release that is experienced by the postsynaptic cell membrane. The phenomenon of synaptic scaling is typically measured by a change in quantal amplitude, which is defined as the amplitude of postsynaptic current in response to a single vesicle of transmitter that has been spontaneously released. In other words, synaptic strength can be probed by measuring quantal amplitude in the form of miniature post synaptic currents (mPSCs), essentially the smallest unit of synaptic strength, and comparing this measure between drug-treated conditions and

control conditions to determine the response to synaptic blockade. This phenomenon was demonstrated early on [235] by treating cultured neurons from rat visual cortex with the voltage-gated Na+ channel blocker tetrodotoxin (TTX) to block spiking activity, or bicuculine to block GABAergic transmission and therefore increase activity. In this study, authors observed compensatory changes in the mean amplitude of postsynaptic AMPAergic mPSCs 48 hours later. Other studies have observed similar findings when examining mPSCs [117]. Our group has utilized similar techniques to examine synaptic scaling in the spinal cord of the embryonic chick, and these studies will be discussed in a following section, entitled "Homeostatic plasticity during embryonic development in the chick embryo".

Another fascinating topic in the history of the study of synaptic scaling involves the question of whether the scaling factor applies uniformly across all synapses (i.e., "uniform scaling") or whether it is applied uniquely to different synapses (i.e., "non-uniform scaling"). Researchers at one time considered that synaptic scaling was expressed in a uniform, multiplicative manner, such that the strengthening of synapses was evenly applied to all synapses of a cell. In theory, this multiplicative expression of scaling would maintain the relative differences in synaptic strengths that could have been established by Hebbian forms of plasticity. The expression of synaptic scaling, however, has more recently been understood to be more complex than a simple multiplicative theory [64, 94, 181, 238], and can be expressed in various non-uniform manners [62], with synaptic strengthening being varied between different synapses within the same cell [238]. Another interesting debate in the field involves the trigger for homeostatic plasticity. At one time, scaling was thought to be driven by changes in spiking, but more recently there has been significant evidence that scaling can be triggered in an action-potential independent manner, by changes in neurotransmission (see below).

1.9.2 Presynaptic homeostatic plasticity

A different form of homeostatic synaptic plasticity is called presynaptic homeostatic plasticity, which involves compensatory adjustments in presynaptic vesicle release. These adjustments are enacted through changes in probability of vesicle release, which are measured by changes in quantal content [45, 46, 80]. Quantal content refers to the number of vesicles that are released into the synaptic cleft in response to an action potential. This can be adjusted in a compensatory manner as a response to changing synaptic efficacy. For example, if there is a reduction in functional post synaptic receptors, for example due to partial pharmacological blockade, then presynaptic terminals can increase their probability of release, causing an increase in the number of vesicles per action potential, ultimately compensating for this reduction and resulting in a maintenance of the evoked response. This form of plasticity was discovered early on in the adult mammalian neuromuscular junction [185]. Here, authors determined that despite changes in miniature end plate potentials (MEPPs), the amplitude of evoked end plate potential was stable. Therefore, the authors determined that mathematically, the quantal content, derived from the ratio of end plate potentials to miniature endplate potentials, must have compensated for this change.

The neuromuscular junction (NMJ) provided a useful system to study this mechanism [80], as it is highly accessible and has only one input. The NMJ of the fruit fly, Drosophila melanogaster has been an especially useful model system for examining presynaptic plasticity, as experimenters can rapidly create transgenic models that expressed altered presynaptic and postsynaptic transmission [45, 80, 183]. For example, a study of presynaptic homeostatic plasticity was conducted at the fly NMJ in which experimenters induced genetic modulations of either postsynaptic receptor density or presynaptic vesicle neurotransmitter concentration via vesicular glutamate transport [140].

The changes which are made to presynaptic probability of release can occur in

either direction. Upregulation of release is known as presynaptic homeostatic potentiation (PHP) while the downregulation of the probability of release is called presynaptic homeostatic depression (PHD). The early work in the drosophila NMJ was seminal to this field, as precise genetic alterations in various aspects of synaptic efficacy could be tested in quick succession, due to the short breeding cycle and lifespan of this model system. For example, genetic reduction of the function of muscle-type glutamate receptor would result in a change in synaptic efficacy expressed as reduced mEPP amplitude, the response to a single vesicle of spontaneous release [183]. Yet, the baseline amplitude of evoked potential was maintained. This suggested that the number of quanta per action potential (quantal content) must be increased. These presynaptic mechanisms of homeostatic plasticity can be induced on a very rapid time scale (within minutes) and their expression can be sustained [69, 80, 181], suggesting that the monitoring of synaptic efficacy occurs quickly, without the need for transcriptional changes or protein synthesis. Still, the identity of the retrograde homeostat, which provides the "error signal" which is thought to trigger these events is not entirely understood, though it could involve a calcium-involved mechanism such as Ca^{2+} calmodulin dependent protein kinase II (CamKII), [45, 140, 183].

To summarize, presynaptic homeostiatc plasticity is characterized by change in probability of presynaptic vesicle release, that is triggered by a change in synaptic efficacy [46, 80]. This change in probability of release can be measured using the "paired pulse" electrophysiological technique [46]. This type of experiment is conducted by providing presynaptic fibers with a priming stimulus pulse that causes vesicle release. This pulse is shortly followed by another, 'test' pulse and the postsynaptic response is measured for each pulse. The ratio of postsynaptic response to the first stimulus compared to the second stimulus reveals the relationship between the amount of vesicle release that was allowed during the first stimulus, compared to that of the second. As such, the amount of facilitation or depression seen in the second response demon-

strates the amount of neurotransmitter vesicles that were available to be released on the first response. If the paired pulse response differs between control preparation and in animals that received synaptic blockade, this would indicate that a change in the probability of vesicle release had occurred.

Lastly, it is important to recognize that presynaptic homeostatic plasticity can be employed in the absence of other forms of homeostatic plasticity, or in combination with them, to precisely control the input/output relationship regarding the postsynaptic response to an action potential in the presynaptic fiber [46, 181]. This presynaptic category of homeostatic plasticity has been observed in several species and systems, from the skeletal muscles to the auditory system [12]. Additionally, it has been observed both in adulthood and in early development. This set of experiments was key in discovering that presynaptic changes can account for changes in synaptic efficacy, to rapidly modulate presynaptic vesicle release.

1.9.3 Homeostatic intrinsic plasticity

Finally, the third category of homeostatic plasticity mechanisms which will be discussed in this introduction is known as homeostatic intrinsic plasticity. This form is enacted via changes in intrinsic excitability of the cell membrane, to regulate its output [138]. Intrinsic forms of homeostatic plasticity can occur relatively quickly, by increasing or decreasing the expression, kinetics, and overall function of various ion channels [51, 79, 148, 233]). For example, Desai et al [51] showed that increases in intrinsic excitability were expressed in cultured neurons from rat visual cortex in response to 48-hour treatment with the voltage gated Na^+ channel blocker TTX. These increases in excitability were measured by examining changes in the balance of inward and outward voltage-dependent ion conductances, and these changes ultimately resulted in much higher firing rates This phenomenon forms the basis of what we refer to as homeostatic intrinsic plasticity, and the hypothesis suggests that

a cell can dynamically change its spiking properties by altering the constellation of ion conductances, resulting in a return towards a target pattern of activity as the cell ultimately reaches some convergence of a number of different cellular solutions [79, 147, 173]. Thus, a cell can dynamically alter its pattern of ion conductances in order to achieve maintenance of some network feature such as firing pattern, [79], and this can occur through both activity-dependent as well as activity-independent mechanisms [148].

Much of the seminal work describing HIP began in the STG of the crustacean [232, 233]. Using this model system, researchers discovered that currents such as I_A, the transient outward K^+ current, were maintained after perturbation due to a compensatory changes in the conductance of other ion channels, such as the I_H inward current [145, 228]. This demonstrates that many combinations of ion conductances may be changing to counteract or balance one another, while maintaining stability of the neuron. In fact, modeling studies revealed how the changes in ion conductances can involve a wide array of unique and ongoing combinations of changes in ion channel function that all can arrive at the same solution, the goal of which is to maintain activity patterns [173]. Since the discovery of homeostatic intrinsic excitability, many of its features have been investigated, such as the impact of the expression of various genes and proteins [24, 145], and its expression in different neural systems [62].

In summary, homeostatic intrinsic plasticity is a form of homeostatic plasticity in which a cell alters various ion channel conductances, ultimately affecting the excitability of the cell membrane. In addition to ion channels our lab has recently demonstrated compensatory changes in resting membrane potential (RMP) that could be expressed through alterations in Na^+/K^+ pump activity [86, 265]. These adjustments in the overall activity level in a network help to push the level of activity back towards a baseline setpoint of some neural feature of activity. Altogether, synaptic scaling, presynaptic plasticity and homeostatic intrinsic plasticity are three forms of homeo-

static plasticity which are critical for the maintenance and healthy functioning of the nervous system.

These three different forms of homeostatic plasticity have been identified across development and throughout the nervous system, but they appear to play a particularly important role during early developmental timepoints that could contribute to critical periods [33, 52]. During early development, for instance, homeostatic plasticity has been shown to be important for proper development of the hippocampus [62], spinal cord motor function [243, 247], as well as in retinal ganglion cells for visual processing [227]. While several of these early life examples are studied in the context of critical periods of development, homeostatic plasticity is not exclusively expressed during these prenatal or neonatal stages. In fact, adult systems have been found to express various forms of homeostatic plasticity as well [224, 240]. However, for our studies, we will focus on embryonic development as the period of interest.

1.9.4 Homeostatic plasticity in the chick embryo spinal cord

Homeostatic plasticity is heavily expressed during embryonic development. During this time, many neural systems begin to generate waves of spontaneous network activity (SNA), even in the absence of sensory input [116, 169]. These waves of SNA are due to the hyperexcitable nature of circuits at these early developmental stages. The systems which express these patterns of spontaneous activity include the retina [2, 30, 254, 255], the hippocampus [14], as well as the brainstem [120] and spinal cord [32, 159, 176, 171].

In the spinal cord, SNA is expressed throughout the motor circuit, during a time when GABAergic chloride currents produce a depolarizing effect [13, 17, 137, 176, 32, 243]. This spontaneous activation of the spinal motor circuit results in observable limb movements in the embryo or fetus. In the chick embryo, these movements are considered highly important for proper development of the motor system [160, 198, 206], as

these movements begin around the same time as motoneurons are reaching their targets [127, 134, 246]. In fact, it is a well-known phenomenon that SNA has an impact on the guidance of motoneuron axons as they extend towards their targets [95, 113]. Not surprisingly, this activity, and the overall excitability of the developing network is extremely important to maintain during the period of early development, when there are constant changes and challenges. Therefore, it is not surprising that the nervous systems of many organisms have evolved mechanisms to maintain this spontaneous activity and adjust excitability in a network at proper setpoint levels. Several of these mechanisms have been identified in the developing system and are prime examples of the expression of homeostatic plasticity during early development. The chick embryo is a widely used model system that is especially useful for the examination of the regulation of SNA in the spinal cord [168, 169, 194, 244]. In the chick embryo, it is well known that there are regularly occurring episodes of SNA that are synchronized across many segments of the spinal cord during early to mid-gestational stages (embryonic days 4-14, HH 24 – 40). These spontaneous movements have been studied for over 100 years in the chick embryo [187] and therefore are a well understood readout of SNA in the developing spinal cord. These rhythmic motor patterns can be recorded electrically or optically [168, 176, 245] using ex vivo preparations of the spinal cord. In addition, these episodes of SNA can be observed in ovo by opening the eggshell and measuring the limb movements, or "kicks" [176, 198, 206]. Measuring these episodes in ovo through the movements they produce can be especially useful when tracking the effect of perturbations such as drugs which alter synaptic activity and therefore embryonic movements. In this way, one can subsequently track the recovery of these movements, which are maintained due to homeostatic plasticity. This kind of recovery is important when studying homeostatic plasticity, as it allows for long term, close observation in the intact system, revealing the timing of homeostatic recovery towards baseline level of spontaneous movement. In fact, our lab has leveraged this system

to measure the changes in SNA during experiments that used pharmacological perturbations to induce homeostatic plasticity, discovering that the expression of various mechanisms of homeostatic plasticity occurred at specific times, with the timeline of behavioral recovery to anchor these observations [250]. In this case, it appeared that some mechanisms were engaged to drive the recovery while others were only expressed afterwards. It is clear that SNA is important for the development of the embryonic chick, and this activity may in fact provide the input for testing, tuning, and ultimately regulating the excitability of the neural populations in the spinal cord [82, 149, 176, 218, 246, 244]. In the context of this regular, spontaneous activity in the spinal cord network of the embryonic chick, prior studies from our group have established several important findings about homeostatic plasticity. To start, we found that the addition of lidocaine - which blocks Na^+ channels and therefore interrupts overall spiking activity - in ovo at embryonic day 8 (E8) resulted in a cessation of the expression of SNA-driven movements. After two days of activity block, the amplitude of both AMPAR and depolarizing GABAR mPSC were increased [82]. This indicates that synaptic scaling had taken place, as a response to the activity blockade, but it was not clear whether spiking activity was the neural feature which was homeostatically monitored in this circuit. In other words, was it possible to trigger scaling by inducing different kinds perturbations? In our group, we identified different triggers for inducing homeostatic plasticity by conducting different kinds of activity perturbations in ovo, tracking the changes in spontaneous motor movements, and later gathering various measures of cellular excitability or synaptic strength in the somatic motoneurons. In this fashion, Wilhelm Wenner [249] found that in ovo treatment with either GABAergic antagonists or AMPA/NMDA ionotropic glutamatergic antagonists starting at E8 resulted in a cessation of spontaneous episodes of motor activity. This cessation was transient, however, as motor activity was homeostatically restored. Interestingly, Wilhelm discovered that 48-hour blockade of GABAergic

signaling, but not glutamatergic blockade, resulted in the scaling of both AMPAergic and GABergic mPSCs [249]. This demonstrated the importance of GABAergic transmission in inducing homeostatic adjustments in quantal amplitude. When the embryonic movements were examined more closely, however, Wilhelm [249] discovered that the movements returned to pre-drug baseline levels within 12 hours of drug treatment, which is sooner than scaling was observed. This finding indicated that there must be some other mechanism that was responsible for the homeostatic recovery of embryonic limb movements, and this mechanism must have been induced prior to scaling taking place. In fact, Wilhelm [250] observed the expression homeostatic intrinsic plasticity at this 12-hour mark, consistent with the timeline of recovery of SNA. This plasticity was mediated by increases in voltage-gated Na^+ currents, and decreases in I_A and I_{KCA} currents, which are fast-inactivating and calcium-activated K^+ channels, respectively. Thus, while synaptic scaling is among the changes that were enacted in response to GABAergic blockade, the homeostatic recovery of SNA is more likely mediated through ionic compensations such as homeostatic intrinsic excitability. This demonstrates that multiple mechanisms of homeostatic plasticity are triggered in response to changes in GABAergic transmission in the developing chick embryo. These results also confirm that the $GABA_A$ receptor, in particular, plays a key role in initiating the process of homeostatic response. Taken together, these results demonstrate that synaptic scaling is not simply triggered by a reduction in overall spiking, but instead the expression of scaling was dependent on one class of synaptic neurotransmission which was perturbed. These results revealed the importance of GABAergic transmission in the homeostatic increase in quantal amplitude as well as the expression of homeostatic intrinsic excitability in somatic motoneurons during embryonic development, as blockade of GABAergic signaling, in contrast with glutamatergic blockade, induced scaling events, measured as increases in GABAergic mPSCs, which were expressed by 48 hours. Next, it was important to further

clarify the role of GABAergic transmission on the induction of homeostatic plasticity mechanisms. Was GABAergic transmission the neural feature that was monitored? After all, perhaps a change in spiking would override any changes in GABAergic transmission. To better define the type of receptor activation that was necessary for the induction of scaling, our group manipulated GABAergic presynaptic release by adjusting tonic nicotinic transmission, which had relatively weak changes on embryonic movements [85]. Using this pharmacological tool, our lab found that altering presynaptic release of GABA vesicles could trigger scaling in somatic motoneurons completely independently from any changes in action potential rate [73]. Further, while we know that lidocaine blocks spiking activity and leads to upscaling [82], our group showed that the lidocaine-induced upscaling can be converted to downscaling by simply increasing the spontaneous release of GABA vesicles injecting nicotine while blocking spiking with lidocaine [73]. Therefore, the induction of homeostatic mechanisms such as synaptic scaling was not mediated simply by the overall change in spiking, but instead was likely initiated by a change in overall GABAergic synaptic neurotransmission. While the mechanisms which are important for sensing a change were more clear, the precise mechanism(s) which were engaged in order to perform the synaptic scaling in this system were still unknown. To discover the mechanisms which underly the expression of synaptic scaling in the embryonic chick spinal cord, our group conducted numerous experiments. For example, Garcia et al [73, 72]) determined that AMPAergic scaling was mediated by the insertion of AMPA receptors which lacked the Glu_A2 subunit, consistent with prior literature [11, 177, 216]. In addition to the expression of synaptic scaling via glutamatergic receptors, there are also different mechanisms which mediate GABAergic synaptic scaling. While glutamatergic scaling is mediated by receptor accumulation, previous findings from our group have shown that GABAergic scaling in chick embryo spinal MNs is mediated by an increase in intracellular chloride concentration [Cl-]in [84, 142]. This was shown

through Nernstian channel dynamics, which revealed an increase in the driving force for chloride after the blockade of GABA receptors, such that this blockade resulted in an increase of the reversal potential for chloride [84, 142]. In addition, Lindsly et al [142] measured an increase in intracellular chloride levels using Clomeleon, a ratio-metric chloride indicating fluorescent marker [125], after chronic pharmacological blockade of GABA receptors. This increase in chloride is evidence of GABAergic synaptic scaling, and could be mediated by various anion transporters, as blockade of chloride accumulators NKCC1 and anion transporter AE3 also resulted in reductions of evoked GABAergic currents [83]. In summary, homeostatic plasticity comes in several flavors with regard to mechanisms of expression. These mechanisms, which are employed to compensate for a sensed change in GABAergic transmission have been examined in the embryonic chick spinal cord over the past two decades. As discussed above,there is robust evidence for homeostatic changes in the spinal somatic motoneurons and interneurons in the embryonic chick. Following this line of work, I wanted to test whether autonomic neurons, also known as SPNs, also express these mechanisms. This is important because it would be the first work establishing that these mechanisms exist in the developing SNS and could therefore play a role in a critical period for establishing baseline tone in this system. Moreover, because we have a firm understanding of the different mechanisms which underly these homeostatic compensations in the embryonic chick spinal cord, as well as their timelines of expression, we are therefore in a position to investigate these mechanisms in the neurons of the SNS. Next, in order to provide the background context in which plasticity mechanisms develop in the SNS, I will first discuss the general development of the SNS during embryogenesis in the chick embryo and provide comparisons with other species.

1.10 Embryonic development of the sympathetic nervous system

During embryonic development, the neural circuits of the SNS that connect the central nervous system with the peripheral nervous system are in the process of maturation. The anatomy of the SNS has been studied extensively since the 19^{th} century [34, 129, 187], and advancements in electrophysiology, fluorescence imaging, and proteomics have provided a wealth of information in recent decades. In this section, I will review a brief background of the benchmarks of SNS development, focusing on the SPNs in the spinal cord and PGNs in the periphery and briefly explore differences between the timeline of development in mammalian and avian species.

The development of the SNS during embryonic stages involves several main steps: the differentiation of neural crest or neural tube tissue, the migration to proper locations, the guidance of axons to their target destinations, and finally, the formation and tuning of functional synapses with target cells. In the spinal cord, the SPNs develop in a very similar fashion to somatic MNs that innervate skeletal muscle. They are derived from the neural tube tissue which gives rise to the CNS, including the brain and spinal cord [214] whereas the PGNs, on the other hand, arise from neural crest tissue. Further, SPNs emerge from the same ventral progenitor domain as the somatic motoneurons, known as the pMN domain, where the same precursor cells express a unique combination of transcription factors [167, 221, 236]. The cells in this progenitor domain express unique transcription factors and homeodomain proteins such as MNX1 or HB9 [135, 136, 214] that can be used to identify motoneurons. These precursor cells from this progenitor domain then exit the cell cycle and enter the differentiation process, therefore generating either somatic or autonomic cell fates [226]. In the chick embryo, the birth of the SPNs occurs between E2 and E4. This stage is associated with stages 18-24 in the classic Hamburger Hamilton chick

embryo staging literature [93]. After the final cell division, cells migrate out of the progenitor domain and target the ventrolateral region of the spinal cord. The SPNS gather to form a distinct anatomical column in the spinal cord known as the preganglionic column [186]. This process and timeline of cell migration differs slightly between avian and murine animals. For example, the location of the SPNs in the spinal cord is different between these two. In most mammals, the majority of SPNs live in the intermediolateral (IML) cell column [190]. This sympathetic nucleus of the spinal cord typically extends from T1 to around L1 depending on the species, and is located in the lateral most edge of the grey matter, situated in the intermediate zone between the dorsal to ventral horns [205] (also see Figure 1.2). On the other hand, in the chick embryo, the SPNs form a distinct cell column in the spinal cord that is more medial and slightly dorsal to the central canal [139, 261]. This spinal column of SPNs is known as the column of Terni in the chick embryo [225] which extends from the upper thoracic to the second lumbar segment of the spinal cord [41]. In the chick embryo, somatic and autonomic motoneurons migrate to a ventrolateral location until E5. While the somatic motoneurons remain in this location and form the lateral motor column (LMC), the autonomic neurons begin, around E5, to migrate to the more dorsomedial position to form the preganglionic column of Terni. This secondary migration of the SPNs is completed by E8 [186] (Figure 1.4). From this region, the SPNs can be molecularly defined by unique combinations of expressions of various proteins such as Nitric Oxide synthase 1 (NOS1) [42, 199], and a low level of Foxp1 [43, 214].

When it comes to the PGNs, which are the synaptic targets of the SPNS, I will begin by discussing the timeline of the developmental process in the chick embryo. The clusters which form the ganglia start to coalesce by E4 [68], and the ganglia have fully formed by E7.5 / E8 [258] but have very few synapses by E10 [104]. First, there is a large increase in the expression of genes which code for certain subunits of nico-

Figure 1.4: The SNS of avian species develops earlier than that of rodents

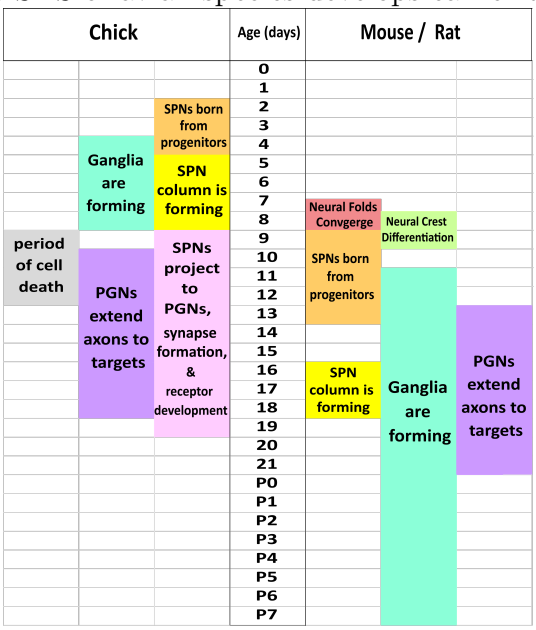

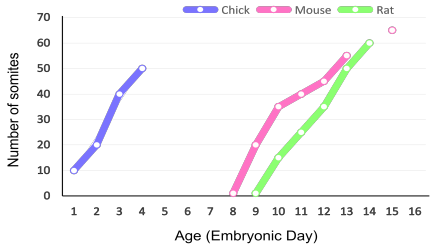

The timeline of sympathetic development differs between avian and murine species, with major milestones highlighted in this chart. It is important to note that there is not a formal consensus on this exact timeline of events, but that these events are reasonable estimates based on a general body of literature

tinic receptors between E8 to E11[55] Next, the anatomical arrival of SPN projections to the ganglia is closely followed by the development of functional synaptic innervation. Both SPN projection arrival and the formation of the SPN to PGN synapse is known to increase dramatically between E11 and E17 [60, 163], a finding which was confirmed in the present study (see chapter 2). Experimenters measured the binding of a nicotinic antagonist, a-bungarotoxin, to nicotinic receptors at progressive ages and this measure increased intensely from E12 to E20 in chick embryo [88], a timeline which roughly matches the arrival of functional synapses. This suggests that once the PGNs are contacted by the SPNs, the synapses begin forming, and the number continues to grow after birth [104]. In fact, the number of preganglionic inputs to the PGNs increases heavily over the first 1-2 weeks of postnatal development [100], as does the number of synapses [16]. This timeline differs in the rat, in which the ganglia do not coalesce until E11 [195] and the diameter of ganglia from the lumbar regions continue to increase tenfold in the first 7 days of postnatal life [98, 100]. Comparatively, the ganglia have fully formed in the chick embryo before the first half of embryonic development is complete at E21 (Figure 1.4).

Together, these findings demonstrate that synapse development dramatically increases after birth in rodent species, while a significant part of the development of these synapses occurs prenatally in the chick (Figure 1.4). It should be noted, however, that some of the prior studies which used electrophysiology to determine the developmental timeline of functional synaptic connections in the SNS were conducted with sharp microelectrodes. This technique has been shown to systematically underestimate the impact of SPN inputs on PGN output, as it induces a significant leak current [157, 212]. Nonetheless, in both avian and murine species, the development of the SNS is protracted compared to development of muscle or cutaneous innervation. Chickens, however, are rather precocial, and can locomote and regulate their body temperature on the day of hatching [209]. This creates a slight mismatch be-

tween species when it comes to discussing the early postnatal period, as autonomic functioning in murine species is less mature at birth. Therefore, the equivalent ages for this process in rat, mouse and chick embryo have been roughly estimated based on anatomical landmarks and number of somites [203] (see Figure 1.4). Next, the projections from the PGNs extend towards their target tissues in the periphery for synaptogenesis. This axon growth cone mediates pathfinding and is thought to be guided by gradients of various neurochemical molecules [4, 78, 132], such as endothelins which are expressed from the vascular system and attract sympathetic neurons [146]. Altogether, the studies which have generated the vast body of knowledge regarding the anatomy, development, neurochemistry, and functional connectivity of the SNS provide an important developmental framework from which to examine both SPNs and PGNs, during a time when they first start to receive functional synaptic input. Thus, I was able to examine cell populations from both the central and peripheral arms of the SNS for their ability to respond in a homeostatic manner to a change in excitatory synaptic input, and to ultimately explore the question of critical period for the development of setpoint of autonomic tone.

1.11 Research objectives of this dissertation

Together, these fields of research: autonomic physiology, critical periods during early development, and homeostatic plasticity coalesce on an important question: Are mechanisms of homeostatic plasticity present in the SPNs and PGNs of the SNS during embryonic development? Understanding the mechanisms which may form the basis of excitability tuning in the developing SNS may ultimately provide insight on the formation of regulatory mechanisms for sympathetic tone. This tone may have a programmed setpoint which is likely established early in development, and as discussed earlier, may be especially vulnerable to perturbations during a critical

period. To address this question, I began by examining evidence for synaptic scaling in the SPNs. Next, I sought to uncover mechanisms of homeostatic plasticity in the PGNs. The SPNs are the autonomic motoneurons of the spinal cord which are the final output from the central nervous system into the periphery for SNS function. These cells are born from the same progenitor cell population as the somatic limb MNs [214], and while there are genetic distinctions [36] they have significantly overlapping receptor expression, and display similar patterns of axon migration [5, 214]. These similarities between SPNs and MNs allow for a jumping off point for studying the SPNs. Therefore, in order to target the capacity for homeostatic plasticity in the SPNs, I began by examining what we already knew about somatic MNs in the embryonic chick. Through a series of important discoveries in the chick embryo spinal cord, our group has found evidence for chloride-mediated scaling in the MNs. As GABA is excitatory in the embryo [13, 180], blocking GABAergic transmission acutely reduces excitatory neurotransmission, as observed in ovo as a reduction of embryonic limb movements [249], and induces various homeostatic mechanisms 48 hours later [250, 249]. This GABAergic scaling in the somatic MNs was found to be mediated by a shift in the reversal potential for chloride conductance [84], and this finding was further confirmed by directly measuring chloride in an imaging study [142]. Thus, I examined the same mechanism of chloride-mediated scaling as the candidate mechanism for probing homeostatic plasticity in the SPNs. To examine this, I first established that SPNs are active during bouts of spontaneous activity, and I had to ensure that I could reliably locate these cells for imaging studies. The methods and results for these experiments will be discussed in detail in the second chapter of this thesis.

In the downstream targets of the PGNs, synaptic input is known to develop slightly later than that of the SPNs, as mentioned previously (Figure 1.2). As such, I elected to delay the perturbation of synaptic input to a slightly later developmental stage.

To determine which age would be ideal for synaptic blockade, I performed a series of electrical studies at different ages to determine synaptic connectivity. Both previous anatomical literature and my own experiments revealed that these synapses are underdeveloped at E10, are functional at E13 and are even stronger at E17. Accordingly, we chose to induce synaptic blockade using in ovo application of ganglionic nicotinic blocker hexamethonium at E13 and examine plasticity 48 hours later. As PGNs receive primarily cholinergic input, I used nicotinic blockade and examined the potential change in intrinsic excitability using whole cell recordings. As the presence of miniature synaptic events was quite rare, I was not able to assess scaling by directly measuring mPSCs. Intrinsic excitability, on the other hand, was measured by examining the frequency/current (f/I) curve response of the cells in current clamp while stimulating at progressively increasing intensities. In this case, we predicted that excitability would homeostatically increase after Hex treatment but instead found that the shift was towards a less-excitable direction. Overall, the differences in expression of homeostatic plasticity between the SPNs in the central arm and the PGNs in the peripheral arm of the SNS during embryonic development are likely important factors in the development the SNS and, potentially, influence the trajectory of autonomic tone maturation.

Chapter 2

Plasticity in preganglionic and postganglionic neurons of the sympathetic nervous system during embryonic development

Ratliff A, Pekala D, Wenner P. 2023

This chapter was published as a manuscript in eNeuro journal [191]

2.1 Abstract

Sympathetic preganglionic neurons (SPNs) are the final output neurons from the central arm of the autonomic nervous system. Therefore, SPNs represent a crucial component of the sympathetic nervous system for integrating several inputs before driving the post-ganglionic neurons (PGNs) in the periphery to control end organ function. The mechanisms which establish and regulate baseline sympathetic tone and overall excitability of SPNs and PGNs are poorly understood. The SPNs are

also known as the autonomic motoneurons (MNs) as they arise from the same progenitor line as somatic MNs that innervate skeletal muscles. Previously our group has identified a rich repertoire of homeostatic plasticity (HP) mechanisms in somatic MNs of the embryonic chick following in vivo synaptic blockade. Here using the same model system, we examined whether SPNs exhibit similar homeostatic capabilities to that of somatic MNs. Indeed, we found that after 2-day reduction of excitatory synaptic input, SPNs showed a significant increase in intracellular chloride levels, the mechanism underlying GABAergic synaptic scaling in this system. This form of HP could therefore play a role in the early establishment of a setpoint of excitability in this part of the sympathetic nervous system. Next, we asked whether homeostatic mechanisms are expressed in the synaptic targets of SPNs, the PGNs. In this case we blocked synaptic input to PGNs in vivo (48-hour treatment), or acutely ex vivo, however neither treatment induced homeostatic adjustments in PGN excitability. We discuss differences in the homeostatic capacity between the central and peripheral component of the sympathetic nervous system.

2.2 Introduction

The Central Nervous System (CNS) has an extraordinary capability to adapt to changing environments. Particularly responsive is the Autonomic Nervous System, which is comprised of parasympathetic and sympathetic nervous system branches. Central neurons of the autonomic nervous system project into the periphery and drive neurons in autonomic ganglia. In turn, these postganglionic neurons (PGNs) innervate peripheral tissues to maintain homeostasis within an organism [110]. Adjustments in autonomic output occur routinely, such as transient changes in vasodilation to maintain body temperature. However, it remains unclear how the autonomic nervous system first establishes the setpoint of the baseline sympathetic tone, thus

ensuring peripheral targets are not chronically hyper- or hypo- active. Prenatal and early neonatal development appear to be particularly sensitive stages for establishing proper sympathetic tone, such that early autonomic disruptions as occurs in preterm birth [9, 178, 202] are associated with long-term autonomic dysfunction and stress-related neuropsychiatric consequences [35, 92, 96, 165, 164]. These results indicate that early development is a critical period for the maturation of healthy autonomic setpoints [29]. Critical periods represent distinct developmental windows of plasticity during which circuit excitability can be defined. Little is known about the mechanisms of plasticity in the developing autonomic nervous system, but identifying such mechanisms will advance our understanding of the maturation of autonomic tone. Homeostatic plasticity (HP) represents a set of mechanisms that regulate excitability and could contribute to establishing the autonomic setpoint. When engaged, HP mechanisms ensure that some feature of neural activity (e.g., firing rate, synaptic strength) is homeostatically recovered following a perturbation. Such mechanisms include compensatory adjustments in synaptic currents and excitability of the cell membrane [227]. Synaptic compensations can occur by alterations in neurotransmitter receptors [231, 235], the driving force for synaptic currents [84], or presynaptic neurotransmitter release [44, 64, 80]. Compensatory changes in intrinsic membrane excitability, achieved by adjustments in overall function of ion channels, have also been described [50, 51, 173, 232, 250]. Because HP mechanisms alter circuit excitability and are often expressed during a distinct period of development [52, 62, 99, 67, 242], they could be important for determining the trajectory of autonomic tone during a critical period. It is currently unknown whether cells of the developing autonomic nervous system express these HP mechanisms. Therefore, we tested the hypothesis that HP is expressed in developing sympathetic neurons of the chick embryo, which is amenable to studying HP mechanisms during early development [246]. Previously, our group identified a rich repertoire of HP mechanisms in motoneurons (MNs) in

the embryonic chick following *in vivo* blockade of synaptic transmission or spiking activity [82, 246, 250]. In the present study, we hypothesized that sympathetic preganglionic neurons (SPNs) would also express HP mechanisms. We found evidence suggesting homeostatic synaptic plasticity was triggered in SPNs following a 2-day, in vivo reduction of GABAergic neurotransmission, which is excitatory at this developmental stage [247]. Embryonic SPNs increased synaptic driving force for GABAergic currents in a compensatory fashion by altering intracellular chloride levels, consistent with previous findings in somatic MNs [84, 142]. Therefore, HP could play a role in establishing the setpoint for autonomic tone in SPNs. Conversely, reducing synaptic input to PGNs, either chronically in vivo, or acutely ex vivo, did not induce a response indicative of HP. The presence of HP in SPNs but not in PGNs is considered in the discussion.

2.3 Methods

2.3.1 Chicken embryos

All animal procedures were performed in accordance with Emory University's animal care committee's regulations. White Leghorn chicken embryos were purchased from Hy-Line Hatcheries, North America. Fertilized eggs were kept in the incubator at $\sim$38° C at 65% relative humidity. Embryos were staged according to the duration of time in the incubator and developmental stages were confirmed using Hamburger and Hamilton (HH) staging [93]. For the present study, embryos were used from embryonic day 3 - 17 (E3-E17, stage 15-43 HH). Sex was not determined in these experiments.

2.3.2 Tissue isolation

Chick embryo spinal cord tissue was surgically isolated in cooled (14-16° C) Tyrode's solution containing the following (in mM): 139 NaCl, 12 D-glucose, 17 $NaHCO_3$, 3 KCl, 1 $MgCl_2$, and 3 $CaCl_2$. The solution was oxygenated (95% O2/5% CO2) throughout the procedure. After isolation was complete, the solution was warmed to 18° C and the tissue was allowed to recover overnight (12-18 hours). The following day, spinal cords were transferred to a recording chamber, which was circulated Tyrode's solution, oxygenated as above, and held at 27 ± 1° C for electrical recording or imaging [181]. For PGN recordings, lumbosacral (LS) segments of paravertebral chain (LS 1 – 7) were isolated from the spinal cord, detaching them at the ventral roots by breaking the gray and white rami, under the same conditions as the cord preparations. However, recordings from this tissue were obtained after 1-2 hours of recovery period. This short recovery time was feasible as preliminary tests revealed that recordings did not differ between acute and overnight preparations.

2.3.3 Retrograde labeling of SPNs and MNs

Embryos were dissected to isolate spinal cords on embryonic day 10 (E10, stage 36 [93]. Ventral roots were left intact on the cord, and the cut end of the ventral root was drawn into a suction electrode (at LS 1 or LS 2) filled with a fluorescent indicator [169]. For the anatomical examination of SPNs, Texas Red (conjugated with dextran, 10,000 MW, neutral; D1828; Invitrogen) was used. In separate cords, Calcium Green-1 (dextran potassium salt, 10,000 MW anionic, C3713; Invitrogen) was used to visualize calcium transients in both SPNs and MNs. In both cases we used a ratio of indicator to vehicle (H2O) of 1 mg : 10 µl. In one cord with intact rami, we labeled with Texas Red from the interganglionic nerve (IGN) rather than the ventral root, to confirm the location of the SPN population without contamination of signal from limb MNs (Figure 2.1B). However, due to the fragility of the white rami,

success rates were low with this labeling procedure, so we used the proximal ventral root for labeling in most experiments (n = 8).

2.3.4 Calcium imaging of SPNs

All images were taken in the medial view of hemisected cords. Regions of interest (ROIs) were drawn around labeled cell bodies to examine changes in fluorescent intensity during episodes of spontaneous network activity (SNA), which are spontaneously occurring synaptic recruitment of the spinal network that can last for over 60 seconds [128, 170]. After a refractory period of several minutes, another episode of SNA can occur spontaneously, or can be initiated with a brief stimulus pulse of the spinal nerves or spinal cord white matter. Both spontaneous and evoked episodes of SNA were recorded optically by measuring an increase in intensity of fluorescence due to calcium influx in these ROIs (5-15 frames/second). A 60-frame average of a non-labeled region of the cord was used for subtraction of background fluorescence from each ROI. Each of these background-subtracted ROIs were then normalized by dividing the intensity values in every frame by a 60-frame average of the pre-episode baseline fluorescence for that ROI. This calculation provided $\Delta F/F$, which follows the change in intracellular calcium levels at baseline and during spontaneous or evoked episodes of SNA. These values were measured in both MNs and SPNs. The cell type was determined based on location in the cord using results from retrograde labeling experiments (described above). Cells that were close to the medial surface and located within the appropriate dorso-ventral position were classified as SPNs, while cells that isolated to a more lateral population of cells, and on the ventral half of the hemi cord, were considered MNs (Figure 2.1).

2.3.5 Chloride imaging

Embryos were transfected at ∼E3 (stage 15-17 HH) with plasmid containing Clomeleon, a chloride indicator (3.40 µg/µL), in a 1:1 ratio with solution of Fast Green (Sigma-Aldrich) for electrode visualization as described previously [142]. The transfection occurred via injection into the neural tube, followed by lateral electroporation using a train of 5 square wave pulses of 50 ms duration, at 25 V, at a rate of 1Hz. At E10, cords were imaged according to previously used procedures [142] on an Olympus Inverted IX70 microscope. Ratios were calibrated on this system in this previous study which associates a FRET-based ratio of YFP/CFP with a concentration of intracellular chloride. For each cord, both ventral and medial images were acquired using the YFP channel and the CFP channel at 10x magnification. Excitation filter bandwidth was 430-450 nm, the emission filter for the CFP cube was 485 ± 15 nm, or for YFP was 530 ± 15 nm. The dichroic filter cutoff was 460 nm. Neutral density filters were used to reduce light from the arc lamp to 2-6% of full intensity. Images were then processed offline using Simple PCI software. ROIs were drawn around motoneuron cell bodies (ventral view) or presumptive SPN cell bodies within the inclusion criteria (from the medial view of the hemicord), determined by location of retrogradely labeled SPNs (Figure 2.1C). The intensity of each ROI was background subtracted using a region of the cord without labeled cell bodies, to remove any impact of autofluorescence. This process was conducted for both CFP and YFP images, using the same ROIs for both images, and FRET ratio values were expressed as YFP/CFP for each ROI. Cords were excluded from analysis if the coefficient of variation (CV) of the FRET ratio values in all ROIs was > 0.15, or if the cells had a ratio of < 1.2 as this value was associated with cells that were unresponsive in calibration experiments using progressively increasing chloride concentrations in our previous study [142].

2.3.6 Extracellular electrophysiology in PGNs

Extracellular recordings of evoked synaptic activity were conducted using two suction electrodes, one for stimulating the rostral end of the paravertebral ganglia and one for recording at the caudal end. Electrical signals were measured using extracellular amplifiers (AC/DC differential amplifier model 3000, A.M. Systems, filtering parameters for capturing synaptic activity: 300Hz high pass, 1KHz low pass). The threshold for inducing a reproducible compound action potential was determined individually for each preparation. This threshold was then tested to determine if it was sufficient to see synaptic activity. A stimulus intensity of 4x threshold was used for each preparation, as it was sufficient for inducing maximal or near maximal recruitment of preganglionic axons. A stimulus pulse of 0.5 ms duration was delivered through the stimulating electrode at the rostral end of the isolated chain of lumbosacral ganglia. Each sweep was repeated 30-60 times at an interval of 60 seconds for before and after drug perfusion, or after washout. The induced neural activity was quantified by rectifying the voltage trace and normalizing the amplitude of synaptic activity to the amplitude of a pre-stimulus baseline period (Figure 2.3B). Synaptic discharge was identified by measuring the signal after the SPN orthodromic volley had dropped back to baseline (typically 12-20 ms post stimulus). A period of 10 ms was selected and an average was performed in each sweep to measure the average amplitude of synaptic discharge.

2.3.7 Intracellular electrophysiology

Whole cell recordings were used exclusively as sharp electrode recordings have been demonstrated to be less reliable for intracellular recordings in PGNs [157, 212]. These recordings were used to examine the relationship between input current and the output spiking activity, providing a measure of excitability for PGNs. Individual neurons from ganglia between LS 1 and LS 3 were examined using whole cell patch clamp

recordings (Axoclamp 2B, Molecular Devices) to establish various measures of intrinsic excitability. Neurons with resting membrane potential (RMP) more depolarized than -40 were excluded from analysis and cells were held at a holding potential of -70 ± 5 mV (before correction for liquid junction potential). Any sweeps in which cells were not maintained in this range were excluded from analysis. To evaluate excitability, a frequency/current (f/I) curve was established by increasing the size of current steps (5 pA intervals, 500 ms duration) in current clamp mode and recording the resulting frequency of action potentials (number/0.5 s). The f/I curve procedure was repeated at least 3 times for each cell and resulting values for each current step were averaged. This procedure was also used to examine additional measures of excitability such as rheobase, threshold voltage, slope of the rising phase of the spike, membrane time constant, peak amplitude, half-width duration, and after-hyperpolarization. Liquid junction potential was measured to be $\sim$ +14 mV. To accommodate for this artificial depolarization, this value was subtracted from voltage measures of RMP and threshold voltage in Table 1.

2.3.8 Experimental and Statistical Analysis

In cases of uneven sampling across preparations, nested sampling techniques were used to estimate effect size and statistical significance, including hierarchical bootstrapping and multi-level modeling. The hierarchical bootstrapping method ensures that each animal is equally represented in the dataset, and data points from the same embryo are not treated as independent from one another. This method was necessary because many other common statistical tests have an intrinsic assumption of independence between all datapoints, as well as homogeneity of variance, and such a dataset would therefore violate these assumptions. Multi-level datasets, such as those which contain repeated measures and multiple cells in a single animal, are thus treated as nested, non-independent groups when using this bootstrapping method,

while the Type-1 error rate is maintained within the appropriately adjusted range to avoid false positives [1, 201]. Finally, linear mixed-effect modeling was utilized (lme4, version 1.1-32, R) to ensure that differences seen between experimental groups were explained primarily by the fixed effect (drug treatment), and that said differences were not explained by random effects such as experimental day or cord number. Statistical test values have been included in figure legends.

2.4 Results

2.4.1 Chloride-mediated scaling in sympathetic preganglionic neurons (SPNs)

To determine if SPNs have the capacity for HP during embryonic development, we looked at the possibility that these cells express GABAergic synaptic scaling, as this form of plasticity is known to be expressed in somatic MNs of the embryonic chick [84, 249]. GABAergic synaptic scaling is typically demonstrated by recording GABAergic miniature post-synaptic currents (mPSCs), in response to 48-hour pharmacological blockade of neurotransmitter receptors or spiking activity and is mediated by trafficking GABAA receptors (GABAARs) into or out of the synaptic membrane [117, 227]. We previously demonstrated that GABAergic synaptic scaling in chick embryo MNs was mediated by a different mechanism. GABAergic transmission in embryonic chick spinal neurons is depolarizing and excitatory at these early stages due to elevated intracellular chloride levels [247]. We had determined that GABAAR blockade led to increases in the intracellular concentration of chloride, thus increasing the driving force for these depolarizing currents [84, 142]. One of the ways we showed this was using Clomeleon, a genetically expressed indicator of intracellular chloride [125, 142]. In order to test for this mechanism of scaling in SPNs, we first confirmed their location in the spinal cord. Cell bodies of SPNs (n = 179) were retrogradely

labeled with Texas RedTM from the LS2 ventral root (Figure 2.1A) or IGN (Figure 2.1B). Spinal cords were hemisected and imaged from medial surface of the hemicord. We observed that 81% of labeled cell bodies on the medial surface were located in a region that spanned from the central canal to halfway towards the dorsal edge (Figure 2.1C). This region is consistent with previous reports of thoracolumbar SPNs [139, 186] also known as the column of Terni in the chick embryo [225]. These criteria were used to isolate the SPNs for Clomeleon labeling experiments.

To determine if it was possible to evoke scaling in the SPNs, we treated embryos in ovo with the $GABA_AR$ antagonist gabazine (GBZ, Sigma-Aldrich, 10 µM) from E8-10 to reduce GABAergic synaptic transmission. This treatment was previously shown to be sufficient to trigger scaling in somatic MNs [249], which are similar to SPNs as they are generated from the same precursor population [214]. Spontaneous network activity (SNA) represents a synchronous recruitment of MNs and spinal interneurons which can be measured by a voltage trace or by calcium transient [128, 170]. These episodes of SNA are significantly driven by GABAergic transmission, which is depolarizing at this developmental stage [13, 137, 169]. It was unclear, however, whether SPNs were synaptically coupled to the network of neurons which drive episodes of SNA at this early developmental stage. Therefore, we set out to confirm that SPNs also express SNA by measuring the calcium signal associated with this activity. We compared the calcium activity in both MNs and SPNs, which were retrogradely labeled from the ventral root using the calcium indicator Calcium Green (see methods). We found that SPNs exhibited calcium transients during episodes of SNA, in synchrony with somatic MNs, which have been shown to express SNA that is driven by GABAergic and glutamatergic input [32, 169, 219]. Calcium transients ($\Delta F/F$) in labeled cells increased by $> 20\%$ (N= 3 cords) in both electrically evoked and spontaneously occurring episodes of network activity (Figure 2.1D). This finding confirms that SPNs receive spontaneous synaptic input at this midgestational stage of

Figure 2.1: The location and activity patterns of SPNs in the E10 embryonic chick were determined using imaging techniques

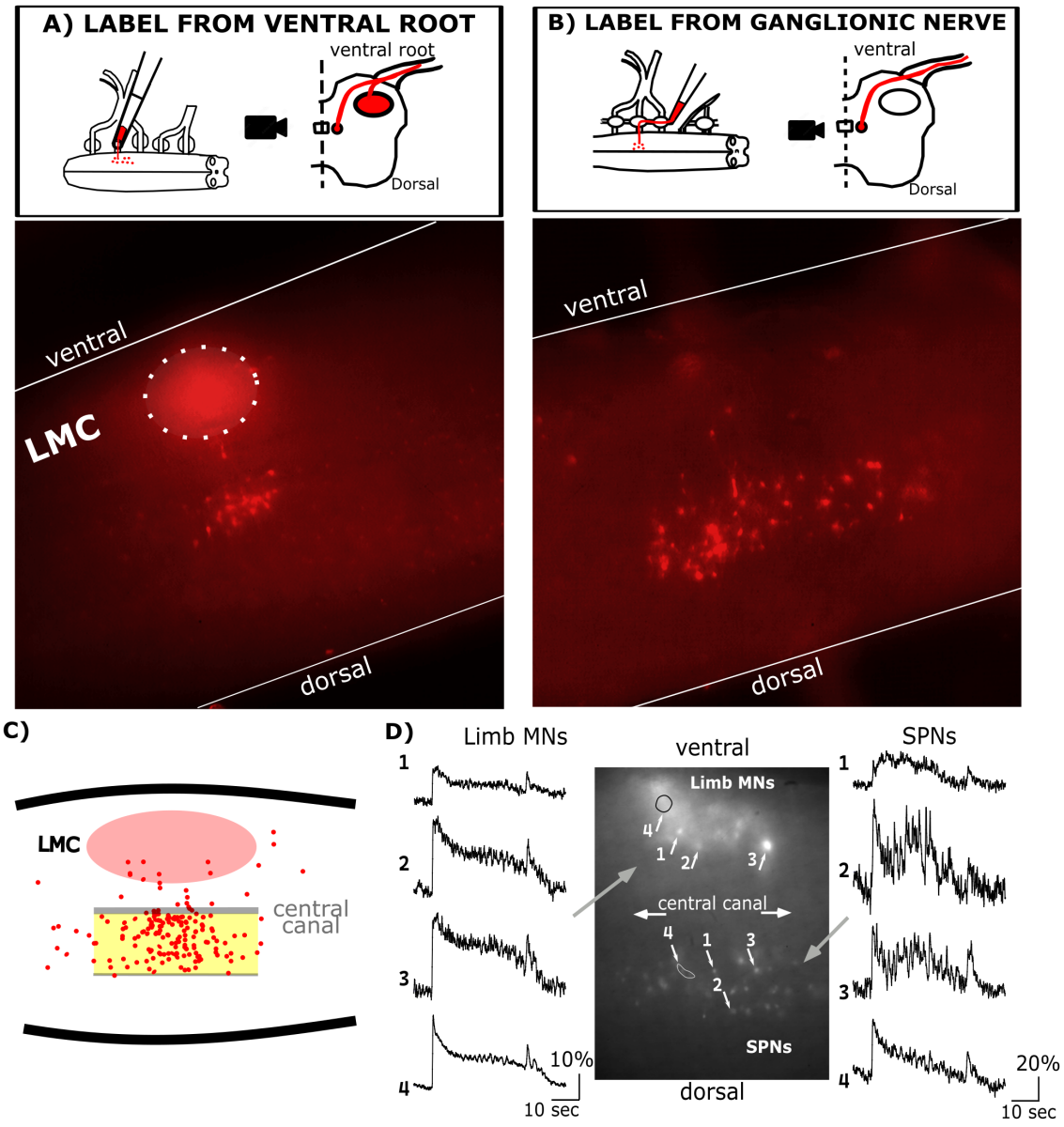

Location and calcium transients of lumbosacral SPNs in E10 embryos. A) Texas Red retrograde labeling from ventral root reveals 2 populations of neurons. One population is consistent with lateral motor column (LMC), the other population is medial, slightly dorsal of the central canal, consistent with Column of Terni. B) In separate experiments, the medial population of SPNs were also retrogradely labeled from the IGN, which did not result in labeling of limb motoneurons in the LMC. C) Of the 179 total cells imaged on medial surface, 81.0% were in the region between the central canal and halfway to the dorsal edge of the cord (highlighted in yellow), where SPNs reside. D) Calcium transients were observed using cells labeled by the calcium indicator Calcium green. This medial view of the hemicord revealed that both limb MNs and SPNs were active during evoked and spontaneous episodes of network activity ($\Delta F/F$ of $> 20\%$, N = 3 cords).

development, and that SPNs express SNA that is likely driven, in part, by GABAergic synaptic transmission, which is depolarizing at this stage. Thus, blocking GABAergic transmission throughout the cord could trigger GABAergic synaptic scaling in the SPNs, as occurs in somatic MNs.

To examine whether intracellular chloride levels are increased in SPNs after 48-hour GABAergic blockade, as would be expected for GABAergic scaling, embryos were electroporated at E3 with plasmids containing the Clomeleon gene, a fluorescence resonance energy transfer (FRET)-based, ratio-metric chloride indicator (Figure 2.2A). Embryos were dissected at E10, and cords were imaged thereafter. We first examined the pattern of expression in the somatic MNs to determine the specificity of the label. As described previously [142], Clomeleon expression was typically in the lateral half of the hemicord when imaging through the ventral surface of the cord, where somatic MNs are located (Figure 2.2B). This pattern of expression in somatic MNs is likely a result of electroporating the plasmids at a developmental stage in which these cells undergo their final mitotic division [101] thus preventing further dilution of the genetic indicator that would occur with additional divisions. Cords were therefore only accepted into the dataset if they displayed this distinct lateral hemicord expression pattern (Figure 2.2B). We imaged somatic motoneurons through the ventral white matter (Figure 2.2B), as we had done previously [142]. We found that ratios were significantly reduced following *in ovo* 48-hr treatment with the GABAAR antagonist gabazine (10 µM) from E8-10, compared to ratios from vehicle-treated embryos (Figure 2.2C). This difference in FRET ratios of YFP:CFP in the somatic MNs was consistent with our prior study in these cells [142] and matched the chloride concentrations that were previously determined using whole cell and perforated patch techniques, thus demonstrating an increase in intracellular chloride concentration associated with GABAergic synaptic scaling [84]. Because SPNs are born at the same time as somatic MNs they should also be labeled with Clomeleon [214]. To

confirm this, we looked for Clomeleon-labeled cells viewed from the medial surface of the hemisected spinal cords (Figure 2.2D) that were in the previously identified location of the SPNs (Figure 2.1C). Indeed, we identified many medially positioned Clomeleon-expressing cells in the SPN location (Figure 2.2D). These cells were then analyzed for Clomeleon ratios to identify differences in chloride levels between treatment groups. Using multiple analyses of FRET ratios, we found significant reductions in YFP:CFP ratios of embryos treated with gabazine for 48 hours compared to those treated with vehicle. This was consistent with our previous work on somatic MNs [142] and suggested that chloride levels were elevated in response to GABAergic blockade (Figure 2.2) as there is an inverse relationship between the ratio of YFP:CFP and the intracellular chloride concentration. While this result demonstrates that intracellular chloride levels have increased in SPNs, we cannot provide a precise change in concentration because we did not redo the necessary calibration experiments on these more superficially located SPNs.

In summary, lumbosacral SPNs, as defined in methods, exhibit an increase in intracellular chloride after 48 hours of synaptic blockade of $GABA_A$ receptors. This suggested that GABAergic synaptic scaling occurred in both SPNs and somatic MNs, indicating the presence of synaptic HP in the central arm of the sympathetic nervous system during embryonic development.

2.4.2 Cellular excitability decreased in PGNs following 2-day synaptic blockade in ovo.

Development of SPN-PGN synaptic activity

In order to further characterize the capacity for HP in the embryonic SNS, we tested the downstream synaptic target of the central SPNs, the PGNs of the peripheral nervous system. This allowed us to test whether PGNs themselves might compensate for

Figure 2.2: Chronic $GABA_A$ synaptic blockade resulted in increased intracellular chloride levels in SPNs

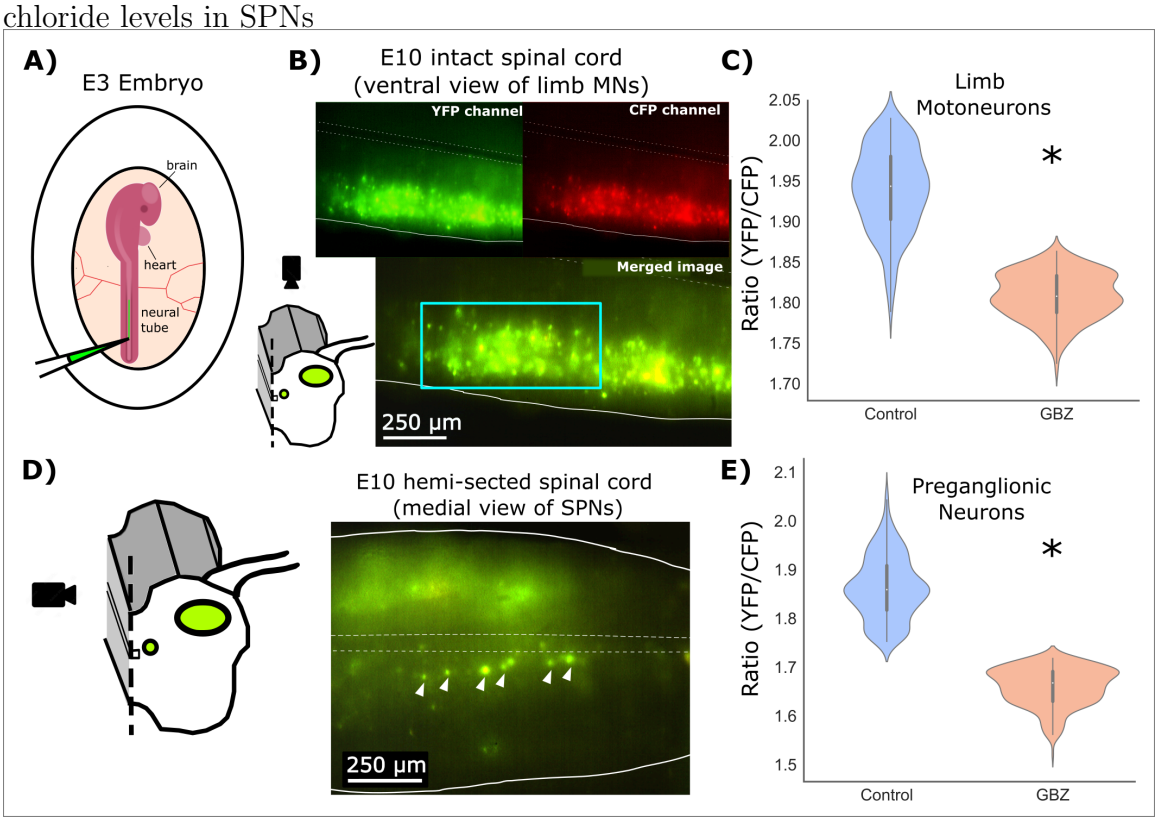

Intracellular chloride levels of MNs and SPNs were altered after synaptic blockade. A) Introduction of Clomeleon plasmids for electroporation into neural tube at embryonic day 3 (E3). B) YFP, CFP, and merged image of ventral view of spinal cord were used to analyze chloride levels in somatic MNs in E10 spinal cord. Schematic at bottom left shows orientation of ventral view C) Analysis of MNs showed significant reduction in YFP/CFP ratio in drug treated group. In order to examine entire dataset while controlling for unbalanced number of cells observed between cords, hierarchical bootstrapping was implemented. This analysis of resampled data revealed lower ratios in GBZ-treated cells (1.79 ± 0.03) compared to vehicle (1.92 ± 0.05, $p = 0.035$). D) Left: Medial view of hemisected spinal cord was imaged for analysis of SPNs. Right: Merged YFP-CFP image, with SPNs designated with white arrow, at E10 in embryos which were labeled with Clomeleon at E3. E) Analysis of SPNs also revealed a reduction in ratio in GBZ-treated cells. Hierarchical bootstrapping test confirmed lower ratios in GBZ-treated cords compared to control cords (GBZ = 1.66 ± 0.04, H2O= 1.86 ± 0.07, $p < 0.0001$). Finally, linear mixed effects test was performed on entire dataset, which determined difference between groups is explained by fixed effect of treatment group, not driven by random effects such as embryo number or experiment date ($p < 0.005$). See supplemental Figure 1 for additional statistical treatment of data.

plasticity occurring in the SPNs or act as a simple relay. As PGNs receive exclusively cholinergic input from SPNs, we attempted to trigger HP using *in vivo* pharmacological block of ionotropic nicotinic receptors, using Hexamethonium (Hex), a ganglionic nicotinic acetylcholine receptor (nACh-R) antagonist.

We first sought to better define the developmental stage at which the SPN-to-PGN connections were established [55, 60, 104, 163] and to ensure the synaptic connections were strong enough to reliably induce spiking activity in the postsynaptic PGNs. To this end, we isolated several segments of the paravertebral chain between the second lumbo-sacral segment (LS2) and LS7 and stimulated the SPN axons using a suction electrode containing the IGN between LS1/LS2 (Figure 2.3A). Therefore, stimulating the rostral end of the tissue allowed us to stimulate any preganglionic axons which were projecting in the caudal direction from LS1 and above [262], while recording the resulting volley through preganglionic fibers as well as synaptically-driven spiking activity in the postsynaptic PGNs. The recording suction electrodes were attached to the IGN at LS 5, 6, or 7. Stimulations were provided every 60 seconds, at 4x threshold for eliciting the compound action potential volley (Figure 2.3B). The PGN discharge was measured as the average of the rectified, filtered voltage trace for the indicated 10 ms period (Figure 2.3B, green box) normalized to the 10 ms pre-stimulus period (Figure 2.3B, gray box). To confirm that activity observed was induced by synaptic transmission, we added the nicotinic antagonist Hex (100 µM) to the circulating solution (Figure 2.3B). At E10, minimal synaptic activity was observed, but did not surpass 2x baseline noise levels (Figure 2.3C, green, dashed line represents mean). Further, the addition of 100 µM Hex did not significantly affect these measures of synaptic discharge in any of the E10 experiments (Figure 2.3C). At E13, 3 out of 4 preparations exhibited synaptic discharge greater than 2x that of the baseline, which was significantly lower with the addition of 100 µM Hex (Figure 2.3C). At E17, all 7 preparations exhibited clear synaptic discharge,

larger than that which was observed at E13 (between 3.1 and 6.2x baseline amplitude, Figure 2.3C). This prominent synaptic activity at E17 was significantly reduced by addition of 100 µM Hex (Figure 2.3C). Importantly, preparations that did not express synaptic discharge were only included in the analysis if the stimulus reliably produced a clear orthodromic volley, demonstrating that the presynaptic SPN projections were successfully stimulated and projected down to that ganglion. Taken together, this evidence demonstrated that E13 is the developmental age at which the impact of synaptic transmission begins to increase rapidly. Therefore, to test for a homeostatic response we chose to begin synaptic blockade at this timepoint.

Intrinsic excitability of PGNs

Measuring scaling was not possible, as the typical method for determining scaling involves measuring the amplitude of mPSCs, but these spontaneous events were infrequent in this preparation, thus preventing us from assessing scaling. Instead, we examined homeostatic changes in intrinsic excitability, as this mechanism of HP has been observed in embryonic spinal MNs following synaptic blockade [250].

Because the SPN to PGN synaptic connection was shown to be functionally intact and able to produce reproducible synaptic discharge beginning at E13, this developmental stage was used to block synaptic input to PGNs and assessed homeostatic changes in intrinsic excitability 48 hours later, at E15. At this time, the sympathetic chain was isolated, and cellular excitability was examined via whole cell recordings of PGNs. Values were compared between embryos treated for 48 hours with 100 µM Hex and those treated with vehicle ($_d$H2O). Neurons had a mean of resting potential of -44.5 mV and were held in current clamp at -70mV $\pm$ 5mV, before adjusting for liquid junction potential. Progressive depolarizing steps (500 ms duration, 5 pA step interval) were given (Figure 2.4A). Surprisingly, following 2-day in ovo blockade of ganglionic nicotinic transmission, f/I relationships from Hex-treated embryos showed

Figure 2.3: Synaptic connection between SPNs and PGNs begins to be functional around E13

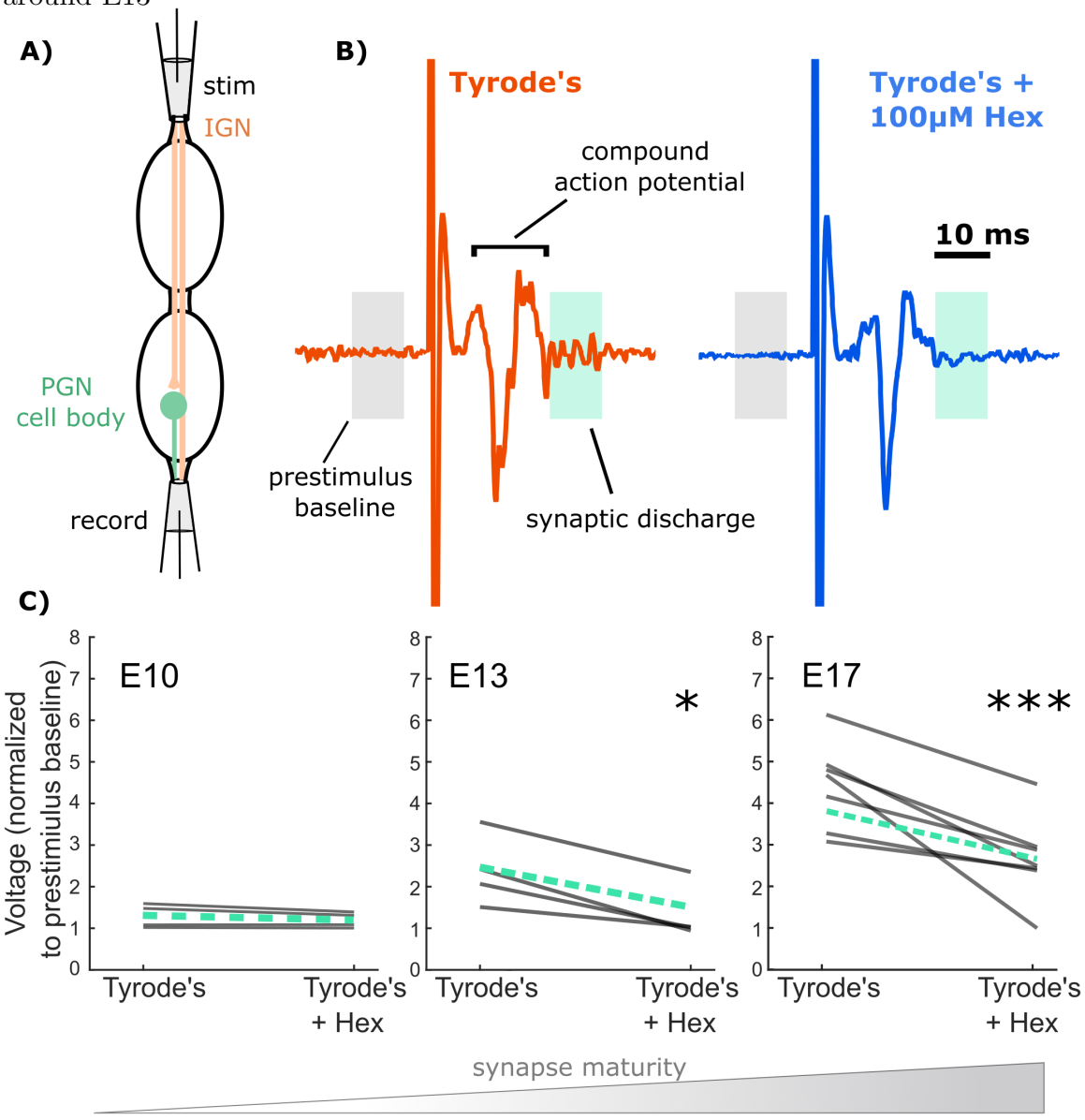

PGNs develop mature synaptic activity between E13 and E17. A) Schematic of PGN extracellular recording set up. B) Example traces at E17 show evoked response, including synaptically-driven discharge in PGNs (highlighted in green box, 10ms), followed by a reduction in discharge after the addition of 100M Hex into the bath. C) The reduction of discharge was calculated across many trials for the following developmental stages: E10, E13, and E17. Paired, two tailed t-tests revealed the following: At E10, there was no difference in discharge after the addition of Hex ($t(3) = 1.8$, $p = 0.17$) At E13, there was a significant reduction in synaptic discharge with Hex ($t(3) = 6.6$, $p < 0.01$). At the E17 stage, the activity was significantly reduced after addition of 100M Hex. ($t(6)=-4.6$, $p < 0.005$).

Table 2.1: Comparison of passive membrane properties and action potential features. Mean values are listed with standard error. Statisical values reflect the degrees of freedom for each measure, compared using a two-tailed, unpaired t-test. ($p < 0.05 = *$)

Table of membrane properties	*Vehicle-treated*	*Hex-treated*	*t-statistic*	*p-value*
Capacitance (pF)	*25.3 ± 3.5*	*23.5 ± 4.5*	*t(15) = 0.31*	*0.76*
Resting membrane potential (mV)	*-56 ± 2*	*-59 ± 1.7*	*t(15) = 0.3*	*0.77*
Rheobase (pA)	*30.4 ± 4.9*	*44.7 ± 6.1*	*t(14) = 1.82*	*0.091*
Input resistance (MOhm)	*1052.7 ±115*	*788.6 ± 110*	*t(12) = 1.72*	*0.11*
Threshold voltage (mV)	*-54 ± 1.3*	*-51 ± 2.4*	*t(15) = -1.19*	*0.25*
Action potential half-width (ms)	*4.4 ± 0.5*	*2.7 ± 0.2*	*t(13) = 2.15*	*0.051*
After-hyperpolarization amplitude (mV)	*10.2 ± 1.6*	*10.5 ± 1.7*	*t(14) = -0.11*	*0.91*
Action potential peak amplitude (mV)	*12.6 ± 2.3*	*24.7 ± 3.5*	*t(14) = -2.94*	*0.011**
Membrane time constant (ms)	*26.8 ± 5.2*	*18.4 ± 2*	*t(15) = 1.3*	*0.21*
Slope of rising phase (mV/ms)	*8.5 ± 3.4*	*8.1 ± 2.2*	*t(14) = 0.25*	*0.81*

a rightward shift compared to those from vehicle-treated embryos, demonstrating that intrinsic excitability in PGNs had been reduced after nicotinic blockade (Figure 2.4B). To validate this finding with more rigorous tests, linear mixed effects and logistic regression for sigmoidal curves were used, confirming the strong effect of Hex treatment in reducing intrinsic excitability (Figure 2.4D). This result was opposite to what we would expect if there had been a compensatory shift towards increased excitability in response to the reduction of excitatory synaptic drive. To better understand the effect of Hex treatment on PGNs, we performed post-hoc analysis of passive membrane properties and evoked action potential properties (Figure 2.4C) and these values are summarized in Table 1.1. Peak amplitude of action potentials was significantly higher in cells from embryos that were treated with Hex compared to those treated with vehicle (Table 1). The half-width duration was also 38% shorter, on average, in the hex-treated condition. However, this measure fell just outside of statistical significance ($p = 0.051$). It is important to recognize that our recordings likely captured a diversity of ganglionic neuron subtypes [65], but the present study was not able to differentiate subpopulations of PGNs. Taken together, these differences suggest that while there may have been some adaptation in various ion channels, there was no homeostatic shift in overall intrinsic excitability.

Figure 2.4: Following chronic nicotinic blockade, PGNs displayed reduced excitability

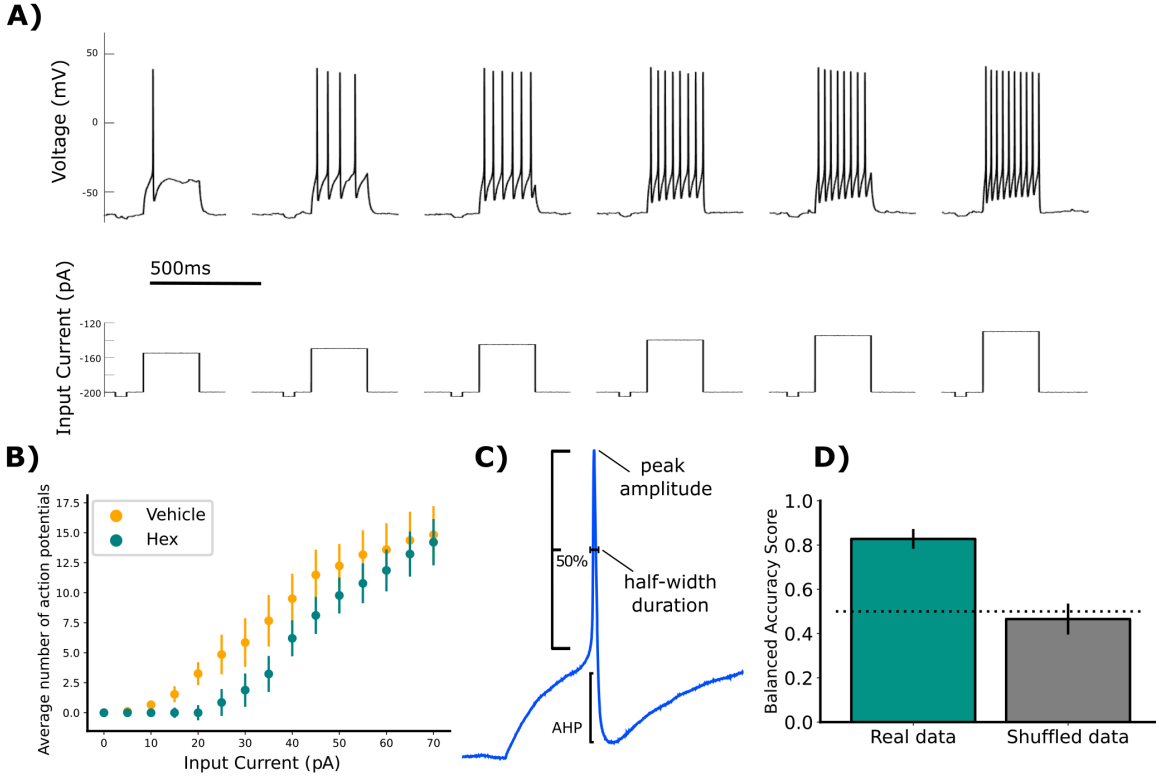

Nicotinic blockade led to a change in excitability in PGNs that did not appear to be in a compensatory direction. A) Progressively increasing depolarizing current steps (500 ms duration, intervals of 5 pA) were delivered every other second. B) Frequency/current (f/I) curve reveals the relationship between treatment condition and excitability of cells. Two-way repeated measures ANOVA revealed a main effect of input current on output number of action potentials, as well as a significant between-group effect of treatment ($F(14) = 32.8$, $p < 0.0001$). Because cords were not evenly sampled, and due to the hierarchical nature of the dataset, a linear mixed effect (LME) model was performed on a linear portion of dataset (20 pA to 55 pA) to verify this effect of treatment group. This analysis showed a significant effect of treatment group ($t(15.49) = -2.28$, $p = 0.037$), and eliminated any effect of potential confounding factors such as experiment date. C) Schematic representation of parameters measured from individual spikes, summarized in Table 1. D) To confirm the effect using all input current values, logistic regression model was trained on a subset of data to predict the treatment group. When given naïve data from the test dataset, the mean accuracy of the model was significantly greater than chance (mean accuracy = 82.7%, $t(28) = 7.29$, $p < 0.001$). In comparison, the model's accuracy when predicting treatment group for a shuffled dataset, was no better than chance (mean accuracy = 46.6%, not different than chance accuracy of 0.50, ($t(28) = 0.63$, $p = 0.54$), further validating the effect of treatment group.

2.4.3 No homeostatic adjustment to synaptically-evoked PGN discharge following acute nicotinic blockade

This decrease in membrane excitability was in the opposite direction than expected for the expression of HP. However, there are some forms of homeostatic synaptic plasticity that occur rapidly, including acute changes in intrinsic excitability that take place within hours of blockade [86]. To determine if we could observe an acute homeostatic adjustment to an evoked response, we reduced synaptic input while examining the SPN-evoked response in the sympathetic chain *ex vivo* over several hours. Here we used E17 preparations which express robust evoked firing, such that it would be possible to observe discharge even after adding Hex (Figure 2.5, also see methods – extracellular recordings). We stimulated SPNs with a brief train of 3 pulses (20 Hz) every 5 minutes, comparing synaptic discharge before and after adding sub-saturating concentrations (50 - 100 µM. n = 3 experiments) of Hex to the bath. We found that this reduction of synaptic input to PGNs led to a reduction of measured synaptic activity, which showed no evidence of recovering to baseline amplitude levels through the observed 4-hour drug application period (Figure 2.5). Importantly, in the 2 experiments where a washout was conducted, activity recovered towards baseline levels, indicating that the lack of recovery during the Hex condition was not due to the deterioration of the tissue.

2.5 Discussion

The autonomic nervous system homeostatically maintains certain features of body function, such as blood pressure. This system adjusts its output within seconds to accommodate challenges to baseline blood pressure. When challenges are no longer present, the output of the autonomic nervous system returns to baseline. It is unknown how this baseline autonomic output is established during development. Spinal

Figure 2.5: Following acute nicotinic blockade, PGNs show no evidence of homeostatic recovery

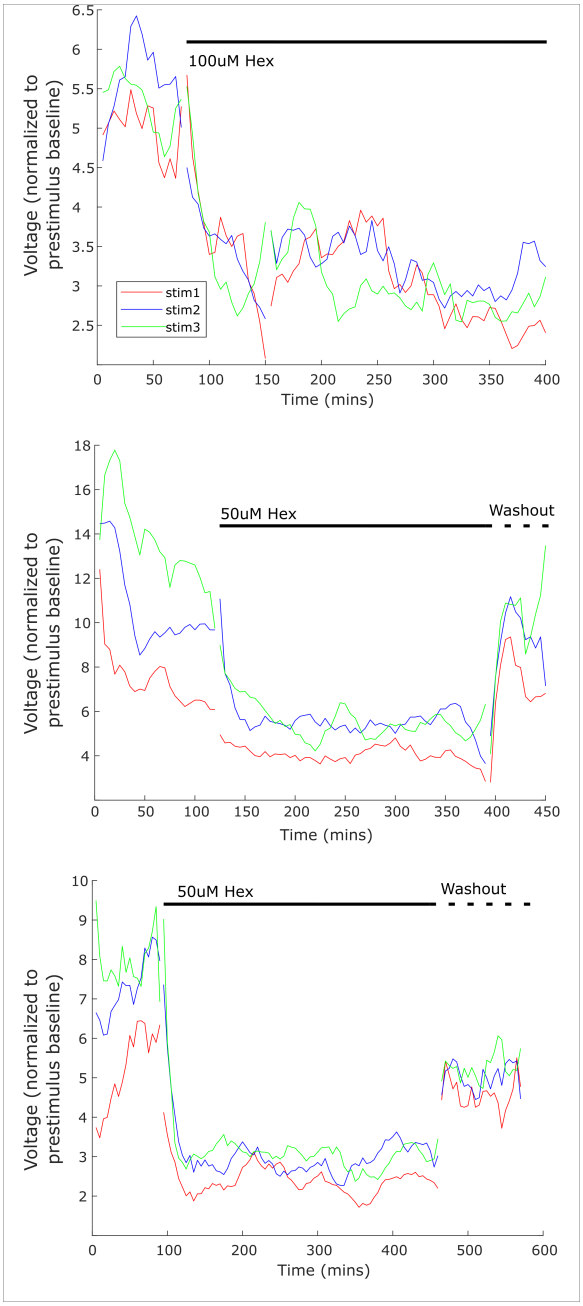

Acute nicotinic blockade resulted in reduction of synaptic activity which did not recover over several hours. Ex vivo preparations of sympathetic chain tissue were used for extracellular recordings in baseline conditions, and during nicotinic blockade using either 50 or 100M Hexamethonium (Hex). Synaptic activity was evoked using a train of 3 stimulations (20Hz interval) every 5 minutes, and the resulting synaptic discharge was calculated at each time point. The synaptic discharge remained reduced for several hours, such that baseline levels of synaptic activity did not recover for 4-5 hours of nicotinic blockade. In two experiments, washout of the drug was conducted. Synaptic activity returned after washout, demonstrating that the tissue was still healthy.

and peripheral neurons of the sympathetic nervous system were examined for evidence of HP during embryonic development. In the central arm of the sympathetic nervous system, SPNs were examined for evidence of GABAergic synaptic scaling. An increase in intracellular chloride concentration was found in the cell bodies of the SPNs 48 hours after *in ovo* $GABA_A$ receptor blockade. This suggests that GABAergic scaling has occurred in SPNs and demonstrates that the mechanism is through chloride accumulation [84]. In the peripheral arm, however, the PGNs did not appear to exhibit homeostatic increases in overall intrinsic membrane excitability. After 48 hours of nicotinic synaptic block, PGNs were less excitable compared to those from vehicle-treated embryos. In separate *ex vivo* experiments at E17, SPN-evoked discharge in PGNs was reduced by acutely inhibiting synaptic transmission, which did not show any signs of recovering within 4 hours of antagonist application (Figure 2.5). Responses to synaptic perturbations of both SPNs and PGNs could contribute to the critical period for the establishment of baseline autonomic activity.

Following 48-hour, *in ovo* blockade of $GABA_A$ receptors at early developmental stages when GABA is known to be excitatory in several circuits [13], intracellular chloride concentrations of SPNs were increased compared to control cords. This indicated that chloride-mediated synaptic scaling had occurred. The finding recapitulated previous studies in somatic MNs of the spinal cord at the same stages, in which the chloride concentrations increased following 24 or 48 hours, but not 12 hours, of $GABA_A$R blockade. In addition, these previous studies in MNs directly demonstrated increases in mPSC amplitude, driven by a depolarization of the chloride reversal potential as demonstrated by both perforated patch and whole cell recordings of mPSCs [84, 142]. These results are the first that we know of to suggest that GABAergic synaptic scaling, or any form of HP, is expressed in developing sympathetic spinal neurons. We have also demonstrated that these SPNs, like MNs, are among the spinal circuitry that participates in SNA during embryonic stages (Figure 2.1D), a

phenomenon which has been shown to be important for proper motor development [169] and maturational tuning of spinal cord synaptic strength [82]. Because SPNs are autonomic MNs that arise from the same progenitor population as somatic MNs [214] it may not be surprising that both SPNs and MNs express SNA and this form of synaptic scaling. In addition, this phenomenon of postsynaptic scaling has been observed in MNs as well as spinal interneurons [142], indicating that this form of HP may be part of a universal mechanism for regulating synaptic strength in the ventral horn of the spinal cord during early development. It is possible that the SPNs exhibit other HP mechanisms, such as those expressed in MNs, but more tests will be necessary to determine this going forward.

The finding that blockade of GABAergic transmission triggers an increase in GABAergic synaptic strength in somatic and sympathetic MNs raises the question: what is the homeostatic goal of GABAergic scaling in this system? While we have not directly addressed this question in the current study, it is clear that the predominant role of GABAergic scaling in somatic MNs of the embryonic spinal cord is the maintenance of GABAergic synaptic input [247]. Our previous work in somatic MNs has shown that GABAergic scaling (by intracellular chloride regulation) is triggered by changes in $GABA_A$ receptor activation rather than changes in spiking activity [73]. If reductions in GABAergic transmission occur during a defined critical period, then increases in intracellular chloride levels could be triggered. If the perturbation is maintained beyond the closing of the critical period, then this could leave the sympathetic circuitry in a hyperexcitable state. This could underlie the vulnerability to perturbations in autonomic signaling during early developmental time points described above [165]. This is the first demonstration we are aware of that shows HP in developing SPNs, which could contribute to a critical period for the maturation of sympathetic circuit excitability. An important next step would be to determine whether this or other homeostatic mechanisms are expressed during a

limited developmental window that could alter sympathetic tone over the long term.

On the other hand, PGNs in the peripheral arm of the sympathetic nervous system did not show evidence of compensatory increases in overall intrinsic excitability following synaptic input blockade (Figures 2.4-2.5). In fact, the difference in f/I curves suggests a reduction in excitability after a 2-day blockade of nicotinic synaptic input. This is consistent with a previous study that demonstrated that sympathetic drive was reduced following *in vivo* silencing of the superior cervical ganglion-pineal circuit [28]. In addition, membrane properties were compared between treatment groups. Only AP peak amplitude significantly differed between treatment groups (Table 2.1), which could suggest a change in voltage-gated Na^+ channel currents. However, any such adjustment did not ultimately result in an overall increase in excitability 48 hours after synaptic blockade with Hex. Moreover, when we examined the PGN circuit *ex vivo* at E17, no recovery of synaptically-induced activity was detected during a 4-hour, sub-saturating application of ganglionic nicotinic receptor antagonist. This suggests that compensatory plasticity is not present on this acute timescale at this age (Figure 2.5). This finding also argues against the expression of rapid forms of HP such as presynaptic HP [44, 80, 64]. Together, our measures of excitability and input/output function of the PGNs after synaptic blockade did not support the expression of HP during embryonic development. In this case, it may be that PGNs do not express compensatory plasticity, instead acting as a simplistic relay to the target tissue at this stage, as some groups suggest [158]. Alternatively, we cannot rule out the possibility that the PGNs express a different form of homeostatic response that was not detected, or that was expressed at a different developmental stage. At E13 and even at E17, PGNs are still relatively immature as several synaptic markers continue to develop well into the post-hatching period [16, 88, 104]. Therefore, the critical period for the expression of HP may exist at a later timepoint for PGNs.

Indeed, while previous work on this topic is limited, some studies suggest that

PGNs have a homeostatic capacity in the adult system [57, 241]. Evidence for presynaptic HP has been shown in adult thoracic PGNs in response to an antibody-mediated perturbation of their synaptic input [241]. The neuromuscular junction (NMJ) expresses this form of presynaptic HP in multiple species [64, 80], and shares similarities with the SPN to PGN synaptic connection. However, we saw no evidence of such presynaptic HP in our work (Figure 2.5). Further investigation is needed to determine whether SPN scaling or reduced PGN excitability play a role in establishing the sympathetic tone and whether these mechanisms could contribute to the development of sympathetic disorders later in maturation [35, 165].

The finding that one sympathetic cell type (SPN) expressed a form of HP in response to 48-hour synaptic blockade, while another (PGN) did not, could suggest that during embryonic development, the central and peripheral components of the sympathetic nervous system each play a different role in the overall maintenance of autonomic setpoint. This discrepancy could be due to intrinsic molecular differences in these cell types. In addition, SPNs and PGNs are at different relative stages of developmental maturity, which may impact their capacity for engaging in homeostatic adjustments. For example, the SPNs undergo their final cell division by E5 and have migrated to their mature location near the central canal to form the column of Terni by E8 [139, 186]. While it is clear that the SPNs are synaptically-driven to express SNA at E10 (Figure 2.1D) and potentially by E4 when somatic MNs express SNA [159], the PGNs do not appear to be synaptically activated until $\sim$ E12 (Figure 2.5, also [60, 163]. Thus, the E13 stage at which PGN input was blocked, is a stage of relative immaturity when compared to the SPNs, and therefore may not have captured their capacity for HP that could exist at later developmental stages. We have demonstrated HP in the developing SNS, and an important next step will be to determine if this plays a longer-term role in autonomic dysfunction following an early life perturbation.

Figure 2.6: Additional statistical analysis further demonstrates increase in SPN chloride levels following chronic $GABA_A$ blockade

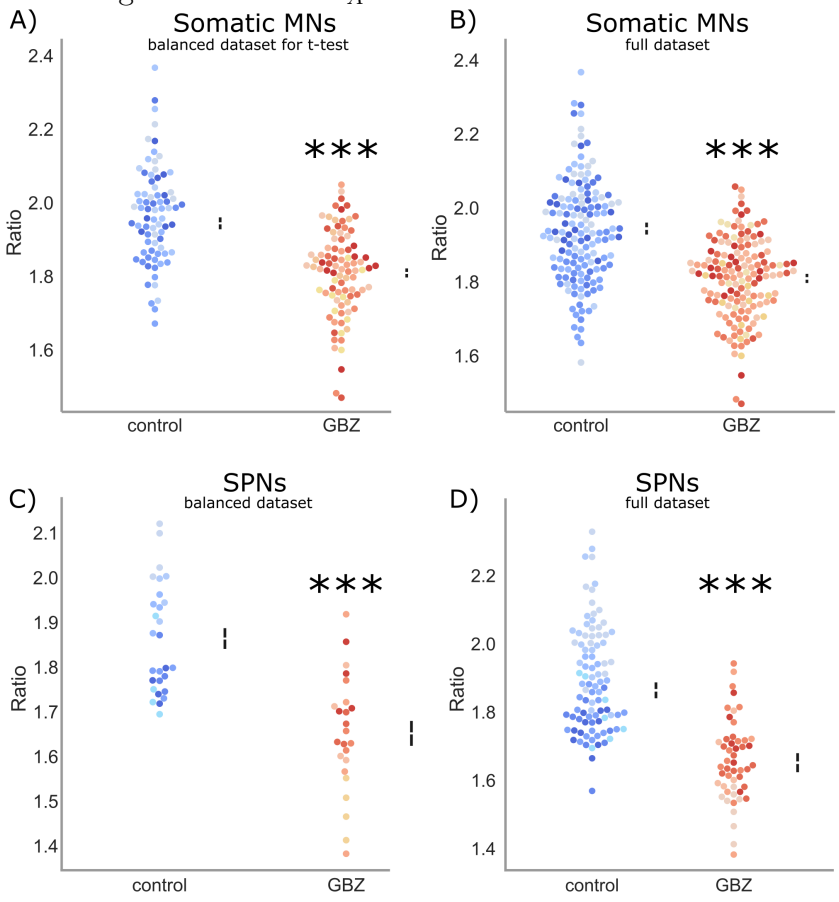

Statistical confirmation of Clomeleon data. A) Motoneuron dataset showed significant difference between control and drug-treated groups. An independent, two sample t-test was performed, restricting data to 10 cells per cord to handle uneven sampling between cords. This test revealed that ratio of YFP:CFP intensity was lower in cells from embryos treated with GBZ (1.81 $\pm$ 0.01) than from those treated with vehicle, (H2O, 1.94 $\pm$ 0.02, $t(175) = 6.7$, $p < 0.001$). B) Full dataset is shown here, including every cell from each cord. This dataset is not suitable for a t-test, however linear mixed effects modeling revealed a significant difference between groups was driven primarily by treatment group, not driven by cord umber or experiment date ($p < 0.001$). C) Analysis of SPNs also revealed a reduction in ratio in treated cells. An independent, two sample t-test using 4 cells per cord revealed that FRET ratio of YFP:CFP were significantly lower in spinal cords from embryos treated with GBZ (1.65 $\pm$ 0.03) compared to those treated with H2O (1.86 $\pm$ 0.02, $t(49) = 5.9$, $p < 0.001$). D) Full dataset is shown here. As number of cells was imbalanced between cords, data was unsuitable for t-test. Therefore, linear mixed effects test was performed on entire dataset. This test determined a significant difference between groups that was explained by treatment group alone, thus not driven the random factors of cord number or experiment date ($p < 0.005$). Bars represent standard error. Notches in bars represent mean.

Chapter 3

A late muscarinic response in PGNs following SPN stimulation may be homeostatic

3.1 Introduction

Previously, I tested the SPNs and the PGNs for homeostatic plasticity mechanisms. Here, I will discuss preliminary studies to test the hypothesis that the PGNs do, in fact, demonstrate preliminary evidence of an acute homeostatic response. In Chapter 2, I showed evidence of chloride-mediated synaptic scaling, a form of homeostatic plasticity, in the SPNs of the chick embryo. In addition, I observed a somewhat unexpected decrease in intrinsic excitability in the PGNs. This shift in excitability moved in a non-homeostatic direction 48 hours after nicotinic blockade *in ovo*. This finding can be explained by several interpretations. First, it is possible that these neurons are simply a relay, and do not express homeostatic compensations in response to activity perturbations, as some theories suggest [158]. Alternatively, some studies have suggested that PGNs do in fact express a form of plasticity that is more Hebbian

in nature [28, 162, 256]. For example, researchers have used chronic light exposure to silence the circuit connecting the hypothalamus, superior cervical ganglion (SCG), and pineal gland *in vivo*. As a result, authors discovered a reduction in axonal branching and expression of the tyrosine hydroxylase an enzyme important for the expression of the sympathetic neurotransmitter in the SCG [28]. This shift towards lower excitability was in a non-homeostatic direction, much like my findings in the PGNs. Thus, it suggests a "positive feedback" relationship between the activity perturbation and the resulting changes within this circuit. In other words, if activity in the circuit were to be reduced, the cells would respond with further reduction of excitability or synaptic strength. Conversely, should activity increase, the cells would respond by strengthening their responses. If this were the case, this shift would be indicative of the expression of a neuroplasticity that is more similar to Hebbian plasticity [18, 97], as opposed to a compensatory expression of homeostatic plasticity, which is a "negative feedback" relationship. This Hebbian-like plasticity appears to also play out downstream from the PGN, as cutting grey rami resulted in reduced excitability in certain targets of the PGNs [256]. Finally, long term stimulation of parasympathetic preganglionic neurons results in a chronic enhancement of their inhibitory output at the target tissue, resulting in a reduction of blood pressure [162]. Again, this result is consistent with a response that is more Hebbian than homeostatic.

The previous findings support the expression of a Hebbian-like plasticity surrounding the PGNs, such that increased activity would result in enhanced circuit excitability, and blockade would result in reduced function. However, another study has found evidence of a mechanism that is consistent with presynaptic homeostatic plasticity in the adult PGNs [241]. Here, experimenters showed that in mice that were injected with antibodies from patients with autoimmune autonomic ganglionopathy, the amplitude of mEPSPs in the superior cervical ganglia was reduced. Researchers did not see an increase baseline level of EPSPs, however, suggesting that perhaps a presy-

naptic increase in vesicle release had occurred. Indeed, authors observed an increase in spontaneous event frequency, consistent with a presynaptic form of homeostatic plasticity. In this chapter we take a closer look at the possibility that homeostatic plasticity could actually be expressed at the SPN to PGN connection in the embryonic chick.

During extracellular studies of acute nicotinic blockade at embryonic day 17 (E17, see Chapter 2, Figure 2.2-2.3), we noticed an interesting finding: that there was a late, long-lasting response that appeared only after the blockade of nicotinic acetylcholine receptors in the *ex vivo* sympathetic chain preparation. This finding was interesting because it only appeared after nicotinic blockade, such that this activity may represent a rapid, compensatory response to the synaptic blockade. This late activity is consistent with earlier electrical characterizations in the lumbar sympathetic ganglia of the anesthetized cat, which suggested that a "late, long-lasting activity" was, in fact, prolonged after nicotinic blockade [107]. Furthermore, this group found that this late activity could be blocked with the muscarinic antagonist atropine, demonstrating that the mechanism of this late-arriving, asynchronous discharge was, in fact, due to synaptic activation of the muscarinic receptors.

The role of muscarinic signaling in the embryonic ganglia has important implications for the interpretation of our findings from Chapter 2. While we did not observe evidence of homeostatic adjustments in intrinsic excitability in these experiments, we cannot rule out the possibility that another form of plasticity, perhaps expressed at a slower latency was induced, and this secondary receptor activation may be the readout. It remained unclear, however, why the muscarinic activity was not expressed under baseline conditions, i.e., in the absence of nicotinic blockade. Could the appearance of this late activity represent a homeostatic response to the synaptic blockade, or was it merely a pharmacological phenomenon? To better understand our previous findings, and to better explain this interesting phenomenon

of hexamethonium-induced late-arriving muscarinic activity, we tested the following hypotheses. First, that the hexamethonium-induced increase in late activity was indeed mediated by muscarinic receptors, as expected based on previous findings [107]. Second, we examined whether this activity was consistent with the idea that more acetylcholine was in the cleft, thus activating the muscarinic receptors. We consider the possibility that this increase in neurotransmitter availability is due to a presynaptic mechanism of homeostatic plasticity. We also discussed the possibility that this increase was a byproduct of an increase in available acetylcholine in the cleft due to the occupation of nicotinic receptors.

To better understand the mechanism and role of non-nicotinic synaptic transmission in the embryonic chick, we first had to characterize the activity and confirm its neurotransmitter identity. Here, we find that the activity was indeed sensitive to Atropine, consistent with it being muscarinic in nature. Next, we performed preliminary tests to uncover whether there is evidence consistent with presynaptic plasticity in this system, and found this to be the case.

3.2 Methods

3.2.1 Chick embryos

White leghorn chickens were used (Hyline Hatcheries, North America), as previously described in Chapter 2. All animal procedures were performed in accordance with Emory University's animal care committee's regulations. Fertilized eggs were kept in the incubator at $\sim$38° C at 65% relative humidity. Embryos were staged according to the duration of time in the incubator and developmental stages were confirmed using Hamburger and Hamilton (HH) staging [93]. For the present study, embryos were used from embryonic day 3 - 17 (E3-E17, stage 15-43 HH). Sex was not determined in these experiments. Embryos aged E17 - E18 (HH stages 43-44) were used for

these studies, as the more developed embryos have more robust activity to test. The amplitude of this late activity was low, therefore this age provided the best chance to see the activity. In addition, some authors have described a slow depolarization that starts around E16 [60].

3.2.2 Tissue isolation

Lumbosacral (LS) segments of chick embryo paravertebral chain (LS 1 – 7) were surgically isolated from the spinal cord, detaching them at the ventral roots by breaking the gray and white rami, in cooled (14-16° C) Tyrode's solution containing the following (in mM): 139 NaCl, 12 D-glucose, 17 $NaHCO_3$, 3 KCl, 1 $MgCl_2$, and 3 $CaCl_2$. The solution was oxygenated (95% O2/5% CO2) throughout the procedure. After isolation was complete, the solution was warmed to 18° C and the tissue was allowed to recover 1-2 hours. Following recovery, the tissue was transferred to a recording chamber, which was circulated Tyrode's solution, oxygenated as above, and held at 27 ± 1° C for electrical recording or imaging [181].

3.2.3 Extracellular recordings

The methods for extracellular recordings using suction electrodes have been described in Chapter 2. To reiterate: Extracellular recordings of evoked synaptic activity were conducted using two suction electrodes, one for stimulating the rostral end of the paravertebral ganglia and one for recording at the caudal end. Electrical signals were measured using extracellular amplifiers (AC/DC differential amplifier model 3000, A.M. Systems, filtering parameters for capturing synaptic activity: 300Hz high pass, 1KHz low pass). The threshold for inducing a reproducible compound action potential was determined individually for each preparation. This threshold was then tested to determine if it was sufficient to see synaptic activity. A stimulus intensity of 4x threshold was used for each preparation, as it was sufficient for inducing maximal or

near maximal recruitment of preganglionic axons. **Three** stimulus pulses of 0.5 ms duration were delivered through the stimulating electrode at the rostral end of the isolated chain of lumbosacral ganglia. Each sweep was repeated 30-60 times at an interval of 60 seconds. These sweeps were repeated in several conditions: before drug perfusion (Tyrode's) after drug perfusion, and after washout. The induced neural activity was quantified by rectifying the voltage trace and normalizing the amplitude of synaptic activity to the amplitude of a pre-stimulus baseline period. Synaptic discharge was identified by measuring the signal after the SPN orthodromic volley had dropped back to baseline (typically 12-20 ms post stimulus). A period of 10 ms was selected and an average was performed in each sweep to measure the average amplitude of synaptic discharge. The recording window was expanded compared to that in Chapter 2, to include data up to 1 s after the stimulus pulse. This allowed us to capture the late activity. In preps that did not exhibit compound action potential volleys, they also did not express synaptic discharge, and the tissue was presumed to be damaged or otherwise not functional and therefore was not examined further.

3.2.4 Pharmacology

To test the nature of the SPN-PGN synaptic activity, we tested blockade of different acetylcholine receptor types. In order to induce acute nicotinic receptor blockade, a sub-saturating concentration of either 50 µM or 100 µM of Hexamethonium (Hex,Tocris Bioscience) in dH_2O, was used, as well as 2 µM d-tubocurare (dTC, Sigma-Aldrich) in dH_2O to further block nicotinic receptor activation. Next, to induce muscarinic receptor blockade, 1 µM concentration of Atropine (Thermofisher Scientific) in dH_2O was used. All drugs were added to the circulating bath and based on flow rate, can be assumed to have reached the tissue well within 2 minutes of drug introduction.

3.2.5 Statistical analysis

Extracellular data from evoked responses were compiled by taking the average values of 10ms windows of interest from the rectified, normalized traces. Next, this value was averaged across repeated trials to produce an average for each embryo. Where appropriate, these averages were compared between before drug and after drug conditions using paired, two-tailed student t-tests.

3.3 Results

To test the nature of this 'late' activity, we repeated extracellular experiments described in Chapter 2. Examining all experiments using E17 and E18 preparations, we found the same compound action potential response, followed by early discharge in 17 out of 19 preparations. The discharge is consistent with that found in Chapter 2 and replicates previous findings as well [3, 103, 107]. Any preparation that did not express synaptic discharge was no longer considered in the following experiments. This fast activity, which was present as early as 12ms after the stimulus, was assumed to be nicotinic, but we again tested this using Hexamethonium (Hex).

To examine the nature of the early activity, we recorded evoked responses in baseline conditions. Next, we induced acute nicotinic blockade using 50 - 100µM Hex administered into bath. This experiment was conducted in 12 out of the 17 preparations that expressed this discharge. In 12 out of 12 cases, we observed a decrease in the early, synaptic activity (as described in Chapter 2, data not shown here), demonstrating that the evoked "early" activity was indeed mediated by nicotinic receptor activation.

Importantly, in 7 out of the 12 preparations that received nicotinic blockade, we also observed an increase in the amplitude of a "late, long-lasting activity" that occurred from approximately 250 to 600 ms post-stimulus, that was not present in

Figure 3.1: Late activity increases as early activity is pharmacologically reduced

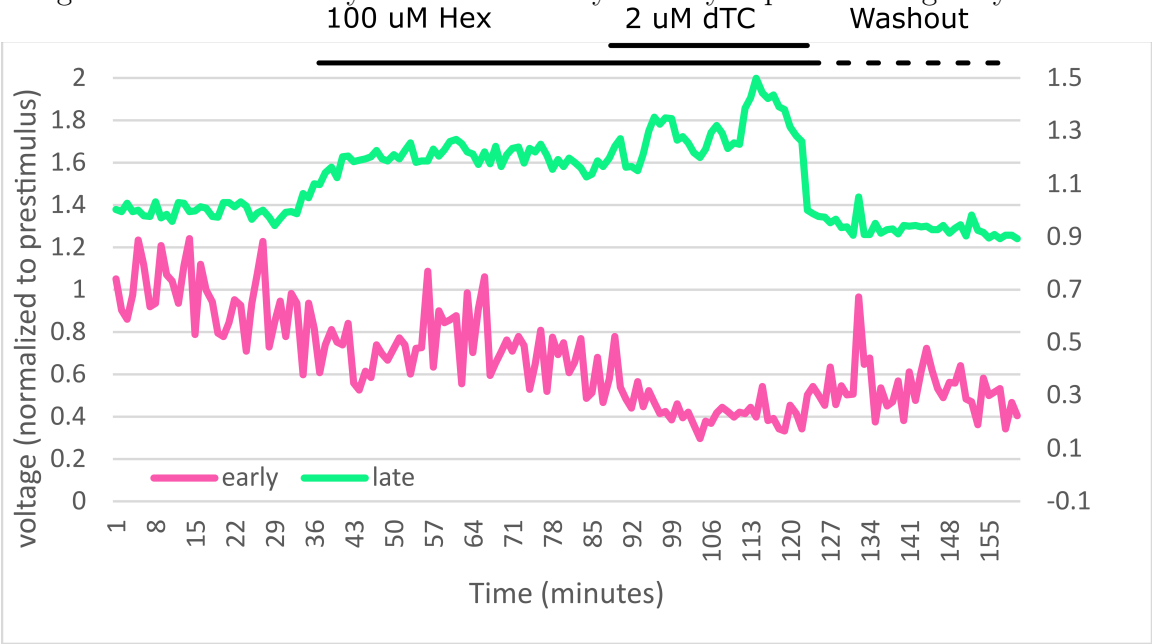

Following blockade of nicotinic receptors, the "late" activity signal increases as the "early", nicotinic activity is suppressed by nicotinic receptor blockade. The circulation of Hex began at 30 minutes, and dTC was added at 90 minutes. The washout began at 120 minutes. The y-axis which denotes the rectified, averaged voltage for the early activity (pink, thought to be driven by nicotinic receptor activation) is on the left, and is normalized to prestimulus baseline. The y-axis for the "late" activity (green, thought to be associated with muscarinic receptor activation), calculated in the same way, is on the right.

predrug baseline conditions (Figures 3.1 and 3.2). The discharge increased, on average, by 28.9% and the range in values was considerable. The lowest increase was approximately 3.6% (though baseline amplitude in this prep was sometimes occluded by noise) and the largest increase was nearly 72%. This late activity began to appear within minutes of the addition of Hex, and the increase appeared to be in parallel with the reduction in the fast discharge (Figure 3.1). This result was consistent with previously described, atropine-sensitive activity, which also increased in amplitude after nicotinic blockade using Hex [107]. The increase in late activity is likely the result of increased activation of the muscarinic receptors, possibly due to greater available acetylcholine at the synapse. In many cases, the late activity could be increased with a higher stimulus or with the addition of 2 µM dTC, a general blocker of nicotinic receptors (see Figures 3.1 and 3.2). Next, in 3 out of the 7 preparations that exhibited late discharge in response to Hex, we tested that this activity was mediated by muscarinic receptors by applying the muscarinic antagonist atropine (1µM) to the bath. In 3 of 3 experiments, bath application of atropine reduced the amplitude of late activity back to baseline levels (Figure 3.2C).

While this is only a first step, these preliminary results support the hypothesis that this discharge was, at least in part, produced by the activation of a muscarinic acetylcholine receptor. Further, this affirms that in the E17-E18 chick embryo, the PGNs express both nicotinic and muscarinic acetylcholine receptors, which can be evoked by stimulus applied to the preganglionic fibers.

This result is important because it opens the possibility that a muscarinic activity could occur in the *in ovo* experiments of chapter two. Still, it is not immediately clear why activation of the muscarinic receptor is triggered by the blockade of the nicotinic receptors. This finding is likely due to an increase in available acetylcholine in the synaptic cleft. We propose two ways that this could occur. First, it could represent a rapid homeostatic response, consistent with an increase in presynaptic vesicle release,

Figure 3.2: Late, muscarinic activity increases after acute nicotinic blockade

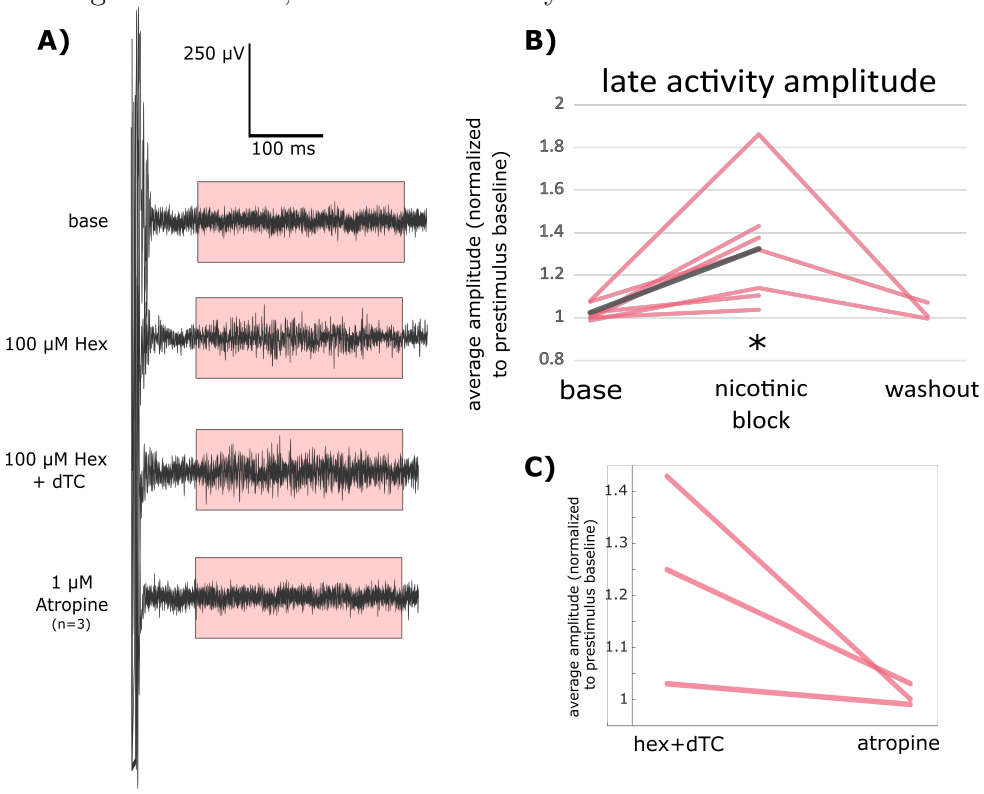

Late activity was induced by nicotinic receptor blockade and abolished by muscarinic receptor blockade. A) Representative traces from one experiment in which late activity (highlighted by red box) is shown baseline conditions, after progressive additions of Hex, dTC and Atropine. B) Averages of the late activity for each preparation, normalized to prestimulus period. This activity was measured in baseline conditions and during nicotinic blockade (average of 7 preparations is represented by black line). Acute nicotinic blockade resulted in increase in late activity (mean 28.9%). A paired, two-tailed t-test revealed that this result was signifcantly significant $t(6) = 3.06$, $p = 0.022$. In 3 out of 7 experiments, a washout was conducted, which effectively returned late activity to baseline levels. C) In 3 experiments, atropine was added. In every case, the addition of Atropine resulted in a reduction in the amplitude of late activity, though this was only a qualitative result (the sample size was too low to examine statistically).

such as the response characterized by presynaptic homeostatic plasticity. Second, this increase could occur because the acetylcholine binding site is occluded by hex, and the acetylcholine in the cleft is therefore unbound and available to bind instead to muscarinic receptors.

Using the data available from these experiments, I have attempted to examine these hypotheses. First, we aimed to test the theory that this activity represents a rapid expression of presynaptic homeostatic plasticity in which more vesicles are released during an evoked response. We could theoretically test the probability of release by assessing the paired pulse ratio before and after the addition of Hex. The paired pulse ratio provides a measure of the probability of presynaptic vesicle release, which is a value that changes when presynaptic homeostatic plasticity is engaged (see Chapter 1 for a more in-depth discussion of this) [12, 181]. While we did not carry out intracellular recordings which are painstakingly slow in this system, we instead used an indirect measure. Here, using an extracellular approach, we stimulated pre-ganglionic fibers with two pulses of the same intensity, at an interval of 50 ms. The probability of release was indirectly approximated by the ratio of discharge (second pulse / first pulse). Therefore, this extracellular data was used as a proxy for paired pulse, and a first approximation of potential change in probability of release. If there were an increase in the probability of release following nicotinic blockade, as would be expected for presynaptic homeostatic plasticity, then we would expect that the ratio would decrease. As such, I have compared the first and second pulses with an interstimulus interval of 50ms, in normal conditions and in conditions of nicotinic blockade using either 50µM Hex, 100µM Hex, and/or 2 µM dTC. Here, in 7 out of 7 preparations tested, I found a modest decrease in the paired pulse ratio in response to the addition of nicotinic blockade (Figure 3.3). On average, the decrease was 12.37%, and the range was from 3% to 18%. The 3 preps with the lowest decreases were those that received the lowest blockade (50 µM Hex), consistent with a dose-dependent

change (Figure 3.3). Together, these results demonstrate that the amplitude of pulse 2 was higher than pulse 1 in baseline conditions. In all cases, this ratio was reduced with the addition of nicotinic blockade. If these results are taken to represent the paired pulse test, this would be consistent with a change in probability of release.

The experiments in this chapter provide several vital findings: first, that muscarinic signaling is active in the chick embryo by E17. Second, muscarinic signaling appears to increase after acute, *in vitro* addition of pharmacological blockade of nicotinic receptors, whether by 50uM Hex, 100uM Hex or a combination of Hex and dTC. These findings are consistent with previous literature [107]. Further, as a preliminary test to better understand the increase in muscarinic activity, we conducted an extracellular proxy of the paired pulse test. Here, the paired pulse ratio of synaptically-evoked discharge decreased after nicotinic blockade. These results are preliminary, but nonetheless they provide an important first approach at explaining the nature of SPN-to-PGN late synaptic transmission and the potential expression of homeostatic plasticity in the SNS of the chick embryo.

3.4 Discussion

The aim of these experiments was to determine the mechanism underlying the finding that muscarinic-mediated late activity is only revealed during conditions of acute nicotinic blockade. The increase in muscarinic activation is likely the result of increased acetylcholine in the synaptic cleft. However, the mechanism which causes this increase could be of a homeostatic nature or simply a byproduct of pharmacology. The increase in muscarinic transmission after a decrease in nicotinic activation is a question that has interesting implications in understanding this system [109], and could provide insight into our findings from PGNs in Chapter 2. Ultimately, we are interested in understanding whether the PGNs possess some cellular mechanism

Figure 3.3: Extracellular paired pulse ratio reveals a reduction after acute nicotinic blockade

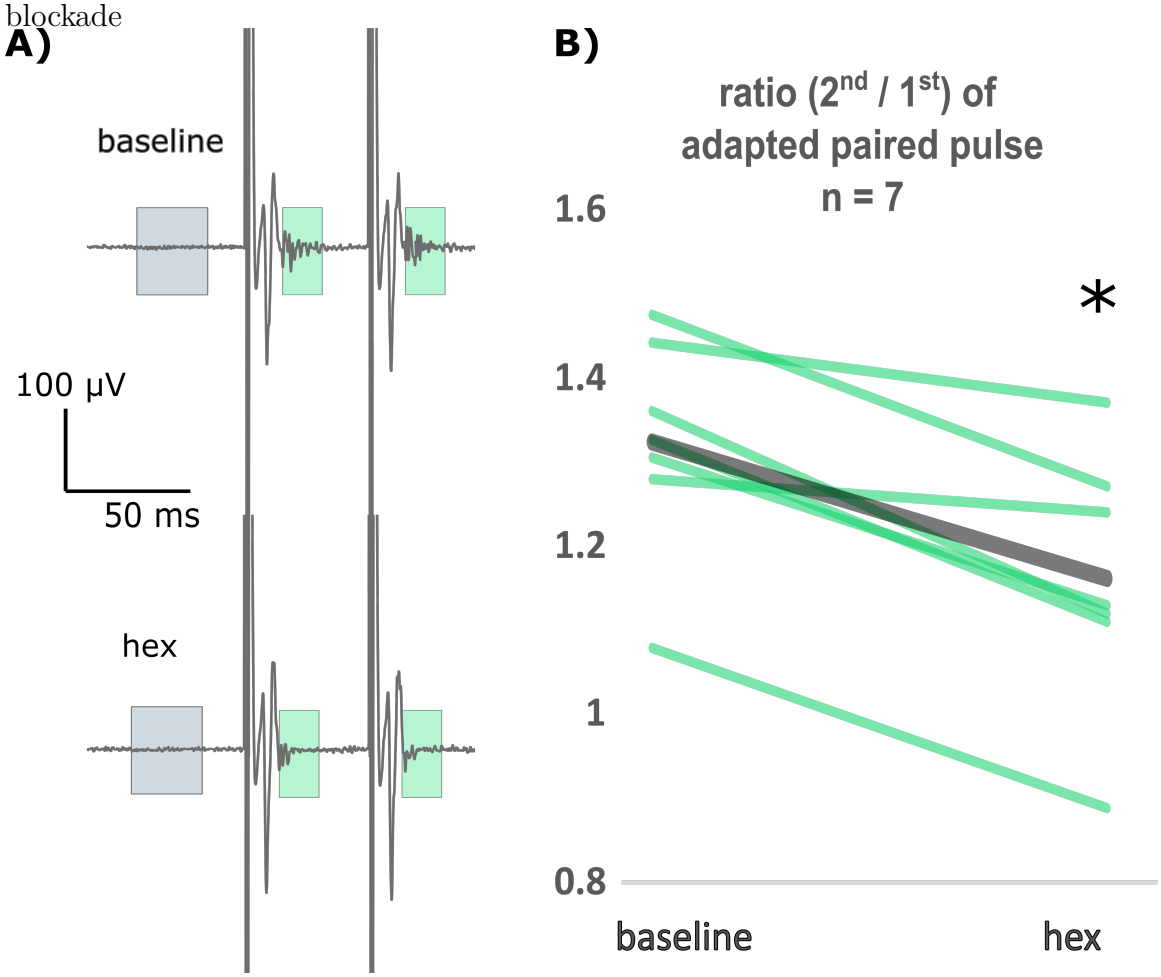

Evoked responses indicate a that the ratio of synaptic discharge in response to 2nd to 1st pulse had changed after nicotinic blockade. Left, the examples traces demonstrate the synaptic response to stimulation of preganglionic fibers (green boxes), which were normalized to prestimulus period (grey box). Right, after nicotinic blockade, the ratio of 2nd to 1st pulse decreased (n = 7, grey line represents mean). A paired, two-tailed t-test revealed that this result was significantly different between treatment groups. t(6) = - 5.59, p = 0.001.

to regulate their own activity in a homeostatic manner. One way this increase in acetylcholine in the cleft could occur is through a presynaptic increase in probability of vesicle release, a well-known mechanism of homeostatic plasticity that occurs at neuromuscular synapses [80, 239]. We examined this question using an indirect approach in extracellular studies. On the other hand, could this phenomenon simply represent the fact that muscarinic receptors are activated by acetylcholine when there is an abundance of the neurotransmitter in the cleft, due to the nicotinic receptors being occupied? We cannot resolve this question with the current study, but future directions are discussed below.

In order to better characterize this finding, we tested whether the activity was due to activation of muscarinic receptors. Within minutes of treatment with atropine, the late activity was reduced to baseline levels, consistent with previous work [107], suggesting that the lumbosacral PGNs of the E17 chick embryo have intact muscarinic signaling at this age. Interestingly, this activity was only apparent after blocking nicotinic receptors. This could be evidence of a homeostatic mechanism of presynaptic release, or it could be the outcome of a pharmacological phenomenon. In either case, it is an important step in understanding the signal transduction in this developing system. In order to test for rapid, presynaptic mechanisms of plasticity in the PGNs, we indirectly examined the paired pulse ratio using extracellular examinations of many fibers and compared baseline conditions to conditions of nicotinic blockade. At baseline, the ratio of the second pulse divided by the first pulse was always greater than one. The change in the ratio of 2nd:1st pulse is consistent with the idea that more vesicles are released following nicotinic receptor block. While these are indirect extracellular measures of a threshold event (action potentials) based on the stimulation of many fibers, it is still clear that the postsynaptic discharge evoked by the second stimulation is reduced in comparison to the first after partially blocking the postsynaptic receptors. Therefore, it is a reasonable next step to conduct further

tests using intracellular techniques to confirm a change in presynaptic homeostatic plasticity. Interestingly, if presynaptic release had increased, I might have expected to see an increase in response during my acute studies in chapter 2 (Figure 2.5). One reason I might not have seen the increase is that the increase in probability of release is known to occur very quickly [181], and therefore the increase might have not been apparent. It is possible that this change was expressed, and actually prevented a more dramatic decrease in synaptic discharge, though this is purely speculative.

It is important to acknowledge the limitations of this study. As previously mentioned, these recordings are only a proxy of a paired pulse test and should only be interpreted as a first step. Further, while these experiments provide insight into the nature of signal transduction in the embryonic PGNs, they were not conducted *in vivo*. Instead, the measures were recorded in an *ex vivo* preparation, using sympathetic chain tissue that was isolated from the rest of the body. Also, these experiments are conducted using a relatively large stimulus which likely do not replicate the tonic activation that the PGN would experience *in vivo*, and therefore these tests should be repeated in the living system and should otherwise be interpreted with caution.

Another method by which the acetylcholine in the cleft could increase after the addition of hex is based on the pharmacology of the blockade. Perhaps the number of vesicles released remained constant, but by blocking the nicotinic receptors, more molecules of acetylcholine were unbound from the receptors and therefore available to bind to the muscarinic receptors. As a future direction, one could test this idea by inducing a similar increase in unbound acetylcholine and see the evoked response. For instance, one could find a way of maintaining transmission of nicotinic receptors, while occluding them from binding with acetylcholine, such as with a competitive agonist. Theoretically, this agonist would occupy the acetylcholine binding location, allowing the ion pore of nicotinic receptors to open normally and should prevent any presynaptic HP because the receptor is not blocked. Alternatively, one could use

methods to detect changes in the amount of neurotransmitter that is released between conditions. This could be achieved using the sniffer-patch method [7].

Demystifying the interplay between nicotinic and muscarinic transmission in the developing system could have important implications for the functioning of the SNS [109]. Ultimately, these approaches, in combination with future directions discussed in the following chapter, will be important to determine whether homeostatic or Hebbian-like forms of plasticity are expressed in the PGNs, and whether this expression occurs during, or outside of, a critical period of development.

Chapter 4

Conclusions and Future Directions

4.1 Summary

Throughout this thesis, I have discussed the importance of understanding the role of homeostatic plasticity in the developing spinal and peripheral neurons of the SNS. Briefly, it is crucial to understand the mechanisms which contribute to the development of ANS setpoint, as early perturbations in autonomic functioning can lead to long-term consequences [165], indicating that this may be a critical period during which expression of homeostatic plasticity is present to ensure proper establishment of baseline excitability. To summarize my results, the studies outlined in Chapter 2 resulted in the following findings. First, that the SPNs are active as part of the network that participates in SNA, at E10. Second, these results demonstrate for the first time that homeostatic plasticity, specifically GABAergic synaptic scaling, is expressed in the SPNs through the mechanism of chloride accumulation, as has been previously determined in the somatic MNs [84, 142]. This is an important finding in the field of SNS development because the expression of homeostatic plasticity during early development could contribute to a critical period in development. Determining this critical period would help to understand and ultimately attenuate the

negative health outcomes due to early vulnerability to perturbations in autonomic functioning. Therefore, in addition to being an important contribution to the field of homeostatic plasticity, formulating a better understanding of a potential critical period in SNS development would be an important step in expanding our knowledge of health outcomes in the neonatal nervous system.

In Chapter 2, I provided evidence to suggest that SPNs express a mechanism of homeostatic plasticity. Could this mechanism in the SPNs contribute to a critical period for the development of autonomic tone? Because a disruption in input during this critical period leads to an increase in excitability through chloride-mediated GABAergic synaptic scaling, it stands to reason that this change could have a lasting effect on the function of these neurons. When the window of plasticity closes, the circuit has established its baseline and it is no longer responsive to homeostatic adjustments, even if the perturbation during the critical period is no longer engaged. Perhaps this is the process by which early perturbations lead to long-term hyperexcitability of autonomic tone, while perturbations that occur outside the window do not have the same result, as has been seen in other systems [33, 52, 75]. Of course, this is only a speculative theory, and many future tests would be needed to confirm this.

Next, the results from chapter 2 revealed that the peripheral neurons of the SNS, the PGNs, did not exhibit a compensatory shift in excitability in a homeostatic direction in response to synaptic blockade. In fact, rather than an increase in excitability, the PGNs showed a reduction in overall intrinsic excitability following a 2-day blockade of nicotinic synaptic activity. This shift was in the opposite direction than would be expected for the expression of a homeostatic adjustment. This result could suggest that the PGNs do not, in fact, express the mechanisms of homeostatic plasticity that are commonly seen in the CNS. In fact, some suggest that the PGNs are merely a relay [158] whose job is to reliably distribute the signal from the spinal component

of the SNS without adjusting the signal. In some ways, it would make sense that the PGNs do not express this plasticity, because the SNS is an entire circuit, with several components of sensory feedback. Each cell population along the circuit plays a different role in the integration, sensation, and response to environmental changes. It is possible that only central components show these forms of plasticity, as they have to adjust to many more inputs.

There is evidence that the PVN of the hypothalamus, the main control center of the SNS is instead the primary place for integration, regulation, and cellular homeostatic plasticity of the system. For instance, in a review of spontaneously hypertensive rats [38], authors discussed several findings that suggest changes in "pre-sympathetic" neurons (neurons which would ultimately innervate the SNS) in the PVN that are consistent with homeostatic mechanisms. For instance, measures of increased excitability in these pre-sympathetic neurons have been attributed to reduction in GABAa receptor-binding [126], as well as changes to chloride cotransporters including NKCC1 [257], and adjustments in reversal potential for GABA. Each of these mechanisms is remarkably similar to those seen in other systems during expression of homeostatic plasticity. This suggests that the PVN expresses activity dependent plasticity that might act as the regulator. Thus, if the output of the SNS is highly regulated by central components that integrate multiple inputs, perhaps it is necessary that the PGNs simply relay their input to the targets.

My findings demonstrated a decrease in excitability that was more Hebbian in nature than homeostatic (Chapter 2 figure 2.4). Perhaps this cell population is highly plastic during this period, expressing a Hebbian-like plasticity. For instance, Calinescu et al [28] observed a reduction in axonal sprouting in the SCG after activity in the pineal-SCG circuit was reduced. This example follows a "positive feedback" pattern, such that reducing the activity in a circuit resulted in further reduction in excitability in the ganglia. Several other studies suggested similar findings, demon-

strating that reducing input to (and output from) the PGNs resulted in an overall reduction of hyperactivity. For instance, chronic inhibition of input to the PGNs can reduce blood pressure in spontaneously hypertensive rats, [162], and removal of output from PGNs to their targets causes a reduction in measures of sympathetic hyperactivity and inflammation [256]. Thus, perhaps the PGNs possess Hebbian mechanisms, and therefore act as an amplifier of the signal. In this way, the PGNs could enhance whatever sympathetic signal was translated from the spinal cord as the environment changes. This theory makes sense when we consider what happens in the case of hypertension. In this disease, the system is chronically activated, such that sympathetic tone is elevated. Yet, the blood pressure remains chronically elevated, suggesting that the PGNs which act on the blood vessels do not respond by desensitizing their reactivity to this overactive input from the CNS. Perhaps hypertension is a failure of central neurons from enacting appropriate controls over their output. Taken together, these studies suggest that the PGNs may, in fact, express Hebbian-like plasticity.

Still, these theories are distinct from other studies which demonstrate a potential mechanism of presynaptic homeostatic plasticity in the PGNs [241]. Here, the expression of homeostatic plasticity happened over time. It is possible that the system actually employs a combination of mechanisms at different timescales. In fact, one interesting theory suggests that cellular responses are multi-phasic and could implement both Hebbian and homeostatic mechanisms, in different phases [215]. If this model were true, then my findings would suggest that I had only captured the first phase of a plastic response, and perhaps extending my window of study would reveal another phase of plasticity. Additionally, if this model were true, the theories posed by other studies could harmonize as they would not be mutually exclusive. Nonetheless, the subject of homeostatic plasticity in the PGNs is not well understood, and marks an important gap in knowledge, motivating future studies.

Although I did not observe a homeostatic response in PGNs in chapter two (chronic or acute), we did see an increase in evoked activity following nicotinic blockade, which could be considered compensatory. This activity appeared much later than the nicotinic activity and was not present in baseline conditions. To test the nature of this activity, I tested the impact of muscarinic blockade, to determine whether these metabotropic acetylcholine receptors played a role in this activity. To this end, muscarinic blockade did in fact reduce the late activity, confirming that this activity was the result of activation of the muscarinic receptors. These findings mirror previous studies in the mammalian lumbar sympathetic chain [107]. Yet, it was still unclear why this activity was only present during nicotinic blockade. The increase of muscarinic activity in the presence of nicotinic activity was an event which has several interesting interpretations. On one hand, this phenomenon could be due to an increase in unbound acetylcholine after an action potential, because the nicotinic receptors were occupied by hex. On the other hand, another theory suggests that the increase in muscarinic activity represents the expression of a presynaptic form of plasticity which is known to be induced rapidly, and results in an increase in the number of vesicles released from the presynaptic cell during an action potential [46, 69, 181]. We conducted an experiment to indirectly examine this theory, and proposed experiments to test the other. To this point, we observed evidence that is consistent with a modest increase in probability of presynaptic release. This could indicate that a presynaptic mechanism of homeostatic plasticity was induced, although further experiments are needed to confirm this theory. The diverse results surrounding the topic of homeostatic plasticity in the PGN demonstrate the necessity of future studies to determine the mechanism which underlies this phenomenon.

In summary, I have described the results from each chapter and how they fit into the current understanding of these systems. Further, I have speculated that these mechanisms might lend themselves to the formation of a critical period for

the establishment of autonomic tone. These findings lay the groundwork for understanding the cellular mechanisms which govern the central-to-peripheral synapse of the sympathetic circuit during an embryonic period of development. The presence of homeostatic plasticity in the SPNs could potentially play an important role in tuning the input/output excitability during a critical period, therefore setting the baseline for autonomic tone. Further, the expression of plasticity in the PGNs was ambiguous, but the increase in excitability could demonstrate that the majority of the tuning of the SNS circuit occurs in the central component of the SNS, while the periphery uses different mechanisms to define input and output relationships. Altogether, these results give insight into the mechanisms which could underly a critical period for the development of autonomic tone, explaining the enhanced vulnerability to ANS perturbations during prenatal and early neonatal timepoints. However, further investigation is required to demonstrate whether the patterns of expression of homeostatic plasticity in the embryonic SPNs and PGNs indeed represent an important mechanistic difference between cells of the central and peripheral arms of the SNS, and whether they contribute to a critical period for establishing a setpoint for autonomic tone.

4.2 Future Directions

In the previous chapters of this thesis, I have introduced the gap in knowledge, explained my experiments and findings, and interpreted my results. As such this thesis project has answered some important questions about the embryonic SNS. That said, the results presented here have also opened several new questions which would be of benefit to explore in the future.

4.2.1 Identify critical periods and determine the timeline of expression

To begin, in order to understand how the plasticity expressed in the SPNs contributes to a critical period, it is important to first understand whether this plasticity indeed represents a critical period, as theorized. To answer this question, one could use the same model system and perturb GABAergic signaling at multiple developmental timepoints, to determine the following: 1) Is GABAergic synaptic scaling induced if the synaptic transmission of GABA is perturbed at a different embryonic stage? 2) What are the ultimate, long-term outcomes in the adult system, in response to early perturbations? And 3) Does the system induce different mechanisms in response to different perturbations? Conducting the GABAergic blockade just as in chapter 2, but at several timepoints would help to define the critical window in which this system is highly plastic, however this method would be complicated by the fact that the effect of GABAergic conductance changes in polarity throughout development [14]. Furthermore, to test for a true critical period that mimics the human population, it would be important to determine whether perturbations that occur early in life result in altered signaling in the adult system. Important considerations for this type of experiment are discussed below.

To answer this important next question, a series of experiments at different timepoints would be required. To begin, it would be important to examine the long-term outcome regarding autonomic tone and excitability of cells in the SNS, in response to a disruption of autonomic signaling early in development. To test this, it would first be important to select the appropriate model, type of perturbation, timepoints for inducing the perturbation, and timepoint for studying the long-term effects. One would need to compare a timepoint for perturbation that is within the window of plasticity and, as a control, one that is instead outside of the window of plasticity, preferably in the fully mature system. To do this, one must first define the critical period of plas-

ticity. As such, one could conduct experiments in which different groups of animals receive perturbations at different stages, and the outcomes are measured thereafter. To define the critical period, one would need a series of different time points of perturbation. Alternatively, tracking homeostatic recovery using non-invasive, chronic recordings could allow this to be achieved.

Once the critical window has been defined, an important study would be to examine the mechanisms that are involved in inducing plasticity. Thus, I would test whether perturbations other than reducing GABAergic scaling result in an expression of homeostatic plasticity. To examine this, I would induce several perturbations during in the same time window and test the outcomes using the same measure. In the case of sympathectomy, one could induce a perturbation by surgically cutting the white rami, which would cease the communication to that ganglion from SPNs at the same segment. This process would likely be exceedingly difficult in a prenatal system, but this has been achieved in adult systems [256]. On the other hand, one could take advantage of pharmacology, as we did in the present study. As a next step, I would be interested in blocking glutamatergic or peptidergic input to the SPNs. Finally, one could induce a less invasive, *in vivo* perturbation of the SNS such as intermittent hypoxia [152], or chronic light exposure [28], to ultimately test the outcome at later stages. Thus, by interfering with signaling at different places in the circuit, during the critical period and also outside of it, to see the changes in long term outcomes in the adult system.

As an outcome measure, I would be interested in testing changes in sympathetic tone that may have occurred as a result of interfering with signaling during a critical period. For example, I could record HRV, or basal blood pressure, as these measures are well known to be representative of sympathetic tone [37], however a direct measure of cellular excitability would also be required to understand the mechanism behind any change seen in sympathetic tone.

4.2.2 Further characterization of SPN and PGN plasticity

Next, further exploration would be useful for determining the nature of the mechanism of scaling in the SPNs. For instances of glutamatergic scaling, the plasticity that occurs is mediated by an increase in the expression of glutamate receptors on the post synaptic surface [72, 106], which is typically identified by an increase in the amplitude of mPSCs [235]. However, our group has found that GABAergic scaling in the somatic motoneurons in the LMC of the embryonic chick are likely mediated by different mechanisms [84, 142]. Is the form of plasticity that was seen in the SPNs different from that which was observed in the somatic motoneurons that innervate skeletal muscle? It would be important to do intracellular measures in the SPNs, to understand whether GABAergic blockade results in increased mPSCs. Additionally, one could examine whether the expression of receptors changes and whether the alteration in intracellular chloride can be rescued using blockade of chloride transporters.

In the PGNs, evidence was consistent with a lack of expression of homeostatic plasticity, and possibly, an expression of Hebbian-like plasticity instead. Some studies support the latter hypothesis, as discussed in the conclusion section. To test the hypothesis that the PGNs had a Hebbian response to nicotinic blockade, one could examine the system for some of the hallmark features of this set of plasticity mechanisms such as long-term depression (LTD) and long term potentiation (LTP). If it turns out that this mechanism does in fact play a role in the peripheral response to changing activity, it would be an important next step to determine the developmental windows during which this plasticity is expressed. In the end, this would be a very important understanding for diseases of the SNS such as hypertension.

Furthermore, it would be useful to examine whether the changes seen in both cell populations – increased intracellular chloride in the SPNs and decreased excitability in PGNs is bi-directional. Thus, one could test the effect of a perturbation in the opposite direction, producing an increase in synaptic signaling and measure the

resulting changes in these cell networks.

4.2.3 Uncover mechanisms of plasticity in additional componenets of the SNS

As a future direction to better understand how the SNS – a system whose job is to maintain homeostasis – is homeostatically regulated itself, one could explore mechanisms of homeostatic plasticity in additional cell populations along the SNS circuit. For example, in upstream centers such as the PVN of the hypothalamus (Figure 1.1) as there is some evidence that mechanisms of plasticity are expressed here [38, 152]. In addition, the downstream targets of the PGNs, the various target tissues, can be examined to see whether the peripheral components of the SNS have any capacity for homeostatic plasticity. It is well known that presynaptic homeostatic plasticity is expressed in the peripheral targets of the motor system, at the NMJ [64].

4.2.4 Examine effect of spontaneous activity on PGNs throughout development

Another important factor in determining the plasticity in the PGNs is identifying the period of time that the perturbation should be induced. In Chapter 2, I examined the synaptic functional connectivity with regard to evoked activity. While this is important for determining the capacity for signal transduction, this does not necessarily translate to the typical, spontaneous input that is experienced by the PGN in normal conditions. In the spinal cord, however, it is well known that there are regularly occurring episodes of SNA which depolarize the somatic motoneurons as well as the SPNs. This activity very likely plays out into the ganglia, with preganglionic axons propagating action potentials to the terminals and causing vesicle release and depolarization of the PGNs, especially as the synapses are more fully developed, but

we did not show the nature of this activation here. Thus, another important future direction would be to determine at what age the SNA is capable of driving naturalistic output in the PGN. To this end, we could measure spinal cord episodes ex vivo, and record output from the attached ganglia, with intact ventral roots and rami. This surgical procedure has proven to be delicate, but can certainly be done, evidenced by the Texas Red imaging done at the IGN in Chapter 2. Still, this ex vivo preparation does not perfectly replicate the in ovo activity, but it would be a more naturalistic approximation than the stimulus that was provided in our extracellular experiments.

4.2.5 Elucidating the impact of nicotinic blockade *in vivo*

Next, to better interpret the results from the experiments in Chapter 2, I would want to test the hypothesis that the PGNs do, in fact, possess a window of homeostatic response, which was not captured by examining excitability at only one timepoint: 48 hours after synaptic blockade, as in the experiments done in chapter 2. In order to test this prediction, it may be useful to take advantage of the spontaneous episodes of spinal cord activity in the embryo. These episodes result in a useful readout of spinal cord activity, and one might monitor this behavioral readout before in ovo nicotinic blockade, and at several timepoints afterward. This would help to determine whether activity recovers over time, and lends itself to determining the precise timing, as introducing additional timepoints has been highly informative in previous studies with pharmacological blockers [250, 249]. In addition to overall movements, we could measure other outputs of SNS activity. The effect of Hex on the output to the SNS likely includes changes in muscle tone, but also changes in blood pressure, heart rate, and possibly pupil dilation.

To track these changes in ovo, I needed a more precise method for measuring behavior, as previous studies have relied on measuring by eye. Hex may not have as obvious an effect as GBZ treatment, and it is important that experimenter bias

is reduced. Furthermore, obtaining chronic recordings of these measures would be even more advantageous than simply adding a couple of timepoints. This means that the data acquisition technique needs to have the following attributes: 1) higher precision than previous techniques, 2) ability to conduct longer-term recordings, and 3) the ability to be conducted while the embryo remained in the incubator, as these measures, and overall health of the embryo, depend greatly on temperature. To this end, I developed and implemented two novel techniques, one using electrical recordings and another which leverages computer vision to conduct these behavioral experiments. In addition, I developed different computational analysis processes to interpret the data with varying results based on age and visibility of embryo. A summary of the different technical approaches and results thus far has been included in the appendix of this thesis.

While the novel techniques described above and in the appendix are currently undergoing troubleshooting, it is important to note that both can be used to identify limb movements, with varying success depending on age of the embryo, and can also both identify heart rate. Therefore, an important future direction would be to conduct an experiment which could examine the trajectory of some meaningful behavior, to measure the effect of 100uM Hex in ovo, and determine if there is any evidence for homeostatic recovery towards baseline levels of that behavior. This could aid in selecting a more relevant time point for examination of the PGN excitability, as well as in interpreting which mechanism of homeostatic plasticity might have been expressed.

4.2.6 Determine whether the plasticity mechanisms are species-specific

Finally, it is crucial to test the assumption that the findings from these studies should generalize to murine and primate species. While the vast majority of anatomy and cel-

lular mechanisms of the SNS are conserved between species, it is known that there are a few unique aspects of the avian nervous system which differ slightly from mammalian systems. It is also unclear whether species differences would result in differences in the critical period, plasticity mechanisms, or overall development of autonomic tone setpoint.

In summary, this doctoral dissertation project has shown evidence for the expression of mechanisms of homeostatic plasticity in the SPNs, as well as evidence that suggests a Hebbian-like mechanism in the PGNs of the embryonic chick. Future studies to build upon this knowledge could provide evidence to further understand the mechanisms, limitations, and overall circuit dynamics of the developing SNS, and how critical periods and homeostatic plasticity might govern the tuning of the network during early and vulnerable periods. It is important to continue to expand the body of literature which examines the intersection between homeostatic plasticity, critical periods during embryonic development, and the homeostatic regulation of the SNS. This would not only help to grow the practical knowledge of the natural world through deeper understanding of these topics, but also because of the implications in human health with regard to the study of prenatal risk factors, early life trauma, stress management and the overall understanding of development, and treatment of human autonomic disease.

Appendix A

Further analyses and approaches for reference

A.1 Novel methods for long-term tracking of embryonic limb movements *in ovo*

In order to perform long-term tracking of behavior, I designed two entirely novel techniques. Using these methods, I am hopeful to examine the behavioral effect of adding 100µM Hex in ovo, as the readout of spontaneous activity has proved incredibly useful in prior studies [250]. The first technique leveraged the electrical fluctuations that resonate across the chorioallentoic membrane of the chick embryo when kicking behavior occurs. In this appendix you will find explanations and figures for each approach.

In the first section, I used electrical recordings (Figure A.1) and designed several techniques for automating kick detection in the resulting signal. While this method proved to be very accurate at depicting limb movements at E13, it was not useful for younger embryos, as the membrane fluctuations produced by kicks at E8 are more difficult to detect, for example. Further, there was a higher rate of mortality as the

insertion of the wire electrode could introduce bacteria causing an infection, or could puncture the vascular membrane, causing bleeding. Nonetheless, chronic recordings of both heart rate and limb movements were made possible with this technique and the related analysis software which I designed (Figures A.1 - A.2). In order to automate the kick detection, I first examined signal over time, and pulled out the different characteristic movements. In addition to the smoth muscle movements which range from 0-1 Hz, there are sharp peaks in the signal which denote the embryonic limb movements, or "kicks" (see red circles in Figure A.1A and dotted circle in Figure A.1B-C). These kicks were confirmed using visual inspection of the embryo, coupled with video recordings. In addition to the raw signal, the kicks are apparent as spikes in the spectrogram of the recorded signal, which is a breakdown of the component frequencies in the signal over time (Figure **??**).

Next, in order to better process this signal and better isolate the frequencies, I leveraged a wavelet analysis technique (Figure A.2. Here, I used signal processing toolboxes in MATLAB to conduct a wavelet transform with a Haar window (Figure A.2C) to deconvolve the data without aliasing the signal. This process produces scalograms of the recorded signal (Figure A.2C - A.2D), which is a breakdown of the recorded signal into scales - which are roughly representative of frequency bands - with respect to time. The "intensity", or power, of the signal at each pseudo-frequency is represented by a coeficient, which is represented visually as the color, or the Z-axis (Figure A.2C - A.2D). The signal shows a peak across many psuedo-frequencies during an embryonic kick. Thus, this process proved to be highly effective at finding the kicks in the signal, though manual confirmation was still necessary (Figure A.2E). Once the kicks were isolated, I could measure the rate of kicking, the speed of an individual kick, and many other measures of locomotion (Figure A.2F).

Throughout this process, I used video recordings to confirm the accuracy of the electrical recordings. These videos proved to be very helpful. It was extremely ad-

vantageous to have the ability to pause, replay, and zoom in on the videos, not to mention the ability to record for a longer period of time through a glass top incubator while temperature remained stable. This led to the development of my next technique, which was to analyze the videos using deep learning neural networks which were designed for computer vision, in particular for the kind of image recognition that underlies many facial recognition algorithms.

However, there were several challenges that occurred using DeepLabCut neural network implementation. The first is due to the nature of the deep learning architecture which DeepLabCut relies on to build its model (Figure A.3). The architecture is based on a Convolutional Neural Network (CNN), which analyzes the x and y dimension of each frame, but by design is agnostic to the temporal dimension (t) of the data. In other words, while DeepLabCut can be highly effective of comparing each pixel to neighboring pixel in a single frame, it re-evaluates each frame independently, as if they are completely unrelated images without an innate chronological order. While this application may be sufficient for some purposes, it provided a challenge for our purposes likely because 1) our training dataset was limited in volume 2) the contrast in the videos was low due to the similarity of the limbs alongside the membranes and blood vessels, compared to the strong contrast that is seen in the videos used to train the original model (dark mouse against a white background, Figure A.3B). Still, this technique had some exciting promise, as huge amounts of data could be used to train the network with minimal human-hours involved (labeling of body parts in approximately 10% of frames in training dataset).

Next, I attempted to use a different visual analysis technique which has more promise for our data, as it can understand the chronology of the series of frames that make up the video. This method is known as 'optical flow', and it involves taking a macroscopic look at the pixel intensities on a frame-by-frame basis to find periods of large fluctuations. This method leverages the latent computational signal of a digi-

Figure A.1: Electrical recording of embryonic movements

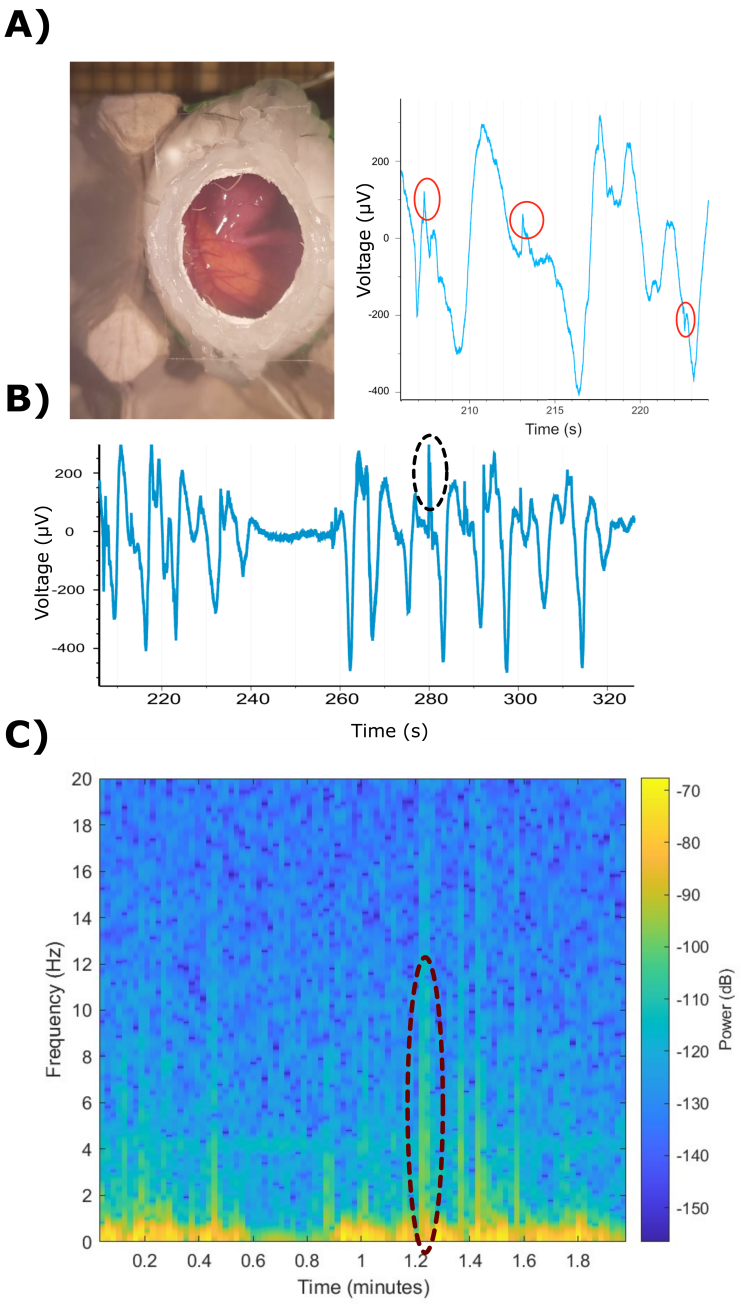

Recording electrical fluctuations were successful in measuring kicking behavior while the embryo remained in the incubator. A) Egg was opened, and electrical wires were implanted into the membrane. The readout (right) included smooth muscle, slow fluctuations as well as sharp 'spikes' in the signal (red circles) which corresponded with the kicks. B) A longer-term recording shows large amplitude, slow fluctuations due to smooth muscle contractions, as well as periods of quiescence, and several large kicks. C) Visualizing the data in panel "B" as a spectrogram revealed a band near 4Hz, consistent with heart rate, and several broadband "spikes" which were synchronous with the kicks.

Figure A.2: Several analytical approaches for electrical signal of embryonic movements

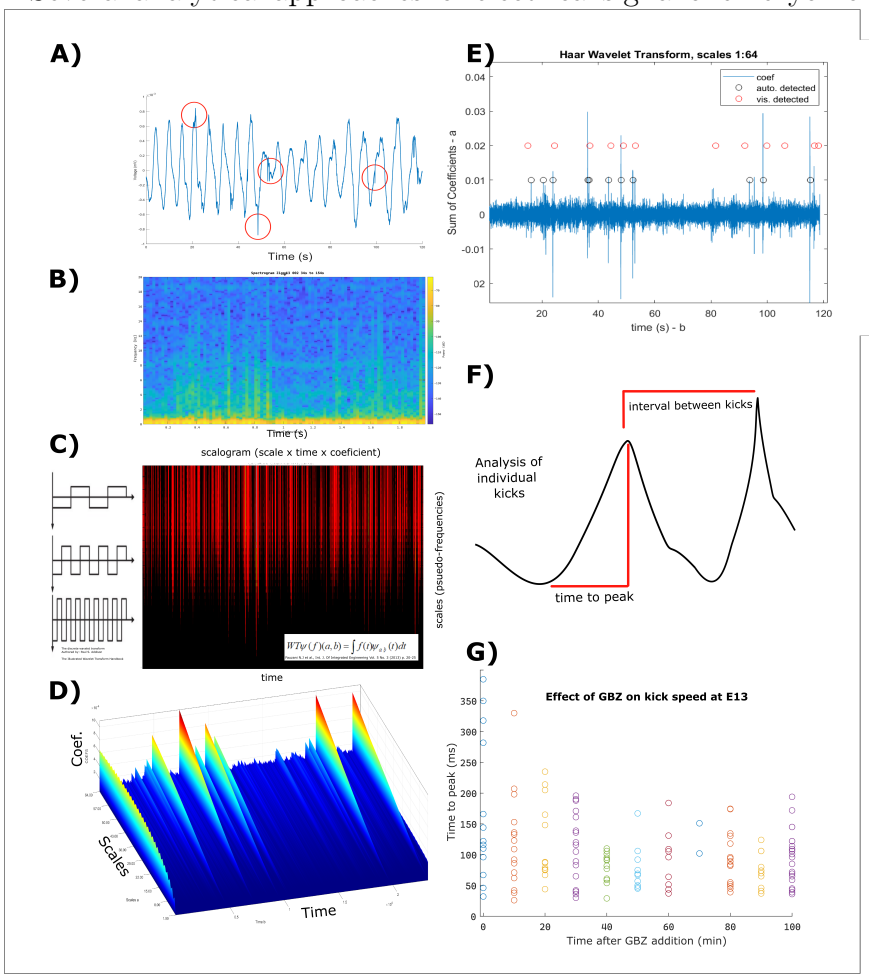

Electrical analysis of embryonic movements in ovo. A) raw signal recorded from E13 embryo. Red circles denote sharp points in the signal that correspond with kicks. B) Spectral analysis of raw signal reveals heart rate (approximately 4 Hz band across signal) as well as 'spikes' that span many frequencies. These events correspond with kicks. C) Conducting a wavelet transform using a Haar wavelet (square shap, left panel) results in a scalogram. Across time (x axis), the coefficient, or "strength" of the signal is expressed as the color of signal (colorbar or z axis). The value of this coefficient is calculated as the coherence between the raw signal and the wavelet, at each size, or 'scale' of wavelet (y axis). Each scale roughly represents a frequency. D) alternative representation of scalogram. Peaks in signal correspond with the times that kicks occurred. E) Calculation of the sum of the coefficient lines. Black circles represent 'kicks' found in the signal after applying a peak detection with threshold parameters. red circles represent times in the signal where the kicks were found using visual analysis of video. F) Using automatic detection to pull out individual kicks for further analysis. Here, measurements sich as slope, time to peak, interval between kicks, length of kicking bout, and interval between bouts. A bout is defined as a period of kicking with no longer than 3 seconds between individual kicks. G) Tracking one measure, time to peak, after the addition of 10 uM GBZ reveals a reduction in time to peak, in other works an increase in the speed of individual kicks at E13.

Figure A.3: Video recordings of embryonic movements and several analytical approaches

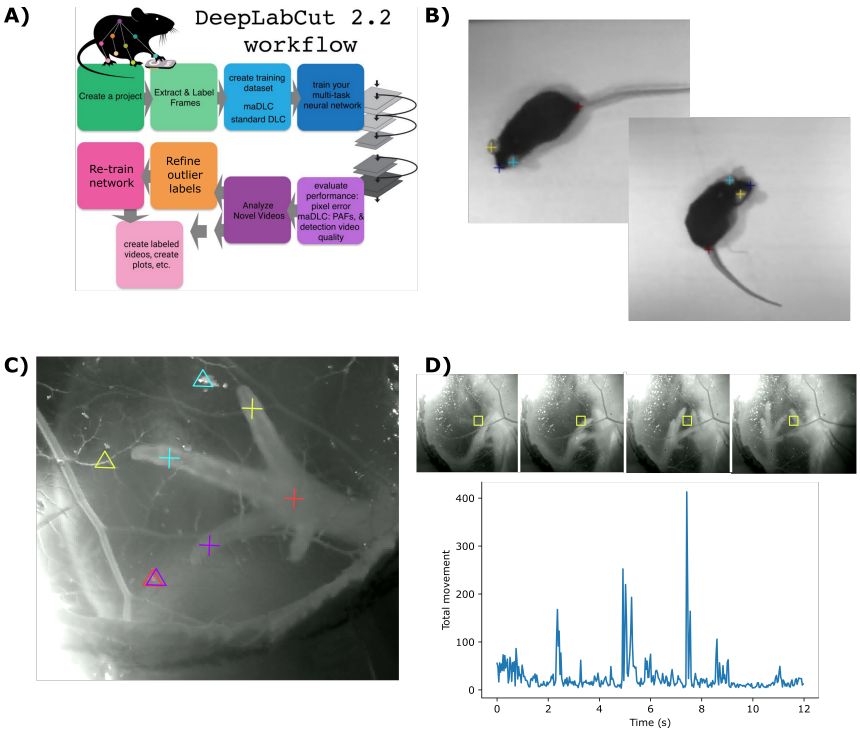

Computer vision techniques for tracking embryonic movements. A) The Deep lab cut workflow. B) The typical training data videos for which the original DLC model was designed. C) The Outcome from first iteration using chicken embryo videos reveal considerable mislabeling, as DLC seems to over-emphasizes edge detection. D) The results from preliminary tests of Optical Flow analysis of video. The peaks in this signal are determined by times in the video with large changes in pixel intensity, and these peaks correlate with the movement of the embryo in the video.

tal video with regard to pixel intensity time, and therefore is more ideal for coarse motion tracking than finely detailed object detection. Therefore, this technique may not be suited for measuring heart rate. Quite simply, the output of this algorithm is measured by the change in intensity values for every pixel, from one frame to the next. On a basic level, once the basic shapes are classified (typically by using an edge detection or corner detection algorithm), optical flow provides the flow vectors of these key features. We can therefore use this tool to estimate latency of movement, velocity of movement, and predict the position of an object in the upcoming frame. In summary, each technique allows for longer term observation in an incubated setting, which is preferable to a room temperature, manually-derived count of limb movements. There are some differences in feasibility of particular kinds of movements with each technique.

A.2 Nicotinic and muscarinic blockade: outcomes for excitability of PGNs

In Chapter 3, I discussed results surrounding the late muscarinic response that appears in the presence of nicotinic receptor blockade. One concern was that this may interfere with my assumption that *in ovo* Hex treatment was sufficient to reduce synaptic input tp PGNs. Therefore, in one experiment, I repeated the measures of excitability from Chapter 2, using ganglionic tissue from an embryo that had received both *in ovo,* pharmacological blockade of both nicotinic and muscarinic neurotransmission (Figure A.4, magenta dot represents the Hex + Atropine condition). In this experiment, each of the following passive membrane properties was measured directly or calculated using other properties: resting membrane potential (RMP), capacitance, input resistance (IR), and the time constant Tau. In addition, the following measurements of evoked action potentials were recorded: threshold voltage, rheobase,

Figure A.4: Intracellular measures following chronic blockade of both nicotinic and muscarinic receptors, N=1

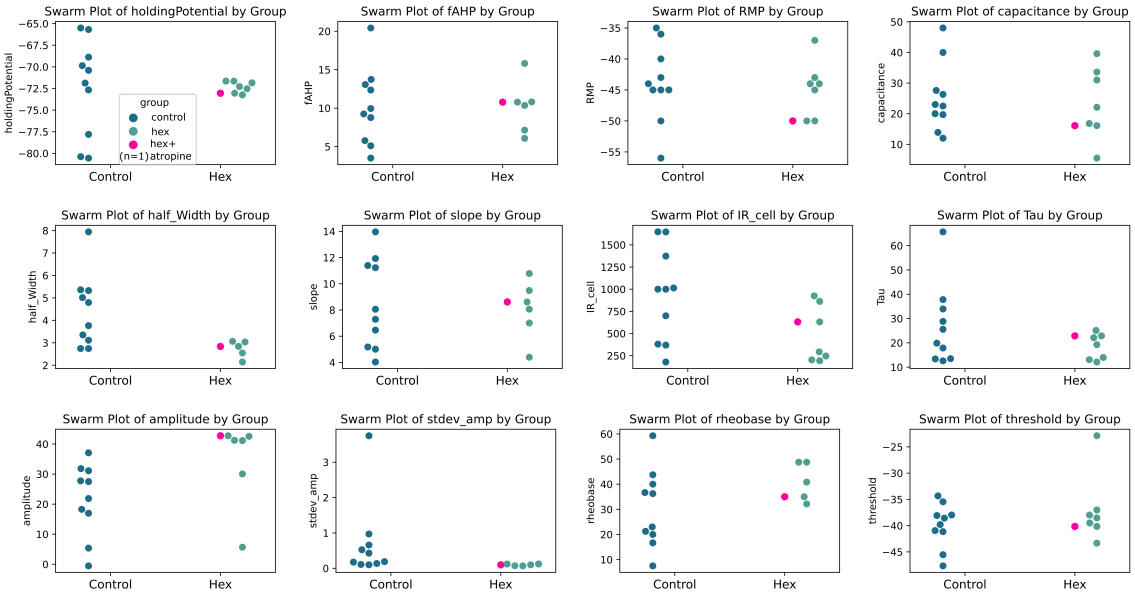

Membrane properties recorded intracellularly from embryos that received either control, nicotinic receptor blockade, or both nicotinic and muscarinic blockade. Each dot represents a single embryo, and was calculated as average of all trials for a particular measure, taken from that embryo (1 cell per embryo). In every measure, these did not differ from the Hex group. Interestingly, this one embryo was among the highest values for amplitude of action potential, which was the one measure that was significantly different between treatment groups.

peak ampliude, rising slope, and half-width duration. For the embryo that received both Hex and Atropine, almost every measures was within the range of values for the Hex-only condition. One exception was the value of action potential amplitude, where the cell recorded from Hex + Atropine condition was nearly equal with the the highest recorded value in the Hex-only condition. Interestingly, this is also the only value that was statistically different between control and test groups, suggesting that the amplitude may be an important feature that is altered after cholinergic blockade, though it is unclear whether this represents a compensatory response akin to homeostatic plasticity. More experiments of this nature would be instrumental for further elucidating this phenomenon.

Bibliography

[1] Emmeke Aarts, Matthijs Verhage, Jesse V Veenvliet, Conor V Dolan, and Sophie Van Der Sluis. A solution to dependency: using multilevel analysis to accommodate nested data. *Nature neuroscience*, 17(4):491–496, 2014.

[2] James B Ackman, Timothy J Burbridge, and Michael C Crair. Retinal waves coordinate patterned activity throughout the developing visual system. *Nature*, 490(7419):219–225, 2012.

[3] David J Adams, S Bevan, and DA Terrar. Modes of hexamethonium action on acetylcholine receptor channels in frog skeletal muscle. *British journal of pharmacology*, 102(1):135–145, 1991.

[4] Ralf H Adams and Anne Eichmann. Axon guidance molecules in vascular patterning. *Cold Spring Harbor perspectives in biology*, 2(5):a001875, 2010.

[5] William A Alaynick, Thomas M Jessell, and Samuel L Pfaff. Snapshot: spinal cord development. *Cell*, 146(1):178–178, 2011.

[6] Mor R Alkaslasi, Zoe E Piccus, Sangeetha Hareendran, Hanna Silberberg, Li Chen, Yajun Zhang, Timothy J Petros, and Claire E Le Pichon. Single nucleus rna-sequencing defines unexpected diversity of cholinergic neuron types in the adult mouse spinal cord. *Nature Communications*, 12(1):2471, 2021.

[7] TGJ Allen. Thesniffer-patch'technique for detection of neurotransmitter release. *Trends in neurosciences*, 20(5):192–197, 1997.

[8] P Ascher, WA Large, and HP Rang. Studies on the mechanism of action of acetylcholine antagonists on rat parasympathetic ganglion cells. *The Journal of physiology*, 295(1):139–170, 1979.

[9] Christina YL Aye, Adam James Lewandowski, Julien Oster, Ross Upton, Esther Davis, Yvonne Kenworthy, Henry Boardman, Grace Z Yu, Timo Siepmann, Satish Adwani, et al. Neonatal autonomic function after pregnancy complications and early cardiovascular development. *Pediatric research*, 84(1):85–91, 2018.

[10] Jaideep S Bains and Alastair V Ferguson. Paraventricular nucleus neurons projecting to the spinal cord receive excitatory input from the subfornical organ. *American Journal of Physiology-Regulatory, Integrative and Comparative Physiology*, 268(3):R625–R633, 1995.

[11] S Bassani, P Valnegri, F Beretta, and M Passafaro. The glur2 subunit of ampa receptors: synaptic role. *Neuroscience*, 158(1):55–61, 2009.

[12] Mark C Bellingham and Bruce Walmsley. A novel presynaptic inhibitory mechanism underlies paired pulse depression at a fast central synapse. *Neuron*, 23 (1):159–170, 1999.

[13] Yehezkel Ben-Ari. Excitatory actions of gaba during development: the nature of the nurture. *Nature Reviews Neuroscience*, 3(9):728–739, 2002.

[14] Yehezkel Ben-Ari, Jean-Luc Gaiarsa, Roman Tyzio, and Rustem Khazipov. Gaba: a pioneer transmitter that excites immature neurons and generates primitive oscillations. *Physiological reviews*, 87(4):1215–1284, 2007.

[15] JA Bennett, PN McWilliam, CS Goodchild, and C Kidd. The location and characteristics of sympathetic preganglionic neurones in the lower thoracic spinal cord of dog and cat. *Quarterly Journal of Experimental Physiology: Translation and Integration*, 71(1):79–92, 1986.

[16] IB Black, IA Hendry, and LL Iversen. Trans-synaptic regulation of growth and development of adrenergic neurones in a mouse sympathetic ganglion. *Brain Research*, 34(2):229–240, 1971.

[17] Wilfredo Blanco, Richard Bertram, and Joël Tabak. The effects of gabaergic polarity changes on episodic neural network activity in developing neural systems. *Frontiers in computational neuroscience*, 11:88, 2017.

[18] Tim VP Bliss and Terje Lømo. Long-lasting potentiation of synaptic transmission in the dentate area of the anaesthetized rabbit following stimulation of the perforant path. *The Journal of physiology*, 232(2):331–356, 1973.

[19] Jacob A Blum, Sandy Klemm, Jennifer L Shadrach, Kevin A Guttenplan, Lisa Nakayama, Arwa Kathiria, Phuong T Hoang, Olivia Gautier, Julia A Kaltschmidt, William J Greenleaf, et al. Single-cell transcriptomic analysis of the adult mouse spinal cord reveals molecular diversity of autonomic and skeletal motor neurons. *Nature neuroscience*, 24(4):572–583, 2021.

[20] Sam A Booker and Peter C Kind. Mechanisms regulating input-output function and plasticity of neurons in the absence of fmrp. *Brain Research Bulletin*, 175: 69–80, 2021.

[21] Sam A Booker, Laura Simões De Oliveira, Natasha J Anstey, Zrinko Kozic, Owen R Dando, Adam D Jackson, Paul S Baxter, Lori L Isom, Diane L Sherman, Giles E Hardingham, et al. Input-output relationship of ca1 pyramidal

neurons reveals intact homeostatic mechanisms in a mouse model of fragile x syndrome. *Cell Reports*, 32(6), 2020.

[22] Rebecca Brooks-Fournier and Richard E Coggeshall. The ratio of preganglionic axons to postganglionic cells in the sympathetic nervous system of the rat. *Journal of Comparative Neurology*, 197(2):207–216, 1981.

[23] DA Brown. The other (muscarinic) acetylcholine receptors in sympathetic ganglia: actions and mechanisms. *Neurophysiology*, 45(1):60–66, 2013.

[24] Pernille Bülow, TJ Murphy, Gary J Bassell, and Peter Wenner. Homeostatic intrinsic plasticity is functionally altered in fmr1 ko cortical neurons. *Cell reports*, 26(6):1378–1388, 2019.

[25] Pernille Bülow, Peter A Wenner, Victor Faundez, and Gary J Bassell. Mitochondrial structure and polarity in dendrites and the axon initial segment are regulated by homeostatic plasticity and dysregulated in fragile x syndrome. *Frontiers in Cell and Developmental Biology*, 9:702020, 2021.

[26] CCAJ BurtGraham. Pentamethonium and hexamethonium iodide in investigation of peripheral vascular disease and hypertension, brit. *MJ*, 1:455, 1950.

[27] John H Byrne, Ruth Heidelberger, and M Neal Waxham. *From molecules to networks: an introduction to cellular and molecular neuroscience*. Academic Press, 2014.

[28] Anda-Alexandra Calinescu, Tiecheng Liu, Michael M Wang, and Jimo Borjigin. Transsynaptic activity-dependent regulation of axon branching and neurotrophin expression in vivo. *Journal of Neuroscience*, 31(36):12708–12715, 2011.

[29] Francesco Cerritelli, Martin G Frasch, Marta C Antonelli, Chiara Viglione, Stefano Vecchi, Marco Chiera, and Andrea Manzotti. A review on the vagus nerve and autonomic nervous system during fetal development: searching for critical windows. *Frontiers in Neuroscience*, 15:721605, 2021.

[30] Leo M Chalupa. Retinal waves are unlikely to instruct the formation of eye-specific retinogeniculate projections. *Neural development*, 4:1–7, 2009.

[31] Anna Chatzidaki and Neil S Millar. Allosteric modulation of nicotinic acetylcholine receptors. *Biochemical pharmacology*, 97(4):408–417, 2015.

[32] Nikolai Chub and Michael J O'Donovan. Blockade and recovery of spontaneous rhythmic activity after application of neurotransmitter antagonists to spinal networks of the chick embryo. *Journal of Neuroscience*, 18(1):294–306, 1998.

[33] J Miguel Cisneros-Franco, Patrice Voss, Maryse E Thomas, and Etienne de Villers-Sidani. Critical periods of brain development. In *Handbook of clinical neurology*, volume 173, pages 75–88. Elsevier, 2020.

[34] J Lockhart Clarke et al. Researches into the structure of the spinal cord. *Edinburgh Medical and Surgical Journal*, 78(192):56, 1852.

[35] Casey Crump, Marilyn A Winkleby, Kristina Sundquist, and Jan Sundquist. Risk of hypertension among young adults who were born preterm: a swedish national study of 636,000 births. *American journal of epidemiology*, 173(7): 797–803, 2011.

[36] Dapeng Cui, Kimberly J Dougherty, David W Machacek, Michael Sawchuk, Shawn Hochman, and Deborah J Baro. Divergence between motoneurons: gene expression profiling provides a molecular characterization of functionally discrete somatic and autonomic motoneurons. *Physiological genomics*, 24(3): 276–289, 2006.

[37] Iwona Cygankiewicz and Wojciech Zareba. Heart rate variability. *Handbook of clinical neurology*, 117:379–393, 2013.

[38] Roger A Dampney, Lisete C Michelini, De-Pei Li, and Hui-Lin Pan. Regulation of sympathetic vasomotor activity by the hypothalamic paraventricular nucleus in normotensive and hypertensive states. *American Journal of Physiology-Heart and Circulatory Physiology*, 315(5):H1200–H1214, 2018.

[39] John A Dani and Daniel Bertrand. Nicotinic acetylcholine receptors and nicotinic cholinergic mechanisms of the central nervous system. *Annu. Rev. Pharmacol. Toxicol.*, 47:699–729, 2007.

[40] Hélène Darville, Aurélie Poulet, Frédérique Rodet-Amsellem, Laure Chatrousse, Julie Pernelle, Claire Boissart, Delphine Héron, Caroline Nava, Anselme Perrier, Margot Jarrige, et al. Human pluripotent stem cell-derived cortical neurons for high throughput medication screening in autism: a proof of concept study in shank3 haploinsufficiency syndrome. *EBioMedicine*, 9:293–305, 2016.

[41] Jeremy S Dasen and Thomas M Jessell. Chapter six hox networks and the origins of motor neuron diversity. *Current topics in developmental biology*, 88: 169–200, 2009.

[42] Jeremy S Dasen, Jeh-Ping Liu, and Thomas M Jessell. Motor neuron columnar fate imposed by sequential phases of hox-c activity. *Nature*, 425(6961):926–933, 2003.

[43] Jeremy S Dasen, Alessandro De Camilli, Bin Wang, Philip W Tucker, and Thomas M Jessell. Hox repertoires for motor neuron diversity and connectivity gated by a single accessory factor, foxp1. *Cell*, 134(2):304–316, 2008.

[44] Graeme W Davis. Homeostatic control of neural activity: from phenomenology to molecular design. *Annu. Rev. Neurosci.*, 29:307–323, 2006.

[45] Graeme W Davis and Corey S Goodman. Genetic analysis of synaptic development and plasticity: homeostatic regulation of synaptic efficacy. *Current opinion in neurobiology*, 8(1):149–156, 1998.

[46] Graeme W Davis and Martin Müller. Homeostatic control of presynaptic neurotransmitter release. *Annual review of physiology*, 77:251–270, 2015.

[47] Harvey Davis, Emma N Bardsley, and David J Paterson. Transcriptional profiling of stellate ganglia from normotensive and spontaneously hypertensive rat strains. *Scientific data*, 5(1):1–7, 2018.

[48] Luiz Fernando Martins de Souza Filho, Jordana Campos Martins de Oliveira, and Ana Cristina Silva Rebelo. Heart rate variability in the evaluation of the autonomic nervous system of premature infants. *Birth Defects Research*, 113 (11):872–875, 2021.

[49] Arianna Del Signore, Cecilia Gotti, Angela Rizzo, Milena Moretti, and Paola Paggi. Nicotinic acetylcholine receptor subtypes in the rat sympathetic ganglion: pharmacological characterization, subcellular distribution and effect of pre-and postganglionic nerve crush. *Journal of Neuropathology & Experimental Neurology*, 63(2):138–150, 2004.

[50] Niraj S Desai. Homeostatic plasticity in the cns: synaptic and intrinsic forms. *Journal of Physiology-Paris*, 97(4-6):391–402, 2003.

[51] Niraj S Desai, Lana C Rutherford, and Gina G Turrigiano. Plasticity in the intrinsic excitability of cortical pyramidal neurons. *Nature neuroscience*, 2(6): 515–520, 1999.

[52] Niraj S Desai, Robert H Cudmore, Sacha B Nelson, and Gina G Turrigiano. Critical periods for experience-dependent synaptic scaling in visual cortex. *Nature neuroscience*, 5(8):783–789, 2002.

[53] Susan A Deuchars and Varinder K. Lall. Sympathetic preganglionic neurons: properties and inputs. *Comprehensive Physiology*, 5(2):829–869, 2011.

[54] Susan A Deuchars and Varinder K. Lall. Sympathetic preganglionic neurons: properties and inputs. *Comprehensive Physiology*, 5(2):829–869, 2015.

[55] P Devay, X Qu, and L Role. Regulation of nachr subunit gene expression relative to the development of pre-and postsynaptic projections of embryonic chick sympathetic neurons. *Developmental biology*, 162(1):56–70, 1994.

[56] Dion K Dickman and Graeme W Davis. The schizophrenia susceptibility gene dysbindin controls synaptic homeostasis. *Science*, 326(5956):1127–1130, 2009.

[57] Sarra Djemil, Antonia M Sames, and Daniel TS Pak. Ach transfers: Homeostatic plasticity of cholinergic synapses. *Cellular and Molecular Neurobiology*, 43(2):697–709, 2023.

[58] Frank J Dowd, Bart Johnson, and Angelo Mariotti. *Pharmacology and therapeutics for dentistry-E-book*. Elsevier Health Sciences, 2016.

[59] Stuart E Dryer and VA Chiappinelli. Properties of choroid and ciliary neurons in the avian ciliary ganglion and evidence for substance p as a neurotransmitter. *Journal of Neuroscience*, 5(10):2654–2661, 1985.

[60] Stuart E Dryer and Vincent A Chiappinelli. An intracellular study of synaptic transmission and dendritic morphology in sympathetic neurons of the chick embryo. *Developmental Brain Research*, 22(1):99–111, 1985.

[61] Rosamond M Eccles. Responses of isolated curarized sympathetic ganglia. *The Journal of Physiology*, 117(2):196, 1952.

[62] Julio Echegoyen, Axel Neu, Kevin D Graber, and Ivan Soltesz. Homeostatic

plasticity studied using in vivo hippocampal activity-blockade: synaptic scaling, intrinsic plasticity and age-dependence. *PloS one*, 2(8):e700, 2007.

[63] Espen Moen Eilertsen, Line C Gjerde, Ted Reichborn-Kjennerud, Ragnhild E Ørstavik, Gun Peggy Knudsen, Camilla Stoltenberg, Nikolai Czajkowski, Espen Røysamb, Kenneth S Kendler, and Eivind Ystrom. Maternal alcohol use during pregnancy and offspring attention-deficit hyperactivity disorder (adhd): a prospective sibling control study. *International Journal of Epidemiology*, 46 (5):1633–1640, 2017.

[64] Kathrin L Engisch, Xueyong Wang, and Mark M Rich. Homeostatic plasticity of the mammalian neuromuscular junction. In *Vertebrate Motoneurons*, pages 111–130. Springer, 2022.

[65] Uwe Ernsberger, Thomas Deller, and Hermann Rohrer. The diversity of neuronal phenotypes in rodent and human autonomic ganglia. *Cell and tissue research*, 382:201–231, 2020.

[66] Uwe Ernsberger, Thomas Deller, and Hermann Rohrer. The sympathies of the body: functional organization and neuronal differentiation in the peripheral sympathetic nervous system. *Cell and Tissue Research*, pages 1–21, 2021.

[67] Michael J Fitzpatrick and Daniel Kerschensteiner. Homeostatic plasticity in the retina. *Progress in Retinal and Eye Research*, 94:101131, 2023.

[68] Cynthia J Forehand, Elizabeth B Ezerman, Eric Rubin, and Joel C Glover. Segmental patterning of rat and chicken sympathetic preganglionic neurons: correlation between soma position and axon projection pathway. *Journal of Neuroscience*, 14(1):231–241, 1994.

[69] C Andrew Frank, Matthew J Kennedy, Carleton P Goold, Kurt W Marek, and

Graeme W Davis. Mechanisms underlying the rapid induction and sustained expression of synaptic homeostasis. *Neuron*, 52(4):663–677, 2006.

[70] Donald N Franz, Parley W Madsen, Robert G Peterson, and Chaichan Sangdee. Functional roles of monoaminergic pathways to sympathetic preganglionic neurons. *Clinical and Experimental Hypertension. Part A: Theory and Practice*, 4 (4-5):543–562, 1982.

[71] Cheryl D Fryar, Yechiam Ostchega, Craig M Hales, Guangyu Zhang, and Deanna Kruszon-Moran. Hypertension prevalence and control among adults: United states, 2015-2016. 2017.

[72] Miguel Angel Garcia-Bereguiain, Carlos Gonzalez-Islas, Casie Lindsly, Ellie Butler, Atlantis Wilkins Hill, and Peter Wenner. In vivo synaptic scaling is mediated by glua2-lacking ampa receptors in the embryonic spinal cord. *Journal of Neuroscience*, 33(16):6791–6799, 2013.

[73] Miguel Angel Garcia-Bereguiain, Carlos Gonzalez-Islas, Casie Lindsly, and Peter Wenner. Spontaneous release regulates synaptic scaling in the embryonic spinal network in vivo. *Journal of Neuroscience*, 36(27):7268–7282, 2016.

[74] Estelle B Gauda and Gabrielle L McLemore. Premature birth, homeostatic plasticity and respiratory consequences of inflammation. *Respiratory Physiology & Neurobiology*, 274:103337, 2020.

[75] Carlo NG Giachello and Richard A Baines. Inappropriate neural activity during a sensitive period in embryogenesis results in persistent seizure-like behavior. *Current Biology*, 25(22):2964–2968, 2015.

[76] Michael P Gilbey and Rueben D Stein. Characteristics of sympathetic preganglionic neurones in the lumbar spinal cord of the cat. *The Journal of Physiology*, 432(1):427–443, 1991.

[77] Simon J Gladwell and John H Coote. Inhibitory and indirect excitatory effects of dopamine on sympathetic preganglionic neurones in the neonatal rat spinal cord in vitro. *Brain research*, 818(2):397–407, 1999.

[78] Natalia O Glebova and David D Ginty. Growth and survival signals controlling sympathetic nervous system development. *Annu. Rev. Neurosci.*, 28:191–222, 2005.

[79] Jean-Marc Goaillard and Eve Marder. Ion channel degeneracy, variability, and covariation in neuron and circuit resilience. *Annual review of neuroscience*, 44: 335–357, 2021.

[80] Pragya Goel and Dion Dickman. Synaptic homeostats: latent plasticity revealed at the drosophila neuromuscular junction. *Cellular and Molecular Life Sciences*, 78:3159–3179, 2021.

[81] David G Gonsalvez, Ilan A Kerman, Robin M McAllen, and Colin R Anderson. Chemical coding for cardiovascular sympathetic preganglionic neurons in rats. *Journal of Neuroscience*, 30(35):11781–11791, 2010.

[82] Carlos Gonzalez-Islas and Peter Wenner. Spontaneous network activity in the embryonic spinal cord regulates ampaergic and gabaergic synaptic strength. *Neuron*, 49(4):563–575, 2006.

[83] Carlos Gonzalez-Islas, Nikolai Chub, and Peter Wenner. Nkcc1 and ae3 appear to accumulate chloride in embryonic motoneurons. *Journal of neurophysiology*, 101(2):507–518, 2009.

[84] Carlos Gonzalez-Islas, Nikolai Chub, Miguel Angel Garcia-Bereguiain, and Peter Wenner. Gabaergic synaptic scaling in embryonic motoneurons is mediated by a shift in the chloride reversal potential. *Journal of Neuroscience*, 30(39): 13016–13020, 2010.

[85] Carlos Gonzalez-Islas, Miguel Angel Garcia-Bereguiain, Brendan O'Flaherty, and Peter Wenner. Tonic nicotinic transmission enhances spinal gabaergic presynaptic release and the frequency of spontaneous network activity. *Developmental neurobiology*, 76(3):298–312, 2016.

[86] Carlos Gonzalez-Islas, Miguel Angel Garcia-Bereguiain, and Peter Wenner. Homeostatic recovery of embryonic spinal activity initiated by compensatory changes in resting membrane potential." eneuro 7 (4), 2020.

[87] Daniel A Goodenough and David L Paul. Gap junctions. *Cold Spring Harbor perspectives in biology*, 1(1):a002576, 2009.

[88] Lloyd A Greene. Binding of α-bungarotoxin to chick sympathetic ganglia: properties of the receptor and its rate of appearance during development. *Brain Research*, 111(1):135–145, 1976.

[89] Anton A Grishin, Ching-I A Wang, Markus Muttenthaler, Paul F Alewood, Richard J Lewis, and David J Adams. α-conotoxin auib isomers exhibit distinct inhibitory mechanisms and differential sensitivity to stoichiometry of $\alpha 3\beta 4$ nicotinic acetylcholine receptors. *Journal of Biological Chemistry*, 285(29):22254–22263, 2010.

[90] AM Gurney and HP Rang. The channel-blocking action of methonium compounds on rat submandibular ganglion cells. *British journal of pharmacology*, 82(3):623–642, 1984.

[91] Maureen Hack, Daniel J Flannery, Mark Schluchter, Lydia Cartar, Elaine Borawski, and Nancy Klein. Outcomes in young adulthood for very-low-birthweight infants. *New England Journal of Medicine*, 346(3):149–157, 2002.

[92] Maureen Hack, Mark Schluchter, Lydia Cartar, and Mahboob Rahman. Blood

pressure among very low birth weight (¡ 1.5 kg) young adults. *Pediatric Research*, 58(4):677–684, 2005.

[93] Viktor Hamburger and Howard L Hamilton. A series of normal stages in the development of the chick embryo. *Journal of morphology*, 88(1):49–92, 1951.

[94] Amanda L Hanes, Andrew G Koesters, Ming-fai Fong, Haider F Altimimi, David Stellwagen, Peter Wenner, and Kathrin L Engisch. Divergent synaptic scaling of miniature epscs following activity blockade in dissociated neuronal cultures. *Journal of Neuroscience*, 40(21):4090–4102, 2020.

[95] M Gartz Hanson and Lynn T Landmesser. Normal patterns of spontaneous activity are required for correct motor axon guidance and the expression of specific guidance molecules. *Neuron*, 43(5):687–701, 2004.

[96] Kristin Haraldsdottir, Andrew M Watson, Arij G Beshish, Dave F Pegelow, Mari Palta, Laura H Tetri, Melissa D Brix, Ryan M Centanni, Kara N Goss, and Marlowe W Eldridge. Heart rate recovery after maximal exercise is impaired in healthy young adults born preterm. *European journal of applied physiology*, 119:857–866, 2019.

[97] Donald Olding Hebb. *The organization of behavior: A neuropsychological theory*. Psychology press, 1950.

[98] Ian A Hendry and Jacob Campbell. Morphometric analysis of rat superior cervical ganglion after axotomy and nerve growth factor treatment. *Journal of neurocytology*, 5:351–360, 1976.

[99] Matthias H Hennig, John Grady, James van Coppenhagen, and Evelyne Sernagor. Age-dependent homeostatic plasticity of gabaergic signaling in developing retinal networks. *Journal of Neuroscience*, 31(34):12159–12164, 2011.

[100] GD Hirst and Elspeth M McLachlan. Post-natal development of ganglia in the lower lumbar sympathetic chain of the rat. *The Journal of Physiology*, 349(1): 119–134, 1984.

[101] Margaret Hollyday and Viktor Hamburger. An autoradiographic study of the formation of the lateral motor column in the chick embryo. *Brain research*, 132 (2):197–208, 1977.

[102] David A Hopkins and J Andrew Armour. Localization of sympathetic postganglionic and parasympathetic preganglionic neurons which innervate different regions of the dog heart. *Journal of Comparative Neurology*, 229(2):186–198, 1984.

[103] JP Horn, KM Sikora, K Clark, MG Springer, and PHM Kullmann. Interaction between h-current and nicotinic epsps in sympathetic neurons serves to modulate synaptic amplification in ganglia. *Autonomic Neuroscience: Basic and Clinical*, 192:114–115, 2015.

[104] KA Hruschak, VL Friedrich Jr, and E Giacobini. Synaptogenesis in chick paravertebral sympathetic ganglia: a morphometric analysis. *Developmental Brain Research*, 4(2):229–240, 1982.

[105] Raymond Hurst, Hans Rollema, and Daniel Bertrand. Nicotinic acetylcholine receptors: from basic science to therapeutics. *Pharmacology & therapeutics*, 137 (1):22–54, 2013.

[106] J Huupponen, Tsvetomira Atanasova, Tomi Taira, and Sari E Lauri. Glua4 subunit of ampa receptors mediates the early synaptic response to altered network activity in the developing hippocampus. *Journal of neurophysiology*, 115 (6):2989–2996, 2016.

[107] W Jänig, R Krauspe, and G Wiedersatz. Transmission of impulses from pre-to postganglionic vasoconstrictor and sudomotor neurons. *Journal of the autonomic nervous system*, 6(1):95–106, 1982.

[108] W Jänig, R Krauspe, and G Wiedersatz. Activation of postganglionic neurones via non-nicotinic synaptic mechanisms by stimulation of thin preganglionic axons. *Pflügers Archiv*, 401:318–320, 1984.

[109] Wilfrid Jänig. Non-nicotinic transmission in autonomic ganglia revisited–an important physiological function? *The Journal of Physiology*, 566(Pt 1):1, 2005.

[110] Wilfrid Jänig. *The integrative action of the autonomic nervous system: neurobiology of homeostasis*. Cambridge University Press, 2022.

[111] Wilfrid Jänig and Elspeth M McLachlan. Characteristics of function-specific pathways in the sympathetic nervous system. *Trends in neurosciences*, 15(12): 475–481, 1992.

[112] Michał Jurczyk, Katarzyna Anna Dylag, Kamil Skowron, and Krzysztof Gil. Prenatal alcohol exposure and autonomic nervous system dysfunction: A review article. *Folia Medica Cracoviensia*, 59(3), 2019.

[113] Ksenia V Kastanenka and Lynn T Landmesser. In vivo activation of channelrhodopsin-2 reveals that normal patterns of spontaneous activity are required for motoneuron guidance and maintenance of guidance molecules. *Journal of Neuroscience*, 30(31):10575–10585, 2010.

[114] H Kawano and S Masuko. Region-specific projections from the subfornical organ to the paraventricular hypothalamic nucleus in the rat. *Neuroscience*, 169(3): 1227–1234, 2010.

[115] Lei Ke, Cynthia M Eisenhour, Merouane Bencherif, and Ronald J Lukas. Effects of chronic nicotine treatment on expression of diverse nicotinic acetylcholine receptor subtypes. i. dose-and time-dependent effects of nicotine treatment. *Journal of Pharmacology and Experimental Therapeutics*, 286(2):825–840, 1998.

[116] Daniel Kerschensteiner. Spontaneous network activity and synaptic development. *The Neuroscientist*, 20(3):272–290, 2014.

[117] Valerie Kilman, Mark CW Van Rossum, and Gina G Turrigiano. Activity deprivation reduces miniature ipsc amplitude by decreasing the number of postsynaptic gabaa receptors clustered at neocortical synapses. *Journal of Neuroscience*, 22(4):1328–1337, 2002.

[118] Eugene A Kiyatkin. Neural effects of nicotine: Peripheral sensory systems and experience-dependent neural sensitization. In *Neuropathology of Drug Addictions and Substance Misuse*, pages 348–360. Elsevier, 2016.

[119] Matthew E Klein, Daniel T Lioy, Lin Ma, Soren Impey, Gail Mandel, and Richard H Goodman. Homeostatic regulation of mecp2 expression by a creb-induced microrna. *Nature neuroscience*, 10(12):1513–1514, 2007.

[120] H Komuro, Y Momose-Sato, T Sakai, A Hirota, and K Kamino. Optical monitoring of early appearance of spontaneous membrane potential changes in the embryonic chick medulla oblongata using a voltage-sensitive dye. *Neuroscience*, 52(1):55–62, 1993.

[121] Paraskevi Krashia, Mirko Moroni, Steven Broadbent, Giovanna Hofmann, Sebastian Kracun, Marco Beato, Paul J Groot-Kormelink, and Lucia G Sivilotti. Human $\alpha 3\beta 4$ neuronal nicotinic receptors show different stoichiometry if they are expressed in xenopus oocytes or mammalian hek293 cells. *PloS one*, 5(10): e13611, 2010.

[122] Michael Krauss, Daniel Korr, Andreas Herrmann, and Ferdinand Hucho. Binding properties of agonists and antagonists to distinct allosteric states of the nicotinic acetylcholine receptor are incompatible with a concerted model. *Journal of Biological Chemistry*, 275(39):30196–30201, 2000.

[123] Andrew C Kruse, Brian K Kobilka, Dinesh Gautam, Patrick M Sexton, Arthur Christopoulos, and Jürgen Wess. Muscarinic acetylcholine receptors: novel opportunities for drug development. *Nature reviews Drug discovery*, 13(7):549–560, 2014.

[124] Paul HM Kullmann, Kristine M Sikora, K Lyles Clark, Irene Arduini, Mitchell G Springer, and John P Horn. Hcn hyperpolarization-activated cation channels strengthen virtual nicotinic epsps and thereby elevate synaptic amplification in rat sympathetic neurons. *Journal of Neurophysiology*, 116(2):438–447, 2016.

[125] Thomas Kuner and George J Augustine. A genetically encoded ratiometric indicator for chloride: capturing chloride transients in cultured hippocampal neurons. *Neuron*, 27(3):447–459, 2000.

[126] Phillip E Kunkler and Bang H Hwang. Lower gabaa receptor binding in the amygdala and hypothalamus of spontaneously hypertensive rats. *Brain research bulletin*, 36(1):57–61, 1995.

[127] Lynn Landmesser and Deborah G Morris. The development of functional innervation in the hind limb of the chick embryo. *The Journal of physiology*, 249 (2):301–326, 1975.

[128] Lynn T Landmesser and Michael J O'Donovan. Activation patterns of embryonic chick hind limb muscles recorded in ovo and in an isolated spinal cord preparation. *The Journal of physiology*, 347(1):189–204, 1984.

[129] John Newport Langley. On the union of cranial autonomic (visceral) fibres with the nerve cells of the superior cervical ganglion. *The Journal of physiology*, 23 (3):240, 1898.

[130] John Newport Langley. On the stimulation and paralysis of nerve-cells and of nerve-endings: Part i. *The Journal of physiology*, 27(3):224, 1901.

[131] WA Large and JA Sim. A comparison between mechanisms of action of different nicotinic blocking agents on rat submandibular ganglia. *British journal of pharmacology*, 89(3):583, 1986.

[132] Bruno Larrivée, Catarina Freitas, Steven Suchting, Isabelle Brunet, and Anne Eichmann. Guidance of vascular development: lessons from the nervous system. *Circulation research*, 104(4):428–441, 2009.

[133] SM Leber, SM Breedlove, and JR Sanes. Lineage, arrangement, and death of clonally related motoneurons in chick spinal cord. *Journal of Neuroscience*, 10 (7):2451–2462, 1990.

[134] Matt T Lee, Mark J Koebbe, and Michael J O'Donovan. The development of sensorimotor synaptic connections in the lumbosacral cord of the chick embryo. *Journal of Neuroscience*, 8(7):2530–2543, 1988.

[135] Seunghee Lee, Bora Lee, Jae W Lee, and Soo-Kyung Lee. Retinoid signaling and neurogenin2 function are coupled for the specification of spinal motor neurons through a chromatin modifier cbp. *Neuron*, 62(5):641–654, 2009.

[136] Soo-Kyung Lee, Bora Lee, Esmeralda C Ruiz, and Samuel L Pfaff. Olig2 and ngn2 function in opposition to modulate gene expression in motor neuron progenitor cells. *Genes & development*, 19(2):282–294, 2005.

[137] Xavier Leinekugel, Ilgram Khalilov, Heather McLean, Olivier Caillard, Jean-Luc Gaiarsa, Yehezkel Ben-Ari, and Roustem Khazipov. Gaba is the principal fast-acting excitatory transmitter in the neonatal brain. *Advances in neurology*, 79:189–201, 1999.

[138] Gwendal LeMasson, Eve Marder, and LF Abbott. Activity-dependent regulation of conductances in model neurons. *Science*, 259(5103):1915–1917, 1993.

[139] Rita Levi-Montalcini. The origin and development of the visceral in the spinal cord of the chick embryo. *Journal of Morphology*, 86(2):253–283, 1950.

[140] Xiling Li, Pragya Goel, Catherine Chen, Varun Angajala, Xun Chen, and Dion K Dickman. Synapse-specific and compartmentalized expression of presynaptic homeostatic potentiation. *Elife*, 7:e34338, 2018.

[141] Yu-Long Li. Stellate ganglia and cardiac sympathetic overactivation in heart failure. *International journal of molecular sciences*, 23(21):13311, 2022.

[142] Casie Lindsly, Carlos Gonzalez-Islas, and Peter Wenner. Activity blockade and gabaa receptor blockade produce synaptic scaling through chloride accumulation in embryonic spinal motoneurons and interneurons. *PLoS One*, 9(4):e94559, 2014.

[143] Vichithra RB Liyanage and Mojgan Rastegar. Rett syndrome and mecp2. *Neuromolecular medicine*, 16:231–264, 2014.

[144] Maristella Lucchini, Lauren C Shuffrey, J David Nugent, Nicoló Pini, Ayesha Sania, Margaret Shair, Lucy Brink, Carlie Du Plessis, Hein J Odendaal, Morgan E Nelson, et al. Effects of prenatal exposure to alcohol and smoking on fetal heart rate and movement regulation. *Frontiers in Physiology*, 12:594605, 2021.

[145] Jason N MacLean, Ying Zhang, Bruce R Johnson, and Ronald M Harris-Warrick. Activity-independent homeostasis in rhythmically active neurons. *Neuron*, 37(1):109–120, 2003.

[146] Takako Makita, Henry M Sucov, Cheryl E Gariepy, Masashi Yanagisawa, and David D Ginty. Endothelins are vascular-derived axonal guidance cues for developing sympathetic neurons. *Nature*, 452(7188):759–763, 2008.

[147] Eve Marder and Astrid A Prinz. Modeling stability in neuron and network function: the role of activity in homeostasis. *Bioessays*, 24(12):1145–1154, 2002.

[148] Eve Marder and Astrid A Prinz. Current compensation in neuronal homeostasis. *Neuron*, 37(1):2–4, 2003.

[149] Eve Marder and Kristina J Rehm. Development of central pattern generating circuits. *Current opinion in neurobiology*, 15(1):86–93, 2005.

[150] Nephtali Marina, Melody Taheri, and Michael P Gilbey. Generation of a physiological sympathetic motor rhythm in the rat following spinal application of 5-ht. *The Journal of physiology*, 571(2):441–450, 2006.

[151] Nephtali Marina, David L Becker, and Michael P Gilbey. Immunohistochemical detection of connexin36 in sympathetic preganglionic and somatic motoneurons in the adult rat. *Autonomic Neuroscience*, 139(1-2):15–23, 2008.

[152] Nadia Oliveira Maruyama, Nathan C Mitchell, Tamara T Truong, and Glenn M Toney. Activation of the hypothalamic paraventricular nucleus by acute intermittent hypoxia: Implications for sympathetic long-term facilitation neuroplasticity. *Experimental neurology*, 314:1–8, 2019.

[153] Francesca Mazzo, Francesco Pistillo, Giovanni Grazioso, Francesco Clementi, Nica Borgese, Cecilia Gotti, and Sara Francesca Colombo. Nicotine-modulated

subunit stoichiometry affects stability and trafficking of $\alpha 3\beta 4$ nicotinic receptor. *Journal of Neuroscience*, 33(30):12316–12328, 2013.

[154] Peyton McDonnell, Pia Fornell, Sarah Ponce, and Laura Dyer. Baseline heart rate in infants with prenatal alcohol exposure: A systematic review and independent analysis. *Birth Defects Research*, 115(4):474–487, 2023.

[155] Stanton F McHardy, Hua-Yu Leo Wang, Shelby V McCowen, and Matthew C Valdez. Recent advances in acetylcholinesterase inhibitors and reactivators: an update on the patent literature (2012-2015). *Expert opinion on therapeutic patents*, 27(4):455–476, 2017.

[156] Bruce E McKay, Andon N Placzek, and John A Dani. Regulation of synaptic transmission and plasticity by neuronal nicotinic acetylcholine receptors. *Biochemical pharmacology*, 74(8):1120–1133, 2007.

[157] Michael Lee McKinnon, Kun Tian, Yaqing Li, Alan Joel Sokoloff, Meredith Lucy Galvin, Mi Hyun Choi, Astrid Prinz, and Shawn Hochman. Dramatically amplified thoracic sympathetic postganglionic excitability and integrative capacity revealed with whole-cell patch-clamp recordings. *Eneuro*, 6(2), 2019.

[158] Elspeth M McLachlan. Transmission of signals through sympathetic ganglia–modulation, integration or simply distribution? *Acta physiologica scandinavica*, 177(3):227–235, 2003.

[159] Louise D Milner and Lynn T Landmesser. Cholinergic and gabaergic inputs drive patterned spontaneous motoneuron activity before target contact. *Journal of Neuroscience*, 19(8):3007–3022, 1999.

[160] Yoko Momose-Sato and Katsushige Sato. Developmental roles of the spontaneous depolarization wave in synaptic network formation in the embryonic brainstem. *Neuroscience*, 365:33–47, 2017.

[161] Anita Montagna and Chiara Nosarti. Socio-emotional development following very preterm birth: pathways to psychopathology. *Frontiers in psychology*, 7: 80, 2016.

[162] Thiago S Moreira, Vagner R Antunes, Barbara Falquetto, and Nephtali Marina. Long-term stimulation of cardiac vagal preganglionic neurons reduces blood pressure in the spontaneously hypertensive rat. *Journal of hypertension*, 36 (12):2444–2452, 2018.

[163] BL Moss and Lorna W Role. Enhanced ach sensitivity is accompanied by changes in ach receptor channel properties and segregation of ach receptor subtypes on sympathetic neurons during innervation in vivo. *Journal of Neuroscience*, 13(1):13–28, 1993.

[164] Sarah B Mulkey and Adre Dú Plessis. The critical role of the central autonomic nervous system in fetal-neonatal transition. In *Seminars in Pediatric Neurology*, volume 28, pages 29–37. Elsevier, 2018.

[165] Sarah B Mulkey and Adre J du Plessis. Autonomic nervous system development and its impact on neuropsychiatric outcome. *Pediatric Research*, 85(2):120–126, 2019.

[166] Yuya Nakano. Adult-onset diseases in low birth weight infants: association with adipose tissue maldevelopment. *Journal of Atherosclerosis and Thrombosis*, 27 (5):397–405, 2020.

[167] Bennett G Novitch, Albert I Chen, and Thomas M Jessell. Coordinate regulation of motor neuron subtype identity and pan-neuronal properties by the bhlh repressor olig2. *Neuron*, 31(5):773–789, 2001.

[168] Michael O'Donovan, Stephen Ho, and Wayne Yee. Calcium imaging of rhythmic

network activity in the developing spinal cord of the chick embryo. *Journal of Neuroscience*, 14(11):6354–6369, 1994.

[169] Michael J O'Donovan, Nikolai Chub, and Peter Wenner. Mechanisms of spontaneous activity in developing spinal networks. *Journal of neurobiology*, 37(1): 131–145, 1998.

[170] Michael J O'Donovan, Agnes Bonnot, George Z Mentis, Yoshi Arai, Nikolai Chub, Neil A Shneider, and Peter Wenner. Imaging the spatiotemporal organization of neural activity in the developing spinal cord. *Developmental Neurobiology*, 68(6):788–803, 2008.

[171] MJ O'Donovan and L Landmesser. The development of hindlimb motor activity studied in the isolated spinal cord of the chick embryo. *Journal of Neuroscience*, 7(10):3256–3264, 1987.

[172] MJ O'Donovan, P Wenner, N Chub, J Tabak, and J Rinzel. Mechanisms of spontaneous activity in the developing spinal cord and their relevance to locomotion. *Annals of the New York Academy of Sciences*, 860(1):130–141, 1998.

[173] Timothy O'Leary, Alex H Williams, Jonathan S Caplan, and Eve Marder. Correlations in ion channel expression emerge from homeostatic tuning rules. *Proceedings of the National Academy of Sciences*, 110(28):E2645–E2654, 2013.

[174] Harika Topal Önal. The effects of ionising radiation. *Recent Researches in Health Sciences*, page 319, 2018.

[175] Richard J O'Brien, Sunjeev Kamboj, Michael D Ehlers, Kenneth R Rosen, Gerald D Fischbach, and Richard L Huganir. Activity-dependent modulation of synaptic ampa receptor accumulation. *Neuron*, 21(5):1067–1078, 1998.

[176] Michael J O'Donovan. The origin of spontaneous activity in developing networks of the vertebrate nervous system. *Current opinion in neurobiology*, 9(1):94–104, 1999.

[177] Maria Passafaro, Valentin Piëch, and Morgan Sheng. Subunit-specific temporal and spatial patterns of ampa receptor exocytosis in hippocampal neurons. *Nature neuroscience*, 4(9):917–926, 2001.

[178] Hugues Patural, Vincent Pichot, Fethi Jaziri, Georges Teyssier, Jean-Michel Gaspoz, Frédéric Roche, and Jean-Claude Barthelemy. Autonomic cardiac control of very preterm newborns: a prolonged dysfunction. *Early human development*, 84(10):681–687, 2008.

[179] Steen E Pedersen and Jonathan B Cohen. d-tubocurarine binding sites are located at alpha-gamma and alpha-delta subunit interfaces of the nicotinic acetylcholine receptor. *Proceedings of the National Academy of Sciences*, 87 (7):2785–2789, 1990.

[180] Carlijn Peerboom and Corette J Wierenga. The postnatal gaba shift: a developmental perspective. *Neuroscience & Biobehavioral Reviews*, 124:179–192, 2021.

[181] Dobromila Pekala and Peter Wenner. The uniform and nonuniform nature of slow and rapid scaling in embryonic motoneurons. *Journal of Neuroscience*, 42 (7):1224–1234, 2022.

[182] Stephen D Persell. Prevalence of resistant hypertension in the united states, 2003–2008. *Hypertension*, 57(6):1076–1080, 2011.

[183] Sophie A Petersen, Richard D Fetter, Jasprina N Noordermeer, Corey S Goodman, and Aaron DiAntonio. Genetic analysis of glutamate receptors in

drosophila reveals a retrograde signal regulating presynaptic transmitter release. *Neuron*, 19(6):1237–1248, 1997.

[184] ML Pierce, J Deuchars, and SA Deuchars. Spontaneous rhythmogenic capabilities of sympathetic neuronal assemblies in the rat spinal cord slice. *Neuroscience*, 170(3):827–838, 2010.

[185] JJ Plomp, G Th van Kempen, and PC Molenaar. Adaptation of quantal content to decreased postsynaptic sensitivity at single endplates in alpha-bungarotoxin-treated rats. *The Journal of Physiology*, 458(1):487–499, 1992.

[186] Anita Prasad and Margaret Hollyday. Development and migration of avian sympathetic preganglionic neurons. *Journal of comparative neurology*, 307(2): 237–258, 1991.

[187] William T Preyer. *Specielle physiologie des embryo: Untersuchungen über die lebenserscheinungen vor der geburt*. Grieben, 1885.

[188] Zilong Qiu, Emily L Sylwestrak, David N Lieberman, Yan Zhang, Xin-Yu Liu, and Anirvan Ghosh. The rett syndrome protein mecp2 regulates synaptic scaling. *Journal of Neuroscience*, 32(3):989–994, 2012.

[189] Davide Ragozzino, Benedetta Barabino, Sergio Fucile, and Fabrizio Eusebi. Ca2+ permeability of mouse and chick nicotinic acetylcholine receptors expressed in transiently transfected human cells. *The Journal of Physiology*, 507 (3):749–758, 1998.

[190] TA Rando, CW Bowers, and RE Zigmond. Localization of neurons in the rat spinal cord which project to the superior cervical ganglion. *Journal of Comparative Neurology*, 196(1):73–83, 1981.

[191] April Ratliff, Dobromila Pekala, and Peter Wenner. Plasticity in preganglionic and postganglionic neurons of the sympathetic nervous system during embryonic development. *Eneuro*, 2023.

[192] Christian A Reynolds and Zeljka Minic. Chronic pain-associated cardiovascular disease: The role of sympathetic nerve activity. *International Journal of Molecular Sciences*, 24(6):5378, 2023.

[193] Mark M Rich and Peter Wenner. Sensing and expressing homeostatic synaptic plasticity. *Trends in neurosciences*, 30(3):119–125, 2007.

[194] Amy Ritter, Peter Wenner, Stephen Ho, Patrick J Whelan, and Michael J O'Donovan. Activity patterns and synaptic organization of ventrally located interneurons in the embryonic chick spinal cord. *Journal of Neuroscience*, 19 (9):3457–3471, 1999.

[195] Eric Rubin. Development of the rat superior cervical ganglion: ganglion cell maturation. *Journal of Neuroscience*, 5(3):673–684, 1985.

[196] Malligurki Raghurama Rukmani, Shekhar P Seshadri, Kandavel Thennarasu, Trichur R Raju, and Talakad N Sathyaprabha. Heart rate variability in children with attention-deficit/hyperactivity disorder: a pilot study. *Annals of neurosciences*, 23(2):81–88, 2016.

[197] Gabrielle Rust, J-M Burgunder, TE Lauterburg, and Armand B Cachelin. Expression of neuronal nicotinic acetylcholine receptor subunit genes in the rat autonomic nervous system. *European Journal of Neuroscience*, 6(3):478–485, 1994.

[198] Young U Ryu and Nina S Bradley. Precocious locomotor behavior begins in the egg: development of leg muscle patterns for stepping in the chick. *PLoS One*, 4(7):e6111, 2009.

[199] S Saito, GJ Kidd, BD Trapp, TM Dawson, DS Bredt, DA Wilson, RJ Traystman, SH Snyder, and DF Hanley. Rat spinal cord neurons contain nitric oxide synthase. *Neuroscience*, 59(2):447–456, 1994.

[200] CB Saper, AD Loewy, LW Swanson, and WM Cowan. Direct hypothalamo-autonomic connections. *Brain research*, 117(2):305–312, 1976.

[201] Varun Saravanan, Gordon J Berman, and Samuel J Sober. Application of the hierarchical bootstrap to multi-level data in neuroscience. *Neurons, behavior, data analysis and theory*, 3(5), 2020.

[202] Sarah D Schlatterer, Rathinaswamy B Govindan, Scott D Barnett, Tareq Al-Shargabi, Daniel A Reich, Sneha Iyer, Laura Hitchings, G Larry Maxwell, Robin Baker, Adre J du Plessis, et al. Autonomic development in preterm infants is associated with morbidity of prematurity. *Pediatric research*, 91(1):171–177, 2022.

[203] Bernard F Schneider and Stata Norton. Equivalent ages in rat, mouse and chick embryos. *Teratology*, 19(3):273–278, 1979.

[204] Petra Scholze and Sigismund Huck. The $\alpha 5$ nicotinic acetylcholine receptor subunit differentially modulates $\alpha 4\beta 2^*$ and $\alpha 3\beta 4^*$ receptors. *Frontiers in Synaptic Neuroscience*, 12:607959, 2020.

[205] Gulgun Sengul and Charles Watson. Spinal cord: regional anatomy, cytoarchitecture and chemoarchitecture. In *The human nervous system*, pages 186–232. Academic Press, Elsevier, 2012.

[206] Andrew A Sharp and Anne Bekoff. Pyridoxine treatment alters embryonic motility in chicks: implications for the role of proprioception. *Developmental psychobiology*, 57(2):271–277, 2015.

[207] Jian-xin Shen and Jerrel L Yakel. Nicotinic acetylcholine receptor-mediated calcium signaling in the nervous system. *Acta Pharmacologica Sinica*, 30(6): 673–680, 2009.

[208] Mohammed Siddiqui and David A Calhoun. Refractory versus resistant hypertension. *Current Opinion in Nephrology and Hypertension*, 26(1):14–19, 2017.

[209] Anil Sindhurakar and Nina S Bradley. Kinematic analysis of overground locomotion in chicks incubated under different light conditions. *Developmental psychobiology*, 52(8):802–812, 2010.

[210] Gopal K Singh, Mohammad Siahpush, Lihua Liu, and Michelle Allender. Racial/ethnic, nativity, and sociodemographic disparities in maternal hypertension in the united states, 2014-2015. *International journal of hypertension*, 2018, 2018.

[211] Peige Song, Yan Zhang, Jinyue Yu, Mingming Zha, Yajie Zhu, Kazem Rahimi, and Igor Rudan. Global prevalence of hypertension in children: a systematic review and meta-analysis. *JAMA pediatrics*, 173(12):1154–1163, 2019.

[212] Mitchell G Springer, Paul HM Kullmann, and John P Horn. Virtual leak channels modulate firing dynamics and synaptic integration in rat sympathetic neurons: implications for ganglionic transmission in vivo. *The Journal of physiology*, 593(4):803–823, 2015.

[213] Larry Squire, Darwin Berg, Floyd E Bloom, Sascha Du Lac, Anirvan Ghosh, and Nicholas C Spitzer. *Fundamental neuroscience*. Academic press, 2012.

[214] Nicolas Stifani. Motor neurons and the generation of spinal motor neuron diversity. *Frontiers in cellular neuroscience*, 8:293, 2014.

[215] Simón (e) D Sun, Daniel Levenstein, Boxing Li, Nataniel Mandelberg, Nicolas Chenouard, Benjamin S Suutari, Sandrine Sanchez, Guoling Tian, John Rinzel, György Buzsáki, et al. Synaptic homeostasis transiently leverages hebbian mechanisms for a multiphasic response to inactivity. *bioRxiv*, pages 2022–06, 2022.

[216] Michael A Sutton and Erin M Schuman. Dendritic protein synthesis, synaptic plasticity, and memory. *Cell*, 127(1):49–58, 2006.

[217] Michael A Sutton, Hiroshi T Ito, Paola Cressy, Christian Kempf, Jessica C Woo, and Erin M Schuman. Miniature neurotransmission stabilizes synaptic function via tonic suppression of local dendritic protein synthesis. *Cell*, 125(4): 785–799, 2006.

[218] Joel Tabak, John Rinzel, and Michael J O'Donovan. The role of activity-dependent network depression in the expression and self-regulation of spontaneous activity in the developing spinal cord. *Journal of Neuroscience*, 21(22): 8966–8978, 2001.

[219] Joel Tabak, Peter Wenner, and Michael J O'Donovan. Rhythm generation in embryonic chick spinal cord. In *Encyclopedia of Computational Neuroscience*, pages 3051–3056. Springer, 2022.

[220] Ch Takeshige and RL Volle. A comparison of the ganglion potentials and block produced by acetylcholine and tetramethylammonium. *British Journal of Pharmacology and Chemotherapy*, 23(1):80–89, 1964.

[221] Yasuto Tanabe, Christopher William, and Thomas M Jessell. Specification of motor neuron identity by the mnr2 homeodomain protein. *Cell*, 95(1):67–80, 1998.

[222] Masaki Tanaka, Teru Ikeda, Seiji Hayashi, Norio Iijima, Fumimasa Amaya, Yasuo Hisa, and Yasuhiko Ibata. Nitrergic neurons in the medial amygdala project to the hypothalamic paraventricular nucleus of the rat. *Brain research*, 777(1-2):13–21, 1997.

[223] Vedakumar Tatavarty, Alejandro Torrado Pacheco, Chelsea Groves Kuhnle, Heather Lin, Priya Koundinya, Nathaniel J Miska, Keith B Hengen, Florence F Wagner, Stephen D Van Hooser, and Gina G Turrigiano. Autism-associated shank3 is essential for homeostatic compensation in rodent v1. *Neuron*, 106(5): 769–777, 2020.

[224] Manuel Teichert, Lutz Liebmann, Christian A Hübner, and Jürgen Bolz. Homeostatic plasticity and synaptic scaling in the adult mouse auditory cortex. *Scientific reports*, 7(1):17423, 2017.

[225] Tullio Terni. Ricerche anatomiche sul sistema nervoso autonomo degli uccelli. *Arch Ital Anat Embryol*, 20:433–510, 1924.

[226] Joshua P Thaler, Sonya J Koo, Artur Kania, Karen Lettieri, Shane Andrews, Christopher Cox, Thomas M Jessell, and Samuel L Pfaff. A postmitotic role for isl-class lim homeodomain proteins in the assignment of visceral spinal motor neuron identity. *Neuron*, 41(3):337–350, 2004.

[227] Nai-Wen Tien and Daniel Kerschensteiner. Homeostatic plasticity in neural development. *Neural development*, 13:1–7, 2018.

[228] AJ Tierney and RM Harris-Warrick. Physiological role of the transient potassium current in the pyloric circuit of the lobster stomatogastric ganglion. *Journal of neurophysiology*, 67(3):599–609, 1992.

[229] Gerard J Tortora and Bryan Derrickson. Essentials of anatomy and physiology. *(No Title)*, 2013.

[230] Gerard J Tortora and Bryan H Derrickson. *Principles of anatomy and physiology*. John Wiley & Sons, 2018.

[231] Gina Turrigiano. Homeostatic synaptic plasticity: local and global mechanisms for stabilizing neuronal function. *Cold Spring Harbor perspectives in biology*, 4 (1):a005736, 2012.

[232] Gina Turrigiano, LF Abbott, and Eve Marder. Activity-dependent changes in the intrinsic properties of cultured neurons. *Science*, 264(5161):974–977, 1994.

[233] Gina Turrigiano, Gwendal LeMasson, and Eve Marder. Selective regulation of current densities underlies spontaneous changes in the activity of cultured neurons. *Journal of Neuroscience*, 15(5):3640–3652, 1995.

[234] Gina G Turrigiano and Sacha B Nelson. Homeostatic plasticity in the developing nervous system. *Nature reviews neuroscience*, 5(2):97–107, 2004.

[235] Gina G Turrigiano, Kenneth R Leslie, Niraj S Desai, Lana C Rutherford, and Sacha B Nelson. Activity-dependent scaling of quantal amplitude in neocortical neurons. *Nature*, 391(6670):892–896, 1998.

[236] Anna Vallstedt, Jonas Muhr, Alexandre Pattyn, Alessandra Pierani, Monica Mendelsohn, Maike Sander, Thomas M Jessell, and Johan Ericson. Different levels of repressor activity assign redundant and specific roles to nkx6 genes in motor neuron and interneuron specification. *Neuron*, 31(5):743–755, 2001.

[237] Rick Van Acker. Rett syndrome: A review of current knowledge. *Journal of Autism and Developmental Disorders*, 21(4):381–406, 1991.

[238] Guan Wang, Jia Zhong, Donovan Guttieres, and Heng-Ye Man. Non-scaling regulation of ampa receptors in homeostatic synaptic plasticity. *Neuropharmacology*, 158:107700, 2019.

[239] Xueyong Wang, Yingjie Li, Kathrin L Engisch, Stan T Nakanishi, Sara E Dodson, Gary W Miller, Timothy C Cope, Martin J Pinter, and Mark M Rich. Activity-dependent presynaptic regulation of quantal size at the mammalian neuromuscular junction in vivo. *Journal of Neuroscience*, 25(2):343–351, 2005.

[240] Ye Wang, Wing-Yu Fu, Kit Cheung, Kwok-Wang Hung, Congping Chen, Hongyan Geng, Wing-Ho Yung, Jianan Y Qu, Amy KY Fu, and Nancy Y Ip. Astrocyte-secreted il-33 mediates homeostatic synaptic plasticity in the adult hippocampus. *Proceedings of the National Academy of Sciences*, 118(1): e2020810118, 2021.

[241] Zhengbei Wang, Phillip A Low, and Steven Vernino. Antibody-mediated impairment and homeostatic plasticity of autonomic ganglionic synaptic transmission. *Experimental neurology*, 222(1):114–119, 2010.

[242] Wei Wen and Gina G Turrigiano. Developmental regulation of homeostatic plasticity in mouse primary visual cortex. *Journal of Neuroscience*, 41(48): 9891–9905, 2021.

[243] Peter Wenner. Homeostatic synaptic plasticity in developing spinal networks driven by excitatory gabaergic currents. *Neuropharmacology*, 78:55–62, 2014.

[244] Peter Wenner and Michael J O'Donovan. Mechanisms that initiate spontaneous network activity in the developing chick spinal cord. *Journal of neurophysiology*, 86(3):1481–1498, 2001.

[245] Peter Wenner, Yang Tsau, Lawrence B Cohen, Michael J O'Donovan, and Yang Dan. Voltage-sensitive dye recording using retrogradely transported dye in the chicken spinal cord: staining and signal characteristics. *Journal of neuroscience methods*, 70(2):111–120, 1996.

[246] Peter A Wenner. Development of the locomotor system—chick embryo. In *The Neural Control of Movement*, pages 221–236. Elsevier, 2020.

[247] Peter A Wenner and Dobromila Pekala. Homeostatic regulation of motoneuron properties in development. *Vertebrate Motoneurons*, pages 87–107, 2022.

[248] Diek W Wheeler, Paul HM Kullmann, and John P Horn. Estimating use-dependent synaptic gain in autonomic ganglia by computational simulation and dynamic-clamp analysis. *Journal of neurophysiology*, 92(5):2659–2671, 2004.

[249] Jennifer C Wilhelm and Peter Wenner. Gabaa transmission is a critical step in the process of triggering homeostatic increases in quantal amplitude. *Proceedings of the National Academy of Sciences*, 105(32):11412–11417, 2008.

[250] Jennifer C Wilhelm, Mark M Rich, and Peter Wenner. Compensatory changes in cellular excitability, not synaptic scaling, contribute to homeostatic recovery of embryonic network activity. *Proceedings of the National Academy of Sciences*, 106(16):6760–6765, 2009.

[251] Damian J Williams, Peter Sidaway, Thomas C Cunnane, and Keith L Brain. Mechanisms involved in nicotinic acetylcholine receptor-induced neurotransmitter release from sympathetic nerve terminals in the mouse vas deferens. *Plos one*, 6(12):e29209, 2011.

[252] DeWayne P Williams, Julian F Thayer, and Julian Koenig. Resting cardiac vagal tone predicts intraindividual reaction time variability during an attention task in a sample of young and healthy adults. *Psychophysiology*, 53(12):1843–1851, 2016.

[253] Jacobus Benignus Winslow. *Exposition anatomique de la structure du corps humain par JacquesBénigne Winslow...* éditeur non identifié, 1732.

[254] Rachel OL Wong. Retinal waves and visual system development. *Annual review of neuroscience*, 22(1):29–47, 1999.

[255] Rachel OL Wong, Markus Meister, and Carla J Shatz. Transient period of correlated bursting activity during development of the mammalian retina. *Neuron*, 11(5):923–938, 1993.

[256] Wenrui Xie, Sisi Chen, Judith A Strong, Ai-Ling Li, Ian P Lewkowich, and Jun-Ming Zhang. Localized sympathectomy reduces mechanical hypersensitivity by restoring normal immune homeostasis in rat models of inflammatory pain. *Journal of Neuroscience*, 36(33):8712–8725, 2016.

[257] Zeng-You Ye, De-Pei Li, Hee Sun Byun, Li Li, and Hui-Lin Pan. Nkcc1 upregulation disrupts chloride homeostasis in the hypothalamus and increases neuronal activity–sympathetic drive in hypertension. *Journal of Neuroscience*, 32(25): 8560–8568, 2012.

[258] Joseph W Yip. Migratory patterns of sympathetic ganglioblasts and other neural crest derivatives in chick embryos. *Journal of Neuroscience*, 6(12):3465–3473, 1986.

[259] Joseph W Yip. Specific innervation of neurons in the paravertebral sympathetic ganglia of the chick. *Journal of Neuroscience*, 6(12):3459–3464, 1986.

[260] Joseph W Yip. Target cues are not required for the guidance of sympathetic preganglionic axons. *Developmental Brain Research*, 32(1):155–159, 1987.

[261] Joseph W Yip. Identification of location and timing of guidance cues in sympathetic preganglionic axons of the chick. *Journal of Neuroscience*, 10(7):2476–2484, 1990.

[262] Joseph W Yip, Yee Ping L Yip, and Christine Capriotti. Segmental specificity of chick sympathetic preganglionic projections is influenced by preganglionic neurons from neighboring spinal cord segments. *Journal of Neuroscience*, 18 (24):10473–10480, 1998.

[263] Joseph W Yip, Yee Ping L Yip, and Christine Capriotti. Specific projections of sympathetic preganglionic neurons are not intrinsically determined by segmental origins of their cell bodies. *Journal of neurobiology*, 35(4):371–378, 1998.

[264] M Yoshimura, C Polosa, and S Nishi. Slow epsp and the depolarizing action of noradrenaline on sympathetic preganglionic neurons. *Brain research*, 414(1): 138–142, 1987.

[265] Hong-Yan Zhang and Keith T Sillar. Short-term memory of motor network performance via activity-dependent potentiation of na+/k+ pump function. *Current biology*, 22(6):526–531, 2012.

[266] Zhong-Wei Zhang and Darwin K Berg. Patch-clamp analysis of glycine-induced currents in chick ciliary ganglion neurons. *The Journal of Physiology*, 487(2): 395–405, 1995.

[267] Zhong-wei Zhang, Jay S Coggan, and Darwin K Berg. Synaptic currents generated by neuronal acetylcholine receptors sensitive to α-bungarotoxin. *Neuron*, 17(6):1231–1240, 1996.

[268] Bin Zhou, Rodrigo M Carrillo-Larco, Goodarz Danaei, Leanne M Riley, Christopher J Paciorek, Gretchen A Stevens, Edward W Gregg, James E Bennett, Bethlehem Solomon, Rosie K Singleton, et al. Worldwide trends in hypertension prevalence and progress in treatment and control from 1990 to 2019: a pooled analysis of 1201 population-representative studies with 104 million participants. *The Lancet*, 398(10304):957–980, 2021.

[269] S Zia, A Ndoye, VT Nguyen, and SA Grando. Nicotine enhances expression of the alpha 3, alpha 4, alpha 5, and alpha 7 nicotinic receptors modulating calcium metabolism and regulating adhesion and motility of respiratory epithelial cells. *Research communications in molecular pathology and pharmacology*, 97(3):243–262, 1997.

[270] Amanda Zimmerman and Shawn Hochman. Heterogeneity of membrane properties in sympathetic preganglionic neurons of neonatal mice: evidence of four subpopulations in the intermediolateral nucleus. *Journal of neurophysiology*, 103(1):490–498, 2010.

[271] Michele Zoli, Susanna Pucci, Antonietta Vilella, and Cecilia Gotti. Neuronal and extraneuronal nicotinic acetylcholine receptors. *Current neuropharmacology*, 16(4):338–349, 2018.